Generation of Decimeter and Centimeter Waves

by

V. I. Kalinin

Russian bk, 1948

Declassified in Part - Sanitized Copy Approved for Release 2012/04/09 : CIA-RDP82-00039R000200090009-2

V. I. KALININ

GENERATION OF DECIMETER AND CENTIMETER MICRO~~RADI~~O WAVES

PHYSICAL PRINCIPLES

The State Publication of Literature
Pertaining to Communication and Radio
Problems

Moscow 1948

PREFACE

This work represents an attempt at more or less systematic exposition of the basic physical principles of generation of micro-radio waves, on the basis of the work done by Soviet researchers. As contrasted with my previous monographs (Decimeter Waves of 1935, and Decimeter and Centimeter Waves of 1939), one of which was probably the first one in world literature published on the subject, in this book I have attempted, as far as possible, to refrain from the "encyclopedism" which evidenced itself in the above-mentioned works in the form of recitation of an enormous volume of experimental data, thus giving them the characteristics of a manual. This characteristic of my previous books I utilize extensively in this one, referring the reader frequently to the former for all the factual data of the work performed during the first period (prior to 1938).

The basic idea of this book is the idea of unity of "generators of electronic oscillations", concrete development of which was given in my doctoral theses The Principles of Kinematic Theory of Generation of Electronic Oscillations, which were formulated during the 1939-1943 period. I am utilizing the thesis data in expounding a number of questions, especially in chapters 6 and 7, which are almost completely based on the thesis, with the exception of places where I cite appropriate references. I have also utilized lecture material given by me from 1941-1948 to students of radio-physics at the Saratov, Leningrad and Rostov Universities, also the data of the scientific radio-physics seminar which was conducted in my laboratory from 1942 to 1943, and of a number of theses worked on and completed there during the 1939-1946 period.

Exposition of the data is of a predominantly concentrated nature. Sometimes this requires the repitition of certain things; however, it affords the opportunity to conduct the narrative in step with the development of basic physical ideas, and not in conjunction with various modifications or particular types of devices. To facilitate initial acquaintance with the basic ideas, all of the non-essential material which can be outlined on the first reading of the book has been set forth in fine print. In reviewing and proofreading the manuscript I have received valuable assistance from the senior scientific associates of the NIIMF SGN radiophysics laboratory, candidates of physico-mathematical sciences, V. L. Patrushev and G. M. Gershteyn, to whom I am deeply grateful. It is up to readers to pass upon the effectiveness of style and adequacy of this book, whose comments and desires will be greatly received.

V. Kalinin

Saratov, Radio-physics laboratory NIIMF SGU, (Sci-Res Inst of Mechanics and Physics, Saratov State University)

March 1948

INTRODUCTION

In speaking of radiowaves of the decimeter and centimeter wavelengths the term "microwave" is frequently used. However, despite its compactness, it is hardly convenient to use this terminology, which is not fully descriptive. In this book we shall use the expression "microradiowaves", only for the sake of brevity, without any pretense toward having found an exact definition.

By microradiowaves we shall denote electromagnetic waves having wavelengths of 1 meter to 1 millimeter, corresponding to frequencies from $3 \cdot 10^8$ to $3 \cdot 10^{11}$ cycles. The microradiowave region is located between the meter wavelengths, of purely electrical properties, and the intermediate wavelengths, with strongly pronounced optical characteristics.

The microradiowave technique is based on electrical methods of generation and radiation of oscillations. Their peculiar "opticity" manifests itself, mainly, in the lower portion of the bandwidth which is of interest to us in directional antennae arrays, in measuring methods, and, especially in specific applications of these waves. In its geometrical dimensions the generating, receiving and measuring apparatus of the microradiowave band is usually comparable to the wavelength, or in some instances, exceeds the latter. This results, as is well known [1,2], in the fact that the usual analytic processes are of little use in this field, and is especially pronounced in the study of specific microradiowave oscillatory and communications systems.

But the most important property of the physics and technique of microradio waves is the utilization of electron inertia in the functioning of the various electronic instruments. The attempt to apply the principle of an inertialess electronic relay to very high frequencies is limited by the minimum technologically feasible dimensions of electron tubes. Manifestation of electronic inertia leads to the scrapping of the usual methods of explaining phenomena taking place within electron tubes. The rapid and intensive development of the microradiowave field in recent years is actually due to the utilization of the electron transit time effect. "The total transit time is not an electronic limitation, but only a limitation of the traditional methods of tackling the problem".[1] The present day state of microradiowave physics and techniques is based on the following important facts: (a) accumulation, beginning with 1920, of an enormous amount of experimental and theoretical data in the field of "electronic generators" (generators operating on the principle of utilization of the electron transit time effect: retarding field devices, magnetrons, various velocity-modulated devices, etc.);

(b) the creation of high-quality oscillatory systems, well adapted to the requirements of ultra-high frequency techniques.

(c) the development of electron optics, which has facilitated development of efficient methods of coupling the electron beam to the oscillatory systems.

In turning to the problem of microradiowave generation it is necessary to note that it is most closely connected to the problems of "electronics of ultra-high frequencies". The substance of the latter boils down briefly to a basic study of the electron transit time phenomena within the electro-vacuum instruments. In the frequency band of conventional radio, the interelectrode electron transit time is on the order of 10^{-9} seconds, and electronic devices function almost without inertia, in view of which the controlled electron currents vary in phase in accordance with the control electrode voltages. An excellent example of this is the classical feed-back oscillator. The 180-degree phase difference between the plate and grid voltages, produced as a result of suitable connection of the feedback winding, ensures action of the tube as a dynamic negative resistance relative to the plate circuit. However, as the frequency increases, the phenomenon of electron inertia, which manifests itself in that the electron transit time between the grid and the plate becomes appreciable as compared with the period of oscillation, results in the violation of normal phase relationships within an electron tube oscillator. A desire to circumvent this limitation still remaining within the limits of classical oscillator systems, has led to the emergence of a number of special electron tube designs, in which, by various means, it has been attempted to neutralize the effect of electron inertia (smaller interelectrode spacings, choice of special electrode shape and material, etc.). Efforts in this direction have advanced the conventional radio-technical methods of wave generation and amplification to frequencies on the order of 2000-3500 megacycles ($\lambda = 15 \div 8.5$ centimeters). However, it is not the overcoming of the effect of electron inertia, but its intelligent utilization which has determined present day successes in microradiowave technology. The latter, naturally, became possible only on the basis of study of electron dynamics and properties of electron flow interacting with super high frequency electric fields. Actually, the "electron inertia" problems and methods are responsible for the specific nature of this problem.

Let us agree to designate as electronic oscillations "oscillations started in a circuit, connected to a thermionic system, due to electronic inertia" [3]. We should not, by any means, associate this phenomenon with the direct oscillation or "fluctuation" of electrons. Corresponding to the given definition we shall call such oscillators, which utilize electronic inertia, generators of electronic oscillations. All of the presently known types of generators of electronic oscillations may, in accordance with their external attributes, be divided into the electric-field type of generator, to which pertain retarding-field generators and various modifications of the velocity modulated devices, and generators with electric and magnetic fields, exemplified by the various magnetron systems. However, it is necessary to emphasize that such a subdivision is of purely external significance; the most important fact, high frequency control of the electron flow, is effected in all types of generators of electronic oscillations by means of electric fields.

It is normal then to anticipate that the mechanics of functioning of the various types of generators of electronic oscillations can be described on the basis of a single system. The probability of such unity in working mechanism, and, consequently, of building up of a more or less general theory is confirmed by the existence of properties common to all generators and characteristic relationships. One of the widely known and important relationships, which, in one form or the other, holds for all of the generators of electronic oscillations, is the "Barkhausen's equation".

$$\lambda^2 V_0 = \text{const},$$

where λ is the wavelength and V_0 is the applied constant accelerating potential. A relationship of this form, first derived by Barkhausen, Kurtz and Zilitinkevich, should be understood not as a condition of continuous dependence between λ and V_0, but only as a connection between these quantities, which characterize the optimum conditions for starting of electronic oscillation within a given device. The last observation is significant, since the only element which determines the frequency of electronic oscillations is the oscillatory circuit. Assumption of the presence of inherent frequencies of electron flow determined by certain "non-circuit" effects (for example, "fluctuation" of electrons according to Barkhausen and Kurtz), is, in the final analysis, completely unreasonable for the usual conditions of operation of electronic oscillation devices (electron flow in high vacuum).

Thus, the natural and unified scheme underlying any generator of electronic oscillations boils down to two basic elements: electron flow as the carrier of charges which can absorb or give up kinetic energy, and the oscillatory circuit as the seat of ultra-high frequency electric fields interacting with the flow of electrons. The magnetic field employed in some types of devices plays a secondary role, ensuring a definite motion of electrons, which is necessary for the effective functioning of the instrument.

References

1. Condon, E. U., Microradiowaves, Review of Physical Sciences, Volume 27, 213, 1945.

2. Slater, J., Transmission of Ultra-Short Radiowaves, GTI, 1943.

3. Megaw, G. C. S., Journ. Inst. El. Eng., 72, 1933, 313-325.

CHAPTER ONE

MICRORADIOWAVE OSCILLATING SYSTEMS

1.1 THE GENERAL REQUIREMENTS TO BE MET BY ULTRA-HIGH-FREQUENCY OSCILLATING SYSTEMS

The electrical oscillating system, which is a certain aggregation of conductors and conducting surfaces characterized by definite geometrical and electrical parameters as well as properties of resonance for certain frequencies, is the basic frequency-determining element in the microradiowave field. This applies to any device employing electron flow in a high vacuum.

In view of the negligible dimensions of ultra-high frequency oscillating systems there arises the especially critical questions of the amount of energy stored by them. Acutally, concentration of electromagnetic energy in some volume V occupied by the oscillatory circuit, the linear dimensions of which are L, requires the production within that space of electric and magnetic fields (E and H). It is absolutely appropriate to pose the question of the maximum allowable energy density, which determines the limits of circuit loading. On the basis of the assumptions that the oscillating system operates in air at atmospheric pressure, with a breakdown potential of $U \approx 30{,}000$ volt/centimeter, and taking the coefficient of safety to be equal to 0.15, Brillouin [1] determines the density of energy by the formula

$$A_1 = \frac{1}{8\pi}\ 15^2 \simeq 10 \text{ ergs/centimeter}^3 \qquad (1.1)$$

Consequently, the possible order of maximum energy storage by the system is given by the formula

$$A \ni = 10V \text{ centimeter}^3, \qquad (1.2)$$

In the process of operation a portion of the resonator energy is used up for useful emission and losses. The measures of energy dissipation are given by the quantities Q and τ, which are given by equations:

$$Q = \frac{\omega A}{W} \qquad (1.3)$$

$$\tau = \frac{1}{\alpha} = Q\frac{T}{\pi} \qquad (1.4)$$

Where ω is the angular oscillation frequency, A is the total energy of the system, W is the energy dissipated per cycle, α is the damping coefficient of the system, and T is the time of oscillation. Q is known as the "figure of merit" of the system and τ as the "time constant".

Energy dissipated per second is given by

$$\frac{dA}{dt} = \frac{\omega A}{Q} \approx 2\frac{A}{\tau} \qquad (1.5)$$

Assuming that for a good resonator $Q \simeq 3000$, i.e., that

Declassified in Part - Sanitized Copy Approved for Release 2012/04/09 : CIA-RDP82-00039R000200090009-2

1000T; then we have

$$\frac{dA}{dt} \approx \frac{V}{100T}, \tag{1.6}$$

if we take the above-given maximum energy density to be equal to 10 ergs/centimeter^3. For a given radiated power, for example, that of 100 watts (10^9 ergs/second), we can obtain the relationship between the volume of the circuit and its period:

$$V = 10^{11}T. \tag{1.7}$$

Assuming a cubically shaped resonator of linear dimensions L and wavelength λ we get:

$$\left(\frac{L}{\lambda}\right)^3 = \frac{10}{3\lambda^2} \tag{1.8}$$

where λ is in centimeters. The last relationship gives an idea of the nature of the oscillatory systems which can be used for a given radiated power. The following cases are possible:

If $\frac{L}{\lambda} \ll 1$ [insert at bottom of page precedes the next paragraph which follows]

which corresponds to decimeter waves, it is possible to employ systems with distributed constants in the form of two-wire or coaxial lines. For $\frac{L}{\lambda} \gg 1$, which corresponds to centimeter waves, it is necessary to employ cavity resonators (endovibrators), which operate on fundamental and harmonic frequencies (for $\frac{L}{\lambda} > 1$).

It is understood that for other values of radiated powers all of these relationships would be somewhat modified. For smaller

[which corresponds to waves of one meter and greater, it is plausible to use circuits with intermediate constants.

If $\frac{L}{\lambda} \approx 1$]

powers it is possible to employ lumped-constant circuits in the field of centimeter waves; as the power is increased, the situation reverses itself.

1.2 OSCILLATORY SYSTEMS WITH LUMPED CONSTANTS

In the microradiowave field a lumped-constant oscillatory circuit can only be used in instances when, for small apparatus dimensions, there is required a negligible oscillator power output. This takes place with low powered generating and receiving devices utilizing miniature "acorn" type tubes. The oscillating circuit can take the form of a coil, capacity being supplied by the inter-electrode tube capacitances. The linear coil dimensions (for $\lambda \lesssim$ 50 centimeters) are reduced to several millimeters.

A very significant factor limiting the possibility of utilizing closed circuit for ultra-high frequencies is the relative increase in the capacitive effects, which results in lowering the quality of the circuit: reduction of its resonance impedance Z_r, figure of merit Q and of the characteristic impedance $\rho = \sqrt{\frac{L}{C}}$. With the exception of a few and considerably obsolete applications involving power on the order of 0.01 and 0.1 of a watt, "coil"-type circuits are never encountered in the decimeter wave band.

A considerably greater role is played by oscillating lumped-constant systems, somewhat modified for the purpose of improving their parameters and boosting the radiated power. The general principle underlying these modifications can be stated to be the increase in conducting surfaces, the purpose of which is to reduce considerably the loss resistances and increase the dissipated power.

Figure 1.1

To serve as intratube oscillating circuits within the magnetron oscillators, the so-called "laminated circuits" were employed by Grekhovaya and Bovsheverov, which are used widely with magnetrons, as well as with some velocity-modulated generators. The capacity of the laminated circuit (Figure 1.1) is the capacity between the semicylinders a_1 and a_2, the inductance being provided by the wide lamination L, connecting these semicylinders. Such a circuit permits the obtaining of considerable power on rather short waves (on the order of several tens of watts for $\lambda \approx$ 30 centimeters). However, no general calculation for the laminated circuit was made, and in the bandwidth of about 5 to 50 centimeters it is possible, with satisfactory results, to use the empirical relationships derived by Grekhovaya and Bov-

Figure 1.2

sheverov. These relationships point to the dependence of the inherent frequency of the circuit on the ratio l_k/l_a (Figure 1.1) and on the area of the circuit winding S, which is given by the following formulas:

$$\lambda/\lambda_0 = 1 - a l_k \cdot \frac{l_k}{l_a}, \qquad (1.9)$$

where $a = 0.287$ and by

$$\lambda^2 = bS, \qquad (1.10)$$

where $b = 172$.

Figure 1.3

Here λ_0 is the natural wavelength of the circuit for which $\ell_k/\ell_a = 1$, and the other characteristics (b and h) are the same as those of a given circuit with natural wavelength of λ.

In figure 1.2 there are shown curves corresponding to the formulas (1.9) and (1.10), which may be used for speedier approximate design of laminated circuits.

Somewhat less satisfactory results are obtained by using these relationships in the design of "simple" and "double" laminated circuits of the type shown in Figure 1.3, which were used in our laboratory for tubes of simple design with retarding fields and a twin-grid modulator (refer to Chapter 5). The experience of our laboratory indicated that laminated circuits can well be set into oscillation with magnetrons for wavelengths up to 4-5 centimeters, with oscillating powers on the order of decimal fractions of a watt (3).

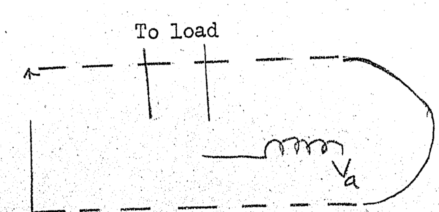

Figure 1.4

Another successful modification of the closed circuit was suggested by Kolster [4] for meter wave generators, but received a further application in the decimeter band. The axially-symmetrical Kolster circuit, shown schematically in Figure 1.4, consists of an axial metallic cylinder M upon which there are mounted the bell-shaped cups S_1 and S_2. The extremities of these cups have flat flanges, F_1 and F_2 which provide the capacity of the system, whereas the cups and the axis form the inductance. The entire circuit can be thought of as a figure of revolution about the axis OO' of the winding shown in Figure 1.5. The inductance of the cups represents the total parallel inductance of the separate windings of Figure 1.5. An approximate value of inductance of this circuit can be computed by means of the following formula of Kolster's:

$$L_{microhenry} = 0.33 \ell \cdot \log \sqrt{\frac{r_1}{r_2}} \qquad (1.11)$$

where ℓ is the length of the cylinder M in centimeters, r_1 is the inner radius of cups S_1 and S_2, and r_2 is the outer radius of cylinder M. The capacity of the circuit is given by Kolster as follows:

$$C_{\mu\mu f} = 0.45 \frac{D_o^2 - D_1^2}{a} \qquad (1.12)$$

where D_o is the outer and D_1 is the inner diameter, and a is the spacing between flanges F_1 and F_2. The method of connecting up this circuit is obvious from Figure 1.4. The effectiveness of circuits of this type is emphasized by their high figures of merit, which, according to Kolster, have Q's on the order of 1000, and, according to other meaasurements, Q's of approximately 200.

Figure 1.6

In the range of sub-meter waves, "spheroidal" circuits of this type were introduced by Hollmann (5), who developed several circuit modifications, permitting very convenient tube mounting and a simple oscillator construction. The bell-shaped cups of Kolster's circuit were replaced by Hollmann with the perfect hemispheres D_k (Figure 1.6). The oscillator circuit here consists of an axial cylinder R' - R'' having a diameter d, upon which are mounted the hemispheres S' and S'', terminated by the flanges F' and F'', of outer diameter D_f. The flange spacing a may be varied by moving the hemispheres along the axial cylinder. When the system of Figure 1.6 is oscillating, a voltage loop appears on the flanges, and a current loop in the middle of the cylinder. To divide the constant potentials applied to the hemispheres, an anode and grid of a tube are connected to the flanges, and the axis cylinder is split in half by a capacitor formed by plates F_i' and F_i''. The purpose of the remaining elements of the system is clear from Figure 1.6. Figures 1.7 and 1.8 show the constructional details of one-tube generators having spherical circuits: the first one with the RCA-834 tube operating on a wavelength of 1.5 meters, and the second one with an acorn tube, operating on a wavelength of about 80 centimeters.

In treating the spherical circuit as a lumped-constant circuit, Hollmann had arrived at the following formula for computing the natural wavelength of the circuit:

$$\lambda_{cm} = 5.7\, D_k \sqrt{0.0625\, D_k^2 \frac{(f^2 - 1)}{a} + 0.55\, D_k + C_r} \qquad (1.13)$$

where $f = D_f/D_k$, and C_r is the capacity of the tube. Applicability of this formula is illustrated by the graph of Figure 1.9, which shows experimental and theoretical values for the two circuits studied. If for quite wide flanges and small spacing a we neglect the capacities of the hemispheres and the tube, the natural wavelength of the circuit can be expressed approximately as:

$$\lambda_{cm} \approx 1.425\, D_k^2 \sqrt{\frac{f^2 - 1}{a}} \qquad (1.14)$$

For narrow flanges ($f \approx 1.2 \div 1.5$), however, these formulas do not hold well, in view of the appreciable effect of the hemispheres' capacity.

Constructional conveniences afforded by the sperical circuit are demonstrated by the following figures. The system of Figure 1.10 shows a generator with tubes placed inside the circuit. Due to the complete symmetry of the arrangement the number of tubes is limited only by the intracircuit space. Externally, this generator has a very simple and smart appearance -(Figure 1.11). Two other modifications of the spherical circuit are shown schematically in Figures 1.12 and 1.13. The last system is interesting from the fact that it permits symmetrical utilization of an even number of tubes operating in pairs every two cycles.

Figure 1.7 Figure 1.8

The oscillatory output of the spherical circuit can be taken off conductively as shown in Figure 1.4 or by lengthening the axial cylinder, thus forming a radiating antenna (Figures 1.8 and 1.11), or by means of a two-wire feeder coupled capacitively with the cups.

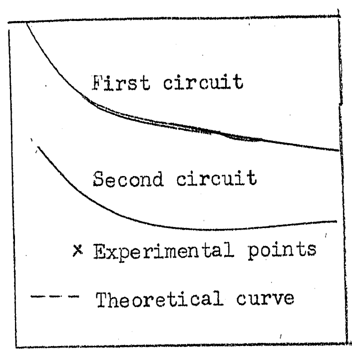

Figure 1.9

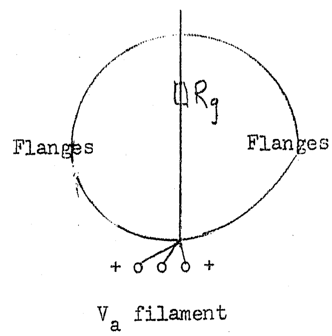

Figure 1.10

The spherical-type circuit, by virtue of its greater figure of merit than that of the "coil" and laminated circuits, found application also as an intratube circuit for the generation of centimeter waves, particularly with magnetrons. Results of the successful application of spherical circuits for the generation of centimeter

Figure 1.11

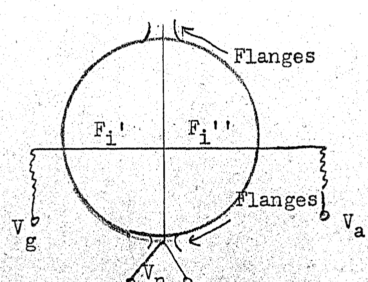

Figure 1.12

waves evidenced themselves in the following: reduction of the natural circuit wavelength for the same geometrical dimensions, increase in the dissipated circuit power, and improvement in the stability of generated oscillations. Figure 1.15 gives the idea of the electrode structure of a magnetron with the internal spherical circuit, designed by L. Dudnik [6], and Figure 1.16 shows the drawing of the entire magnetron tube with dimensions shown in millimeters.

Some of this magnetron data is given in Table 1. 1

A lumped-constant oscillatory circuit has recently been revived in its several original forms [7]. A basic sample is furnished by a circuit consisting of the usual variable condenser with an inductance consisting of a metallic strip fastened to a ceramic ring, which is mounted coaxially with the rotor of the condenser (Figure 1.17). The stator of the condenser is connected to one end of the strip, and the metallic contact fastened to the rotor slides along the strip as the rotor is turned, covering a 270-degree arc. Simultaneously with the increase in capacity, the length of the strip within the circuit increases. With this design, as the capacity is varied from 12 to 85 micromicrofarads, the inductance changes from .014 to .099 microhenries, which makes it possible to cover the frequency band of 55 to 400 megacycles. In order to avoid any resonance phenomena due to the part of the strip behind the contact, it can be connected to the rotor of the condenser. Such connection is employed in another circuit design shown in Figure 1.18. There the capacity is varied by means of an eccentric head, which serves as the rotor of the condenser. This model covers a considerably greater frequency band, from 400 to 1600 megacycles.

Figure 1.13

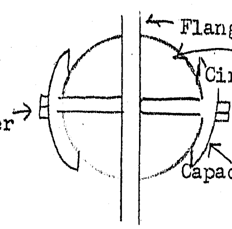

Figure 1.14

Figure 1.15

Figure 1.16

Table 1.2

CHARACTERISTICS OF THE BUTTERFLY CIRCUIT

	Minimum Frequency	Maximum Frequency
Frequency	220 megacycles	1100 megacycles
Inductance	0.011 microhenry	0.0041 microhenry
Capacity	48 micromicrofarads	5 micromicrofarads
Q	650	300
$R = \omega L/Q$	0.023 ohms	0.095 ohm
$\sqrt{L/C}$	15.2 ohms	28.6 ohms
$Z = Q\sqrt{L/C}$	9800 ohms	8600 ohms

Table 1.1

CHARACTERISTICS OF INTERNAL CIRCUIT MAGNETRONS

	Plate			Electrode	Cathode		Circuit			Circuit	Working parameters					λ centi-	Power
Tube Number	d_a	l_a	h	material	d_h	l_h	D_f	D_k	a	conductor	I_f	U_f	U_a	I_s	H	meters	watts
1	4	10	0.4	Mo	0.2	14	24	20	2	Cu	3.8	2.1	850	20	900	11	
2	4	10	0.4	MO	0.2	14	24	20	2	Cu	3.5	2.0	830	10	1250	12	
3	4	10	0.4	Mo	0.2	14	20	20	2	Cu	3.9	2.9	560	25	800	13	

Note: I_f is in amperes; U_f, volts; U_a, volts, I_s, ma; H, volts.

Another and possibly more efficient design provides for a tuning system without sliding contacts. The inductance is shown both as a non-closed (Figure 1.19) or closed (Figure 1.20) strip, to which are connected the plates of the stator of the condenser, in the form of metallic sectors. The principle of tuning of these systems is clear from Figures 1.21 and 1.22. These circuits are of the "semi-butterfly" (Figure 1.19) and "butterfly" (Figure 1.20) types. The first circuit has a tuning range of 400 to 1200 megacycles, and the second circuit that of 220 up to 1100 megacycles. The latter has an outside diameter of 2.5 inches $\cong$ 62 millimeters and is characterized by the following data [see Table 1.2].

The inductance of the butterfly circuit shown in Figure 1.20 can be determined approximately by the formula

$$L = \frac{\pi^2}{6}(r^2 - r_1^2)\left[\frac{1}{t+w} + \frac{1}{\sqrt{r^2 - r_1^2}}\right] \text{ cm} \qquad (1.15)$$

where r is the inner strip diameter, r_1 is the outer rotor bearing radius, and t and w are the respective thickness and width of the strip (all in centimeters).

A photograph of one of the smaller types of butterfly circuit design for a frequency band of 900 to 3000 megacycles is shown in Figure 1.23, where next to it, for comparative purposes, are shown an acorn tube and a detector.

The extreme simplicity and solid mechanical design of circuits of this type, together with good performance characteristics, afford the opportunity for widespread utilization of such lumped-constant circuits, especially for measuring apparatus.

Figure 1.17

Figure 1.18

1.3 OSCILLATING SYSTEMS WITH DISTRIBUTED CONSTANTS

Oscillating systems with distributed constants in the micro-radiowave field are represented by twin-conductor and coaxial lines or by coils, the dimensions of which are comparable with the wave-lengths (intratube grid circuits). One of the most characteristic parameters of a line is its characteristic impedance, given by formulas:

$$\rho = 120 \log (b/a) \qquad (1.16)$$

(for a twin-conductor line, Figure 1.24 a)

and

$$\rho = 60 \log (b/a) \qquad (1.16)$$

(for a coaxial line, Figure 1.24b)

Figure 1.19

Figure 1.20

Figure 1.21

Figure 1.22

The problem of the natural frequency of a line has many solutions. For a no-loss line of characteristic impedance ρ, with a complex input impedance Z_0 and terminated resistively or capacitively, the natural resonant frequency is determined from the relationship:

$$\frac{1}{Z} = \frac{1}{iZ_o} + \frac{1}{i\rho \tan\alpha l} = 0 \qquad (1.17)$$

where Z is the total impedance of the system, $\rho \tan \alpha l$ is the input impedance of the line, $\alpha = \frac{2\pi}{\lambda}$ is the phase constant, and l is the length of the line. From this relationship it follows that:

$$Z_o = - \rho \tan \alpha l \qquad (1.18)$$

For the frequently encountered case of a capacity C_o connected in the input of the line (usually the tube capacity) this equation leads to the well-known Kirchoff-Abraham formula:

$$\frac{2\pi l}{\lambda} \tan \frac{2\pi l}{\lambda} = \frac{C_1 t}{C_o}, \qquad (1.19)$$

from which it is possible to determine the values of λ, the natural wavelength of the line, where C_1 is the per unit capacity of the line.

For a small initial capacity of the system, its basic wavelength is proportional to its length l. However, for a short line and considerable initial capacity C_o this linear relationship does not hold, and for a sufficiently small l, λ is given by the following formula:

$$\lambda = \frac{1}{2\pi} \sqrt{l \frac{C_o}{C_1}} \qquad (1.20)$$

Figure 1.23

This formula characterizes a system intermediate to a line with distributed constants and a closed Thomson circuit [8].

When studying such parameters as the resonant impedance and figure of merit of a line, we cannot assume a no-loss line, as is done in solving the problem of natural frequencies with sufficient practicial accuracy. It is necessary to take into account the actual resistance of a line, which per unit length of a pure copper line is given by the following formula:

$$R_1 = 83.2 \frac{\sqrt{f}}{a} 10^{-9} \text{ ohms/centimeter} \qquad (1.21)$$

for a twin-conductor line, and by formula

$$R_1 = 41.6 \sqrt{f}\left(\frac{1}{a} + \frac{1}{b}\right) 10^{-9} \text{ ohms/centimeter} \qquad (1.22)$$

for a coaxial line.

Here f is the frequency in cycles, and the values of a and b are the same as given by Figure 1.24. If the conductors of a twin-conductor line are closely spaced, R_1 increases and can be determined by multiplying the value obtained from the formula (1.21) by the "proximity coefficient", which depends on the relationship b/a, and is determined from the graph of Figure 1.25.

Figure 1.24

A uniform resonant line, which is equivalent to a parallel circuit and has a large input impedance, can be short-circuited at the output and thus have a length equal to an odd number of quarter wavelengths, or open circuited at the output, with a length equal to an even number of greater wavelengths.

In both cases, and on the basis of the transmission line voltage and current equations, the resonant impedance of the transmission line is given by the formula:

$$Z = \frac{8 \rho^2 f}{R_1 n c} \qquad (1.23)$$

Here n is the number of quarter wavelengths of the line, C is the velocity of light (Centimeters/second). Taking into account the values of the unit and characteristic impedances, we arrive at the following formulas of Z for the coaxial (1.24) and twin-conductor (1.25) lines:

$$Z_{coaxial} = \frac{11.11 \sqrt{f}\, b_{centimeters}}{n} F \qquad (1.24)$$

$$Z_{twin\ conductor} = \frac{23.95 \sqrt{f}\, b_{centimeters}}{n} G \qquad (1.25)$$

The factors F and G depend on the ratio a/b and are determined from the graphs of Figure 1.26. As is expected from formulas (1.24) and (1.25) the resonant impedance of the lines is proportional to the diameter of the outer conductor or the conductor spacing, and, to what is especially significant, the square root of the frequency. We note that at the same time, for circuits with lumped constants, the resonant impedance decreases with frequency, which circumstance emphasizes the advantage of transmission lines. Formulas (1.24) and (1.25) show that the resonant impedance of transmission lines may reach very high values. Analogously, the magnitude of the figure of merit Q determined by the usual method can be determined by the formula:

$$Q = \frac{2\pi f \rho}{R_1 c}$$

which for a coaxial line becomes:

$$Q_{coaxial} = 0.0839 \sqrt{f}\, b\, H, \qquad (1.27)$$

and for a twin-conductor line is given by

$$Q_{twin\ conductor} = 0.0887 \sqrt{f}\, b\, J. \qquad (1.28)$$

Here the factors H and J are also functions of the ratio b/a, shown graphically in figure 1.27. It is interesting to note that 2 is a maximum for b/a = 9.2, and that Q is a maximum for b/a = 3.6 (since it depends on the maximum value of the ratio ρ/R).

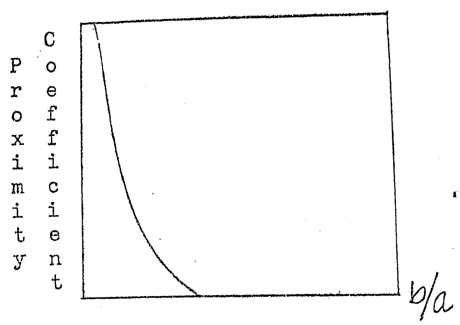

Figure 1.25

The given expressions point to the favorable possibilities afforded by long lines at ultra-high frequencies. For example, for a coaxial quarter-wave line having an outer diameter b of 1 centimeter, at a frequency f = 60 megacycles (λ = 5 centimeters) and b/a = 3.6, Q is equal to 650. As the outer diameter b is increased up to 10 centimeters, Q goes up to 6500. Increasing the frequency to 600 megacycles (λ = 50 centimeters) for the same b = 1 centimeter, gives a Q $\approx$ 2000. The actual values of Q are, of course, somewhat lower than the calculated values due to unaccounted radiation and other losses; however, in this case we deal with values of Q common to quartz crystal oscillators. These circumstances determine the possibility of employing coaxial lineas as stabilizing devices at ultra-high frequencies, the basus of which was laid in the meter wave region (9)

F - Coaxial

G - Twin Conductor

Figure 1. 26

If in meter-wave band devices, it is possible to distinguish a special stabilizing system along with the basic oscillatory circuit, then in the sub-meter-wave band such a stabilizing system coincides both structurally and electrically with the basic oscillatory circuit. The employment of resonant lines in this case becomes especially convenient and affords an opportunity for comparatively simple and at the same time mechanically sound generator design. Even the supports can be made in the form of "metallic insulators", i.e., of quarter-wave lines having an almost infinite impedance at the resonant frequency. Due to its considerable charging capacity $C_1 \ell$ the energy stored by the line $(C_1 \ell U^2)/2$ might be considerably greater than that of a lumped-constant circuit of the same frequency. This circumstance was made use of by Rohde and Schwarz (10) in the design of the original spark generator, and subsequently numerous investigators employed resonant lines as a circuit element or even as the component of the thermionic system. It is natural that the most successful application is that of the coaxial and not of a twin-conductor line. A good example is Barrow's generator (11), which is a feed back oscillator employing a special ultra-high frequency tube (type 316A or the 955 "acorn" type). This circuit is shown in Figure 1.28. This oscillator has tuned circuits in both of the filament wires, and a grid-plate system in the form of coaxial lines with movable stubs.

Figure 1.27

For a further increase in frequency the resonant circuit should be coupled more tightly with the electrodes of the electron tube that excites it, in order to utilize fully the advantages of a distributed-constant system. The first design of a tube with a coaxial resonant line was suggested by Muromtsev and Noble (12) as early as 1932. This high-power tube (up to 16 kilowatts), the circuit of which is given in Figure 1.29, operated on a wavelength $\lambda \approx$ 2.8 meters. Pfetschev and Müller(13) made use of this idea in the submeter wave band, introducing a resonant coaxial line inside the tube and operating on wavelengths from 80 to 20 centimeters. Rice's magnetron (14) operated on a wavelength $\lambda \approx$ 4.8 centimeters and has electrodes which represented the immediate extension of the exterior coaxial line. The various designs of electron-beam generators widely employ resonant coaxial lines (designs of Katsman (15), Grekhovoy and Ashbel (16), and others).

Figure 1.28

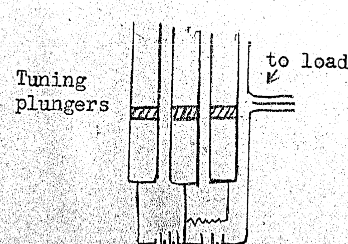

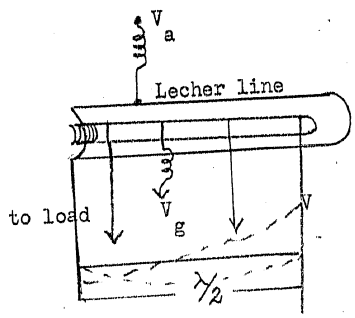

Figure 1.29

All this testifies to the availability to present-day ultra-high frequency technology of highly extensive and far reaching possibilities of employing long lines, especially coaxial ones, for oscillatory and frequency-stabilizing systems.

1.4 CLOSED-CAVITY OSCILLATING SYSTEMS

A desire to create a high-quality oscillating system, easily energized and capable of dissipating considerable power and conveniently coupled to the electron stream, has led in recent years to the practical realization of an old idea: obtaining and utilization of an oscillating electromagnetic field within a closed conducting surface. Starting with Maxwell's equations, it can be shown that within a cavity of highly conducting material, for certain conditions, there is set up a certain spacial standing-wave pattern. In view of this, a closed surface must possess resonant characteristics and be equivalent to some oscillatory circuit. Such "volume" or "space" resonators might be made to any geometric shape. To the simplest of these shapes (sphere, cylinder, prism, parallelepiped) correspond the simplest configurations of electric and magnetic fields described by the rigorous solutions of the Maxwell's equations. The more com-

Declassified in Part - Sanitized Copy Approved for Release 2012/04/09 : CIA-RDP82-00039R000200090009-2

plicated shapes of cavity resonators are subject only to an approximate analysis. Electric cavity resonators are analagous to Helmholtz's acoustical resonators, and the mathematical theory underlying the latter is, to a certain extent, useful in the study of the electrical systems. The usual purpose of computations on such oscillatory systems is the determination of their natural resonant frequencies and certain other characteristic parameters. The most important of these parameters are the figure of merit Q, characteristic impedance ρ, and the resonant impedance Z_r. Besides the immediate application and solution of Maxwell's equations[17] in the study of cavity resonators, there are also employed methods of reducing the resonator to an equivalent Thomson type circuit[18], or to an entire network of closed oscillatory systems.

Spatial oscillatory circuits, which are in the nature of closed conducting surfaces within which there is set up a high-frequency electromagnetic field, are frequently called "endovibrators" to distinguish them from the open type systems -- "exovibrators" which have external electromagnetic fields which are radiated in space. The term "endovibrator", which was introduced by Neyman[19], is quite appropriate since it corresponds well to the actual phenomenon. We shall employ this term in our future exposition.

In the design of endovibrators there are observed a number of features which result in considerable reduction of losses due to Joule's effect and dielectric hysteresis and almost do away with losses due to radiation, as well as the formation of external fields. Actually, the conducting surfaces of an endovibrator can be made quite large, especially at the points of current loops.

The adequacy of mechanical construction makes it possible to get by without the insulating elements, analagous, for example, to coil casings in the conventional circuits. The complete continuity of the endovibrator surface can be broken only for the purpose of establishing the following two necessary corrections: coupling to the energy source, and to the load. Due to the negligible attenuation of the system both of these couplings may be very loose; the other couplings are practically zero in view of "self-shielding" of the system. Due to this, the external surface of an endovibrator remains free of oscillatory currents and voltages, which is very convenient in electrical and purely structural respects. All of the cited endovibrator advantages coupled with the variety of their geometrical shapes yield the possibility of highly effective utilization of these systems in microradiowave technology.

Figure 1.30

The most elementary are the "convex endovibrators" having the shapes of a sphere, ellipsoid, cylinder, prism, parallelepiped, etc., (Figure 1.30). Fields that are set up as a result of oscillations within endovibrators of simple configurations can be qualitatively visualized quite simply and descriptively. Figures 1.31 and 1.32

Figure 1.31

Figure 1.32

depict the fields set up during oscillation of the simplest types of spherical cavity resonators.

Figure 1.31 shows the case of "oscillations of the first order":

a is "the fundamental"; b is "the harmonic". The magnetic field lines are shown by solid lines, while the electric field lines are shown dotted. The conduction current flows around the inside surface of the sphere in the direction of its meridians. The case of "oscillations of the second order" is shown by the closed lines of force (Figure 1.32), i.e., by the absence of charge on the inner surface of the endovibrator.

In analagous fashion it is possible to represent the oscillations of the "first" and "second" order within endovibrators of cylindrical, rectangular and other shapes. Cavities of such simple shapes, especially the parallelepiped and cylinder, have been employed predominantly for measuring purposes, or as oscillatory systems energized by tubes placed inside of them. However, the operation of electron-beam generators and amplifiers requires a tighter coupling of the endovibrator with the electron stream, which imposes certain specific requirements upon the endovibrator design of which the basic ones are as follows:

(a) A sufficiently high resonant impedance Z_r on the order of 10^5-10^6 ohms. This follows from the fact that the amplitude of the oscillatory potential set up within the circuit is given by the equality

$$V_1 = I_1 Z_r.$$

Since the order of magnitude of $V_1 \approx 1000$ volts for $I_1 \approx 10$ milliamperes, then Z_r is in the order of 10^5 ohms.

(b) The length of the path travelled by the electrons across the electric field of the endovibrator should be so small that the electron transit time should not exceed the time of half a cycle, otherwise it will result in the worsening of power interactions. This means that the separation between the endovibrator walls in the region of electron flow should not exceed $\frac{v}{c} \cdot \frac{\lambda}{2}$, where c is the velocity of light and v is the electron velocity [20].

In regard to the parameters Q and Z_r, cavity resonators of the simplest forms fully satisfy the first requirement; however, the fulfillment of the second requirement is connected with entirely natural difficulties, the nature of which is obvious from Table 1.3, which gives certain data relative to simple shapes of endovibrators.

The quantity δ represents the surface attenuation by the walls and is given by the relationship

$$\delta = \sqrt{\frac{\rho}{\pi \omega}} \qquad (1.29)$$

where ρ is the specific resistivity of the material in $\frac{\text{ohms} \cdot \text{centimeters}}{\text{centimeters}^2}$, and ω is the angular velocity of the field.

[See next page for Table 1.3]

Thus, in actual practice, for the most advantageous constructional and electrical coupling of the oscillatory system to the electron stream, it becomes necessary to complicate the shape of endovibrators, settling upon such variants, which, while being convenient from the standpoint of the second requirement, satisfy the first requirement to a considerably lesser degree.

Table 1.3

SOME DATA ON ENDOVIBRATORS OF SIMPLE SHAPES

	Square Prism	Right Cylinder	Sphere
	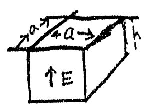	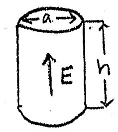	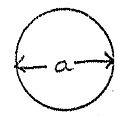
Natural wavelength	1.41 a	1.31 a	1.14 a
Q	$\frac{0.353\lambda}{\delta} \cdot \frac{1}{1+\frac{a}{2h}}$	$\frac{0.383\lambda}{\delta} \cdot \frac{1}{1+\frac{a}{2h}}$	$0.318\frac{\lambda}{\delta}$
Z_r	$170\frac{h}{\delta} \frac{1}{1+\frac{a}{2h}}$	$185\frac{h}{\delta} \cdot \frac{1}{1+\frac{a}{2h}}$	$104\frac{\lambda}{\delta}$
Q for = 10 centimeters; copper walls; a = h	24,100	26,200	26,500
Z_r in ohms for the same conditions	$6.67 \cdot 10^6$	$7.88 \cdot 10^6$	$8.63 \cdot 10^6$

For copper and wavelength of λ = 10 centimeters this relationship holds:

$$\frac{\lambda}{\delta} = 8.32 \cdot 10^4$$

The basic more complicated types of endovibrators actually employed are shown in Figure 1.33. Figure 133a shows the "biconical" construction which represents a sphere with two inset cones having their vertices in the center of the common axis. In order to pass the electron stream, the vertices of the cones should be slightly truncated and covered with grids, which influence the flow of electrons. Mutual proximity of these truncated vertices insures the concentration between them of the basic portion of the electric field of the system, which is very convenient in view of a number of circumstances:

Figure 1.33

(a) It is most efficient to couple the electron stream at the point of the electric field maximum.

(b) for variable spacing of the grids of the truncated vertices, the system can be tuned at the expense of varying its lumped capacity.

(c) the presence of lumped capacity simplifies the determination of the natural wavelength of the system, allowing us, to a first approximation, to employ Thomson type formulas.

The remainder of the types of endovibrators shown in Figure 1.33 essentially satisfy the same requirements. Shape b represents the same "biconical" type with cylindrical lateral surfaces, c is a "bicylindrical" endovibrator and d is a "toroidal" one.

All of these forms are characterized to a greater or lesser degree by the above mentioned properties.

It is interesting to note that the bicylindrical endovibrator (Figure 1.33 c) represents a transition stage of continuous transformation of a cylindrical resonator into a coaxial line, which can be attained by means of pushing into the cylinder a coaxial rod. Several phases of this transition are shown in Figure 1.34. The initial and final phases of this transformation -- a hollow cylinder (I) and a closed coaxial line (VI) are subject to an exact analysis; the analysis of the most interesting intermediate forms is more difficult. Their analysis can be performed by means of special approximate methods, or it is possible to undertake experimental research into their fields and parameters. In actual practice such oscillatory systems are very convenient from the structural standpoint and have found rather wide applications in wavemeters and dielectric constant measuring systems [21,22].

A toroidal endovibrator (Figure 1.33 d) can be visualized as a surface of revolution as a result of revolving a turn of wire attached to plates of a condenser (Figure 1.35) about an axis passing through the center of the plates. In view of the rather sharp separation of the electric and magnetic fields in this system, its

Figure 1.34

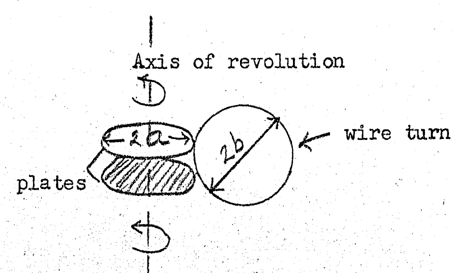

Figure 1.35

natural wavelength may be, to a first approximation, computed by Thomson's formula, which, taking into account the notation of figure 1.35, assumes the following form [23]:

$$\lambda_{o(\text{centimeters})} = 2\pi a_{(\text{centimeters})}\sqrt{\frac{\pi b}{2d(1 + \frac{a}{b})}} \qquad (1.30)$$

The characteristic impedance of this system is given by

$$\rho_{(\text{ohms})} = 60\frac{b}{a}\sqrt{\frac{2\pi d}{a + b}} \qquad (1.31)$$

The ohmic resistance for the case of copper shell is given by

$$R_{(\text{ohms})} \approx 4.55\cdot 10^{-3}\,\frac{1}{\sqrt{\lambda_{(\text{centimeters})}}}\left(\frac{1}{4\pi} + \frac{b}{a + b}\right) \qquad (1.32)$$

The figure of merit of a toroidal endovibrator is determined from formulas (1.31) and (1.32) and for a copper shell is given by the expression

$$Q = \frac{\rho}{R} = 1.658\cdot 10^{5}\,\frac{b}{a}\sqrt{\frac{2\pi d\lambda}{b + a}}\left(\frac{1}{1 + \frac{4\pi b}{a + b}}\right) \qquad (1.33)$$

Toroidal endovibrators permit the most varied toroidal cross-sections, which allows a continuous transformation between the two basic forms: toroidal, bicylindrical with two axial rods and capacity between them; biconical with spherical surface and biconical with a cylindrical lateral surface.

In conclusion, there is cited the Table 1.4 (page 31) of data characteristic of the more complex forms of endovibrators.

Figures given in Tables 1.3 and 1.4 relate to perfect closed systems. In actual operation, due to losses introduced by the necessary couplings and connections, the values of Q and Z are lower, remaining, however, considerably in excess of Q and Z_r of the conventional oscillating systems and even of quartz oscillators.

[See next page for Table 1.4]

The simplest type of endovibrator external coupling is a simple aperture, through which there is radiated the electromagnetic energy of an oscillating endovibrator, or through which it absorbs the outside energy. Such an aperture represents a unique "diffraction" type of antenna [24,25]. By means of such an aperture, for example, it is possible to couple the circuits of a klystron (Figure 1.36).

The coupling of endovibrators with a source of energy or the load may be effected, in the main, by the same means, as the coupling

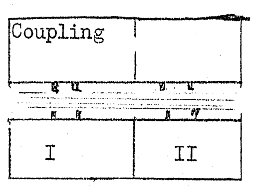

Figure 1.36

Figure 1.37

of the usual oscillatory systems, i.e., by one of the methods shown in Figure 1.37. The case a of figure 1.37 corresponds to inductive coupling, b to capacitive coupling and c to tap coupling. The magnitude of the coupling coefficient and the equivalent coupling

Table 1.4

SOME DATA ON THE MORE COMPLEX TYPES OF ENDOVIBRATORS

	Biconical endovibrator	Toroidal endovibrator	Bicylindrical endovibrator
Natural wavelength	(full cones) 2a	$2\pi a\sqrt{\frac{b}{2d(1+\frac{a}{b})}}$	$\backsim$1.2 a
Q	0.1095 λ/δ Optimum θ = 34 degrees	$3.316\cdot 10^5 \frac{\pi^2 b^2}{a+b(4\pi+1)}\sqrt{\frac{2\pi d}{a+b}}$ (copper walls)	0.04 λ/δ
Z_r	32 λ/δ Optimum θ = 9 degrees	$19\cdot 10^6 \frac{b^3}{4\pi ab+a^2}\left(\frac{2\pi d}{a+b}\right)$ (copper walls)	3 λ/δ
Q for λ = 10 centimeters (copper walls)	9120	3700	3000
Z_r in ohms for the same	$2.66\cdot 10^6$	$9.5\cdot 10^5$	$2.5\cdot 10^5$

resistance depend on the area of the coupling loop in case a, upon the length and location of coupling wires in case b, and upon the choice of points A and A_1 in case c.

However, when the problem deals with the joint operation of an endovibrator with a vacuum tube, or in general with some thermionic system, it stands to reason to speak not about connection, but of the more general idea of coupling the endovibrator to the thermionic system, mainly with the electron stream. The endovibrator might be looked upon as an element external to the thermionic system, connected to it by one of the above-mentioned methods, or as an element directly coupled to the electron stream, and is partially or fully evacuated. There can also take place such intermediate cases as: the tube electrodes might be regarded as the extension or supplement of some of the endovibrator components, or the endovibrator, if not evacuated, is coupled directly to the electron stream through the glass of a thermionic tube placed in the region of the maximum electric field of the system.

All of these variants are widely employed in present day ultra-high ffequency technology, and in actual practice it frequently happens that the most convenient oscillatory systems are these which contain resonator elements of various types. We shall dwell upon them in the next paragraph, citing here several examples of endovibrator applications.

(a) An endovibrator, externally coupled to a vacuum tube, has been used for a long time in the meter wave band, mainly, as a stabilizing system. An example of this is furnished by Neyman's generator shown in Figure 1.38, wherein a toroidal endovibrator of considerable

Figure 1.38

dimensions (indicated in millimeters on the drawing) is energized by a conventional twin-tube circuit, and by varying the condenser capacity it is possible to cover a wave band of 3 to 8 meters.

(b) Employment of the endovibrator as a conventional circuit in a variety of "3-point systems". In connecting the tube electrodes

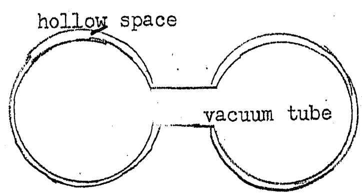

Figure 1.39

to the appropriate points of an endovibrator, it is possible to obtain the usual (for vacuum tube generators) selection of the limiting circuit resistance and thus obtain a conventional generator system. Examples of such systems are given in Figures 1.39 and 1.40. In the first instance a tube is mounted within a toroidal endovibrator. The anode and grid are connected to the inner surface of the endovibrator near points of maximum potential difference, the cathode is conducted through a tuning line, the point of contact of the inner conductor of the line with the toroidal surface being movable (conductor moved along the hollow space within the toroidal surface). The idea of the second design is identical, the only difference being in the use of a cylindrical instead of a toroidal endovibrator.

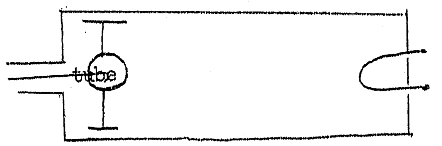

Figure 1.40

(c) A cylindrical cavity open at one end may serve as a resonator and a filter for pertinent frequencies. Thus, with the aid of the 368A type vacuum tube, operating on a second harmonic, it is possible to obtain waves of $\lambda \approx$ 9-10 centimeters, if a generator operating on its fundamental frequency is placed inside a waveguide tuned for $\lambda \approx$ 9-10 centimeters (6.3-7.6 centimeters in diameter), as is shown on Figures 1.41 a and b.

(d) Tighter coupling between the oscillatory system and the electron stream can be obtained by designs providing for intratube grids only for the purpose of setting up electric fields in the path of the electron stream. One of the examples of such a design is furnished by Katsman's tube (26), inside of which and along the path of the electron stream there are located two pairs of grids terminated by ferro-chromium rings, by means of which contact is effected with the walls of rectangular endovibrators, wherein, in the appropriate opening, a tube is inserted (Figure 1.42). Such a combination of the endovibrator and a tube affords the possibility of speedy replacement of the latter without interruption of the operation of the entire device.

(e) Finally, the introduction in the microradiowave practice of "resonant tanks" and "klystrons" led to systems wherein the electron stream is coupled directly to the endovibrator and the latter

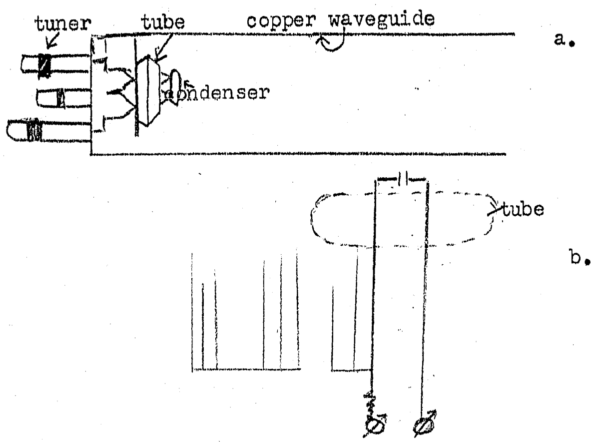

Figure 1.41

Figure 1.42

represents an integral part of the electron tube. In the first publication on the "resonant tank" (27) it was mentioned superficially that "its oscillatory circuit represents a hollow resonator, organically coupled to the retarding field energizing tube". Further on, however (28), its basic secret was disclosed and construction

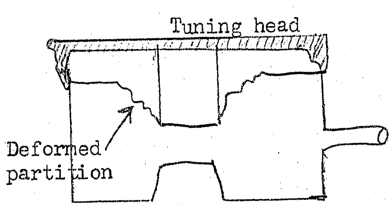

Figure 1.43

Figure 1.44

proved to be basically analagous to that of the "reflex klystron". The essence of the latter is the placing inside a tube of a toroidal or bicylindrical endovibrator, across the electric field of which passes a stream of electrons which is later "reflected" from the retarding electrode, as is shown in Figure 1.43. Some trimming of the endovibrator may be accomplished by means of mechanical deformation of its partitions, which, in appropriate places, might be crimped.

In an analagous manner the electron stream is coupled with the endovibrator in a more complicated klystron design of the Varian (29) brothers, the principal current of which is shown in Figure 1.44. The presence within it of two oscillatory circuits, with feedback between them, imposes rigid conditions on the precision of their mutual tuning. For circuits with high figures of merit

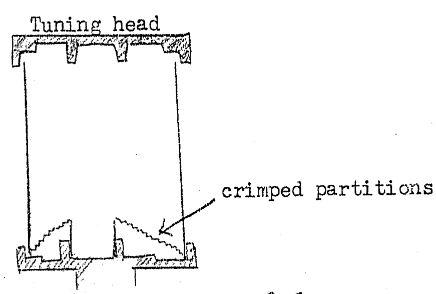

Figure 1.45

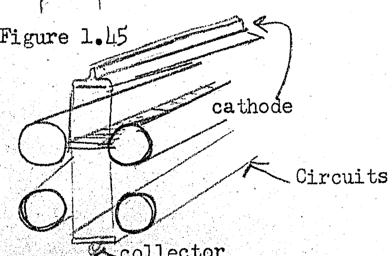

Figure 1.46

mistuning may occur as a result of the slightest manufacturing inaccuracy or temperature deformation. The width of the gap between the grids must be maintained constant with a precision of 0.001 centimeters, which requires the adoption of special measures for circuit trimming. The most convenient method of trimming is presented by controllable deformation of resonator partitions as shown in Figure 1.45.

Finally, in order to increase the oscillatory power without a change in frequency, there was suggested a modification of the toroidal endovibrator, which consists of shaping it in the form of long cylinders, with the further possibility of rolling them into a ring [30], (Figure 1.46).

In many of the examples discussed, the design of the instruments, as well as their operation is made complicated by the necessity of hermetical sealing of considerable metallic surfaces with the glass portions of the tube. A simple burning out of the filament meant the interruption in service of the entire instrument, thus making it more difficult and expensive to replace tubes. Therefore, it is natural to attempt to couple the electric field of the endovibrators with the electron stream "through the glass of the tube", making the tube and the endovibrator as two mechanically independent components. An example of such a design is furnished by Haeff's [31]

circuit

Figure 1.47

velocity-modulated amplifier, shown schematically in Figure 1.47. In it the ultra-high frequency signal to be amplified is applied to a grid, which controls a narrow beam of electrons. This electron beam passes through a gap within a bicylindrical endovibrator where there takes place the interaction of the beam with the high frequency electric field. With this arrangement the tube is frequently simply mounted inside the circuit, and, therefore, may be easily replaced. The oscillatory circuit itself permits simple tuning for a given frequency independently of the tube.

The design advantages of such a system of circuit and tube coupling are obvious, in view of which a number of theoretical and experimental attempts have been made to apply it to the energizing of double- as well as single-circuit klystrons, which, however, did not receive adequate develo ment in view of the simultaneous progress in tube and "circuit" technology, which resulted in the development of certain "combination" systems, to be dealt with in the concluding paragraph of this chapter.

1.5 NEWEST "COMBINATION" OSCILLATORY SYSTEMS

Our review of oscillatory systems employed in the microradiowave field should be supplemented by a discussion on the more interesting designs evolved during recent years, which frequently embody the elements of all of the basic types of oscillatory systems: lumped-constant circuits, long lines, and cavity resonators, all at the same time.

(a) In the US literature there is frequently used the term "tank circuit", which stands for a circuit similar to a resonant concentric line. One of the examples of this is furnished by an interesting design of a stable ultra-high frequency oscillator by Peterson (32), who employed such a "tank circuit" in conjunction with a special 316A type of tube, which operates on the conventional feed-back principle. The external appearance of this generator and a schematic circuit cutaway view are shown in Figures 1.48 and 1.49. As can be seen from these drawings, this circuit is similar to that of a bicylindrical endovibrator. Its inner conductor is in the form of a rod with a plunger, thus resulting in certain capacity with reference to the wall of the outer cylinder. The scheme of circuit mounting and load connections (R'_L) is shown in Figure 1.50. For the outside "tank" diameter of about 10 centimeters (4 inches) its capacity was equal to 130 micromicrofarads, and inductance to about .018 microhenries. In operating on a frequency of 100 megacycles (λ = 3 meters) the Q of the circuit was about 2500.

(b) A different example of the use of the term "tank circuit" is furnished by the work of Linder (33), who made a magnetron anode appear as a line short-circuited on one end, labeling it, however, as the "tank circuit anode".

The anode of Linder's magnetron represents merely an incompletely split cylinder, and it can be fashioned in the form of a strip of copper with a drilled cylindrical opening and a slit parallel to the cylinder's axis (Figure 1.51). A load is connected to the split cylinder ends. In order to generate wavelengths $\lambda \simeq$ 8-9 centimeters, the length of the cylinder slit was 2.3 centimeters, its

Figure 1.48

Declassified in Part - Sanitized Copy Approved for Release 2012/04/09 : CIA-RDP82-00039R000200090009-2

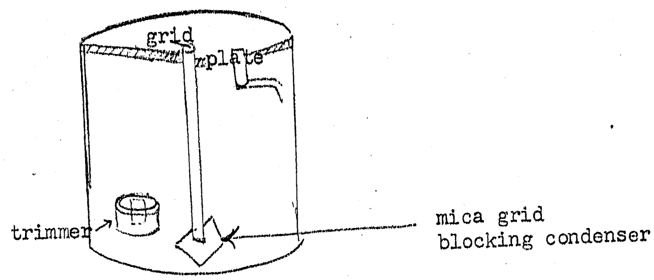

Figure 1.49

width about 0.06 centimeters, for a cylinder diameter of 0.7 centimeters. The considerable size and unit length capacity of the system permit it to dissipate considerable power, without increasing its natural wavelength. With tantalum anodes, the dimensions and design given, 20 watts of oscillator power was obtained at the operating anode temperature of 1800 degrees Kelvin and efficiency of about 22 percent. An output of 15 watts at 20 percent efficiency represents a condition obtainable with continuous tube operation. At the same

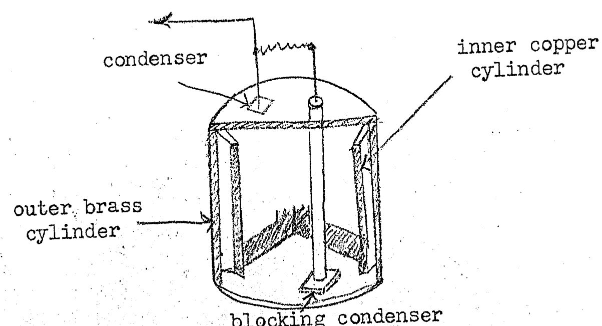

Figure 1.50

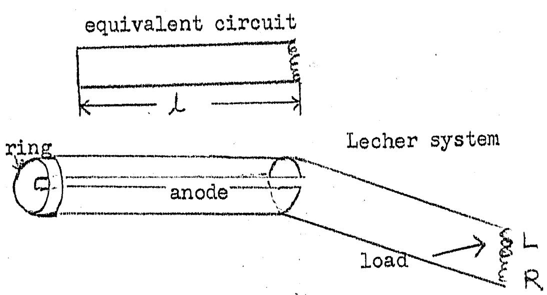

Figure 1.51

time power output obtained from a magnetron with a small anode and small laminated circuit did not exceed 2.5 watts at the same frequency.

(c) A "cylindrical circuit" (7) formed by two coaxially slit cylinders revolving one inside the other, as shown in Figure 1.52, which illustrates the method of tuning (position a corresponds to the maximum frequency and position b corresponds to the minimum frequency). Large resonant impedance is obtained at the inner surface of the outer cylinder, at which point the appropriate tube electrodes are to be connected. Figure 153a illustrates the method of mounting of the 6F4 acorn type tube. Appropriate cuts are made in the outer and inner cylinders, and the tube is mounted upon the outer cylinder in such a way that the grid terminals are taken out over

Figure 1.52 Figure 1.53

one cylinder cut, while the anode terminals are taken over the other cylinder cut (capacitive connection). The presence of the tube limits somewhat the possibility of rotation of the inner cylinder.

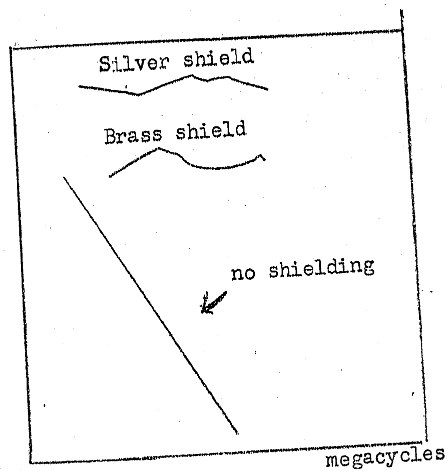

Figure 1.54

Figure 1.55

In shaping the inner cylinder appropriately we can obtain the desired frequency variation relationship. Thus, Figure 1.53b depicts the shape of the rotor for logarithmic law of frequency variation. As the capacity is varied, inductance of such a circuit remains practically constant and can be computed by means of the formula:

$$L_{centimeters} = \frac{1000\ a^2_{centimeters}}{(9a_{centimeters} + 10\ \ell_{centimeters})} \qquad (1.34)$$

where a is the inner radius of the outer cylinder, and ℓ is its length. A cylindrical circuit oscillator covering the bandwidth of

Figure 1.56

450 to 1050 megacycles (wavelengths of 66.7 to 28.6 centimeters) is

Declassified in Part - Sanitized Copy Approved for Release 2012/04/09 : CIA-RDP82-00039R000200090009-2

characterized by the following data: $a = 1$ inch, $\ell = 2$ inches, inter-cylindrical gap = 1/65 inch. Its inductance is about 0.01 microhenries, and the maximum capacity is 16 micromicrofarads, with 2 micromicrofarads being due to the tube capacities, 0.5 micromicrofarads due to the outer cylinder slit and 13.5 micromicrofarads due to the intercylinder capacity. The losses of such a circuit are due primarily to radiation, and the value of Q may be approximately determined by the formula:

$$Q = 0.4 \cdot 10^{12}/(9a + 10\ell)a^2f^2,$$

where f is the operating frequency in megacycles. Radiation losses, which increase with the frequency, can be reduced by good shielding as shown by the graphs of Figure 1.54, showing the relationship between Q and the frequency with no shielding, silver and brass shields. As is seen from these graphs, shielding insures good constancy of Q over the entire tuning band. In order to widen the bandwidth and create a multiband oscillator including, for example, the frequencies from 5-10 to 1000 megacycles, additional "bandchanging" coils can be added to the cylindrical circuit, resulting in its slight design modification, as shown in Figure 1.55.

(d) In conclusion it is interesting to mention the oscillatory circuits designed for a more convenient mounting of the so-called "lighthouse tubes", tubes with disc-shaped seals designed specially for operation with coaxial systems. Being an outgrowth of the above-described (Paragraph 1.1) "butterfly" type circuits, they represent an "inverted butterfly", wherein the inductance is connected to the rotor, and the stator is shorted by a conical support (Figure 1.56), or they represent a "coaxial butterfly" the principle of which is illustrated in Figure 1.57. The latter design is employed for feedback generators in the 1000-1300 megacycle band (wavelengths of 30-23 centimeters). Theccircuit is mounted between the plate and the grid of the "lighthouse tube" (Figure 1.58a) and, together with the tube, forms a portion of the inner conductor of the basic coaxial system. The field of the latter is coupled to the field of the circuit through lateral openings in the circuit (refer to Figure 1.57). The tuning of the system is effected by the movable plates p and c. Having set these plates in the optimum positions, it is possible to obtain a simple design shown in Figure 1.58b, where the feedback is controlled by the movable rod S.

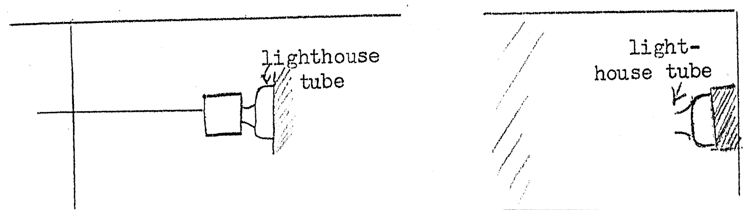

Figure 158

All of the described oscillatory systems herein, including the "butterfly" and "semibutterfly" circuits, are interesting from the standpoint of their simple and reliable mechanical design, as well as from the standpoint of their electrical characteristics, which are sufficiently good, in order to ensure a widespread utilization of these systems especially in laboratories and for measuring purposes. In conclusion we give a joint Table 1.5 (page 40) which characterizes the frequency stabilities of oscillators employing these circuits. The last column's stability factor represents the relative variation in frequency $\Delta f/f$ for a 2:1 change in the plate voltage. By the resonant frequency of the tube we mean the frequency at which the plate grid circuit is resonant as these terminals are short circuited.

Table 1.5

STABILITY TABLE OF THE NEW OSCILLATORY SYSTEMS

Oscillator frequency band megacycles	Tube type	Resonant frequency of the tube megacycles	Type of circuit	Operating frequency megacycles	Stability factor X10-6
50-250	316-A	700	"Semibutterfly"	50 100 200 250	100 250 1000 3000
250-1000	368-A	1900	Twin "butterfly" circuit connected to one tube	250 500 800 1000	200 360 850 1350
250-1000	703-A	1700	"Butterfly	250 500 800 1000	100 250 700 5000
1050-1350	464 ("light house" type)	--	Coaxial "butter-fly"	1050 1200 1350	1400 1700 4000
6-500	464 ("light house" type)	--	Cylindrical cir-cuit with band-switching coils	200 500	400 1500
500-1000	6F4	1400	Cylindrical cir-cuit	500 800 1000	180 1200 7000

CHAPTER I REFERENCES

1. L. Brillonin, Review of Physical Sciences, No 4, 1941
2. M. T. Grekhova and V. M. Bovsheverov, ZhTF, V, 69, 1935
3. A. N. Sus, Thesis, SGU, 1946
4. F. Colster, PIRE, 22, 1335, 1934.
5. H. Hollman, Hochfr. Elektroak. 50, 109, 1937
6. L. A. Dudnik, IEST, No 3, 1939, 32
7. E. Karplus, Gen. Rad. Exp. XIX, No 5, 1944; PIRE, 33, 426, 1945
8. V. I. Kalinin, Decimeter and Centimeter Waves, Svyaz'izdat, 1939
9. Collection of Data on Frequency Stabilization and Control, No 3, NIIS, October 1936
10. L. Rhode and H. Schwarz, Hochfr. Elektroak. 41, 207, 1933
11. W. L. Barrow, Rev. Sci. Instr. 9, 170, 1938
12. I. Muromtseff and H. Noble, PIRE, 20, 1328, 1932
13. O. Pfetscher and K. Müller, Phys. ZS. 35, 654, 1934; Hochfr. El. 45, 1, 1935
14. C. W. Rice, Gen. El. Rev. 39, 363, 1936
15. Yu. A. Katsman, IAN, Physical Series IV, 506, 1940
16. N. I. Ashbel', ZhTF, X, 1301, 1940
17. V. I. Bunimovich, ZhTF, IX, 984, 1939
18. M. Neyman, Electrosvyaz', No 4, 7, 1940
19. M. Neyman, IEST, No 9, 1, 1939; No 10, 21, 1939
20. E. Studenkov, UFN, XXV, 444, 1941
21. V. A. Patrushev, IAN, Physical Series IV, 571, 1940
22. C. Works, T. Dakin and F. Boggs, PIRE, 33, 245, 1945
23. M. Neyman, IEST, No 2, 33, 1940
24. M. Neyman, IEST, No 6, 1, 1940
25. A. Pistol'kors, ZhTF, XIV, 693, 1944

26. Yu. Katsman, Tubes for Ultra-High Frequencies, Doctoral thesis, LETI, 1945
27. Allerdings, Dällenbach, and Kleinsteuber, Hochfr. and Elektroak. 51, 96, 1938
28. W. Dällenbach, Hochfr. and El. 61, 161, 1943
29. R. Varian and S. Varian, Journ. Appl. Phys., 10, 321, 1939
30. V. Kovalenko, IAN, ch. fiz., 4, 449, 1940
31. A Haeff, Electronics, Febr. 1939, 30
32. A. Peterson, Gen. Rad. Exp. 12, 5, 1937
33. E. Linder, PIRE, 27, 732, 1939

Declassified in Part - Sanitized Copy Approved for Release 2012/04/09 : CIA-RDP82-00039R000200090009-2

CHAPTER II

REVIEW OF THE BASIC METHODS OF MICRORADIOWAVE GENERATION

2.1 BASIC METHODS OF MICRORADIOWAVE GENERATION

During their half-century existence radiophysics and radio technology underwent a course of unique, dialectical development. The first experimentally produced electromagnetic waves were the microradiowaves emitted by spark-discharge transmitters. Later on, after considerably lengthy retreat into the long wave region, as early as the 1920-1930 decades of this century, radiophysics, and, following it, radio technology, equipped with more refined devices turned back to the microradiowave band.

The contemporary history of microradiowaves begins with the work of a number of researchers in the 1920-1928 period. Discovery of electronic oscillations in triodes with retarding field by Barkhausen and Kurtz[1] and Zilitinkevich [2], and then in diodes placed in a magnetic field (magnetrons) by Slutskin and Shteynberg [3], Zacek [4] and Okabe [5], gave a stimulus to numerous further researches in this direction, which led, on one hand, to a detailed study of the physics of the phenomena, and, on the other hand, to the recently evolved special microradiowave technique (A detailed review of literature on electronic oscillations prior to 1939 and a more detailed exposition of the basic works are contained in my book, Decimeter and Centimeter Waves, Svyaz'izdat, 1939). Historical origins of the present day velocity-modulated instruments should be sought in the retarding field idea and in the numerous researches provoked by it into the electron dynamics of ultra-high frequency fields, and not in the electron beam tubes of the beginning of this century, as is being done my some authors (6) .

Simultaneously with the perfecting and development of the new types of electronic oscillationggenerators, there took place an increase in the band of frequencies generated by negative-grid triodes with conventional feedback arrangements. Utilization of specially designed tubes and appropriate oscillatory circuits permits at the present time the employment of the feedback principle for frequencies of about 3000-4000 megacycles, i.e., for wavelengths of 10-8 centimeters, which is very convenient in many instances.

Thus, in the waveband of interest to us we deal with the following basic methods of oscillation generation:

(a) A tube generator employing feedback and special tubes and circuits,

(b) Various types of the retarding field arrangement,

(c) A magnetron with several modes of oscillation,

(d) Various modifications of the velocity-modulated devices.

2.2 FEEDBACK OSCILLATORS

The classical feedback oscillator arrangement employs as its basic element an electron tube operating on the principle of static control of the electron stream, thus representing a practically inertialess electronic relay. The principle of static control may be explained briefly as follows: the grid of the tube exerts an electrostatic effect upon the space charge about the cathode, varying in

Declassified in Part - Sanitized Copy Approved for Release 2012/04/09 : CIA-RDP82-00039R000200090009-2

accordance with the changes of grid potential V_g, the current flowing through the tube from zero to its saturation value I_s. In a statically controlled tube the current cannot exceed its I_s value at any instnat, and at any point of the interelectrode space.

The inertialessness of the tube manifests itself in that the time of the alternation of potential at its electrodes is considerably greater than the interelectrode transit time. In view of this, the alternating grid potential, and the plate current controlled by it, vary in phase, and for the appropriate feedback connection, ensuring the out-of-phase relationship between the grid and plate voltages, the following oscillatory power being supplied to the tube's circuit:

$$P = \frac{1}{T}\int_0^T i_a u_a dt \tag{2.1}$$

The quantity P is a maximum for a phase difference between the plate current i_a and plate voltage u_a equal to 180 degrees ($P < 0$). Any violation of this phase relationship impairs the oscillatory output of the tube and lowers the efficiency of the process.

The conventional scheme of a triode oscillator can be employed in the ultra-high frequency range only with the observance of certain special conditions with respect to the tubes and oscillatory circuits. In tubes of the conventional types and dimensions, the effect of the electronic inertia becomes strongly pronounced already at frequencies in the order of 300 megacycles (λ = 1 meter). The time of the electron transit between the gris and the plate ceases to be a negligible quantity and is of the order of the time of the oscillatory cycle, in view of which there are violated the necessary phase relationships between i_a and u_a. The plate current is no longer in phase with the controlling alternating grid potential, but lags behind it by some phase angle ψ, which depends upon the "transit angle" of the electron between the grid and the plate

$$\theta = \omega \tau \tag{2.2}$$

This "transit angle" parameter θ, which is equal to the product of the angular velocity ω and the time of transit τ, represents a very convenient universal characteristic of electron inertia in a given thermionic system. The angle of lag of the plate current behind the control grid potential is determined not simply by the transit angle θ, but, based on the assumption of zero electron velocity at the grid surface, it is given by a fairly complicated function of θ (7)

$$\tan \psi = \frac{\sin\theta - \theta\cos\theta}{\theta\sin\theta + \cos\theta - 1} \tag{2.3}$$

For sufficiently large transit angles θ, there is liable to occur a reversal in the characteristics of the tube, leading to a 180 degree phase displacement between i_a and u_a without the benefit of feedback.

As the frequency is raised, in addition to the inertia of electrons, there takes place an increase in capacitive effects, which lowers the resonant impedance of the circuit. This latter circumstance in its turn requires an increase in the curvature of the tube characteristic, which is accomplished either by the more intensive filament operation, or, for all other factors being equal, by using a higher-emission cathode. The requirement of higher cathode emission is dictated also by the presence of noticeable displacement currents at ultra-high frequencies. Actually, let us assume a diode with minimum zero cathode potential. Since in this case no displacement current flows, and the instantaneous value of the total current in a closed circuit must be the same, then, obviously, the emission cathode current should be equal to the sum of the conduction and displacement currents in the plate circuit. These relationships are, of course, more complicated in the multielectrode systems, but the basic idea is the same.

Furthermore, since at the ultra-high frequencies, the tube becomes an element of the oscillatory system, of predominantly capacitive nature, it is necessary to reduce as much as possible the interelectrode capacities.

For a number of years attempts were made to generate submeter radiowaves by means of the conventional low-power oscillator tubes, employing distributed-constants circuits, or single-turn wire circuits. Results of these experiments showed that the lower limit of waves that can be generated by means of "conventional" tubes employing feedback, is about 80-100 centimeters.

By changing the tube design it is more or less possible to compensate for the deleterious effects of the above factors. One of the basic methods of a change in the tube design is the reduction of the tube dimensions. It can be shown that if all of the tube dimensions are reduced n times, then the curvature of the tube characteristic, the plate current and the amplification factor remain constant, whereas the values of the interelectrode capacities, lead-in inductances and the time of the electron transit also decrease n times. Unfortunately, however, the allowable plate dissipation and cathode emission decrease by a factor of n^2. Thus, a reduction in the tube dimensions without the appropriate reduction of electrode voltages is possible only at the expense of cathode emission and increase in the thermal anode stability. Analagous results are obtained with the increase of the difference in the tube electrode potentials, in order to reduce the electrode transit time without reducing the tube dimensions. These considerations are illustrated in Table 2.1, in which are listed the various changes in the tube parameters as the wavelength and tube dimensions are reduced down to 20 percent of their initial values, assuming the following:

(a) constant plate potential (the first column), (b) constant density of filament emission (second column), (c) constant power dissipation per unit of plate surface (third column),

[See next page for Table 2.1]

The most significant limitation is imposed by the allowable cathode emission. The present day special ultra-high frequency tubes are characterized by the employment of high emission cathodes (predominantly of the oxide type), and particularly of flat emitters. A very important design problem is presented by the dissipation of heat away from the plate and the grid of the tube. It is solved by making the grid out of very fine high-melting-point wire (tungsten, molybdenum) and shaping the anode in such a way as to ensure maximum dissipation of heat by conduction and radiation. There is widespread use of anodes in the shape of solid graphite pieces, an aperture or recess in which forms the anode proper.

Table 2.1

DEPENDENCE OF TUBE PARAMETERS UPON WAVELENGTH AND LINEAR TUBE DIMENSIONS

Parameter	Assumed to remain constant: V_a	I_{em}/S_f	P/S_a
	(in percent)		
Wavelength	20	20	20
Linear dimensions	20	20	20
Electrode potentials	100	12	28
Amplification factor	100	100	100
Interelectrode capacities	20	20	20
Lead-in inductances	20	20	20
Impedance of the circuit	100	100	100
Plate current	100	4	14
Curvature of the characteristic	100	34	53
Electron transit time	20	57	38
Input impedance	100	34	53
Cathode emission density	2500	100	360
Power dissipation density	2500	12	100
Oscillatory power output	100	0.5	4

In order to decrease the surplus and parasitic capacities and inductances, an entirely different lead-in construction is employed for the ultra-high frequency tubes. Instead of the conventional "legs" with "plates" where the platinum or molybdenum lead-in wires extend almost for a centimeter parallel to each other within the glass itself, thus forming considerable capacities, there are utilized lead-ins through "eyes" sealed directly into the glass bottom of a tube and located, whenever possible, perpendicularly to the lead-ins. In recent years use has been made of the so-called disc-shaped lead-ins, which provide for the convenient mounting of tubes with concentric lines coupled with the improvement in the electrode heat dissipation ("lighthouse" tube, refer below).

Let us look over a number of tube designs and oscillator circuits, which characterize present day progress in the field of ultra-high frequency application of the feedback principle.

To begin with, many various miniature tube designs were employed in the submeter waveband (approximately, for λ up to 25-30 centimeters). These tubes are represented by a number of makes of the "extremely close clearance" tubes, geometrically similar to the conventional types, with analagous lead-ins, and also by several types of acorn-tubes distinguished for their original lead-in connections. The latter are very short (Figure 2.1) and are located in the equatorial plane, which is the plane along which are welded the top and bottom portions of the tube. To this series belong the 955, 958 and 6F4 type triodes and the 954 type pentode. An idea of their parameters is furnished by Table 2.2.

Table 2.2

Parameters of Certain Tubes

Parameter	955 Triode	954 Pentode
Filament voltage	6.3 volts	6.3 volts
Filament current	0.15 amperes	0.15 amperes
Plate voltage	180 volts	250 volts
Control-grid voltage	--5.0 volts	--3.0 volts
Screen-grid voltage	--	100 volts
Plate current	4.5 milliamperes	2 milliamperes
Coefficient of amplification	25	--
Internal resistance	12,500 ohms	1.5 megohms
Mutual transconductance	2000 microhms	1400 microhms
Input capacity	1.0 $\mu\mu$ farads	3.0 $\mu\mu$ farads
Output capacity	0.6 $\mu\mu$ farads	3.0 $\mu\mu$ farads
Capacity, plate to control grid	1.4 $\mu\mu$ farads	0.005 $\mu\mu$ farads

A conception of one of the early forms of oscillator with acorn-tube is given by Figure 2.2.

More effective application may be made of miniature tubes and acorn tubes with the high-frequency circuits described in the first chapter, where several schematics are also given (see Hollmann's "spherical oscillator", Barrow's "tube oscillator", and oscillators with "cylindrical" circuits and "butterfly" type circuits).

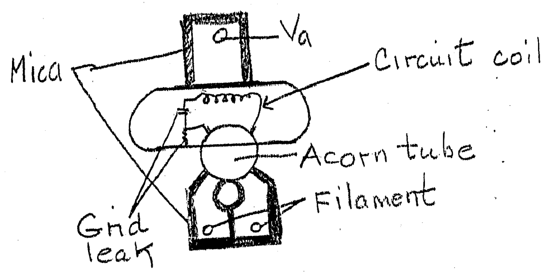

Figure 2.2

The power of the oscillations obtained with miniature tubes does not exceed tenths of a watt. From the standpoint of power, considerably better results are obtained with various special oscillator tubes (miniature tubes and acorn tubes were developed mainly for application to receiving apparatus). The prototype of a whole series of rather successful models was the 316-A tube [8], later somewhat improved by Tsvetovskiy and Dzhibelli [9]. In this type the fastening of the electrodes on thick straight outlet leads which pass directly through the glass base of the tube (Figure 2.3) calls for attention. The anode is a tantalum cylinder equipped with three plates which radiate and conduct heat away. The grid consists of tungsten wires located along the generatrices of the cylinder and fused to two wide rings on each side. The power ratings and efficiency coefficient obtained with this tube are illustrated in Figure 2.4, from which it may be seen that this tube develops more than 5 watts of oscillating power at a wavelength of about 50 centimeters with an efficiency of the order of

Declassified in Part - Sanitized Copy Approved for Release 2012/04/09 : CIA-RDP82-00039R000200090009-2

10 percent. By using a high-quality oscillator system it is possible to increase the efficiency and the stability of the oscillations of an oscillator which operates with a tube of this type. The Barrow "tube" generator (See Chapter 1, Section 2, Figure 1.28), developed for a range of 400 to 40 centimeters, serves as an example of a rather successful design of a laboratory oscillator such as this. The upper portion of the oscillator is a screening metal cylinder into which three concentric tuning lines are introduced: two of them tune the filament circuit and the third is the basic circuit included between the anode and the grid. All of the lines are tuned by pistons which move along them and are fixed at any position desired. The oscillating power is taken off by means of a coaxial line attached to the plate-grid circuit at some optimum point near the tuning piston. The operation of this generator with a 316-A tube is characterized by the following figures:

Frequency (megacycles)	700	500	300
Wave-length (centimeters)	43	60	100
Power (watts)	2	6	8
Efficiency (Percent)	5	20	25

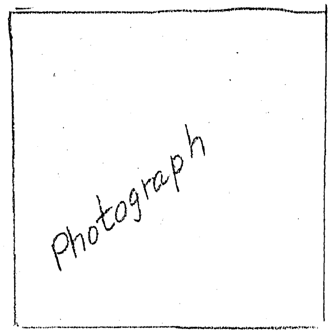

Figure 2.3

The plate dissipation of a tube of the type described may be increased by adding to it a "book-case structure" [10] (Figure 2.5): a number of parallel tantalum plates, from 4 to 12 in number, are located on a common holder and have semi-circular notches located one above the other, in which the grid and cathode are situated. The overall structure of the electrodes acquires a somewhat asymmetrical character. The grid (Figure 2.6) is formed of a number of loops of very fine (ϕ=0.04 millimeters) tungsten wire whose ends are welded to heat-dissipating plates which have the form of a book cover which is placed on its back on the lead-in of the grid.

The operating conditions of ultra-high-frequency tubes are considerably improved if their electrode arrangement is equipped with dual lead-out wires: the plate and grid are fastened on thick parallel molybdenum wires which pass throughout the entire tube (Figure 2.7). The very short leads of the heated filament are made on one side and as far as possible from the plate and grid leads. The plates of such tubes may consist of a piece of graphite [8] or have a "bookcase" design [10]. The construction of the grid is identical to that described above. For the same electrode dimensions, tubes with dual leads make it possible to increase the frequency by approximately 1.2-1.4 times. Typical and natural for them is their inclusion in the center of a half-wave Lecher system. An example of the make-up of an oscillator with such a "two-sided" tube is illustrated by Figure 2.8, where the tube is included in the middle of a "box-type Lecher".

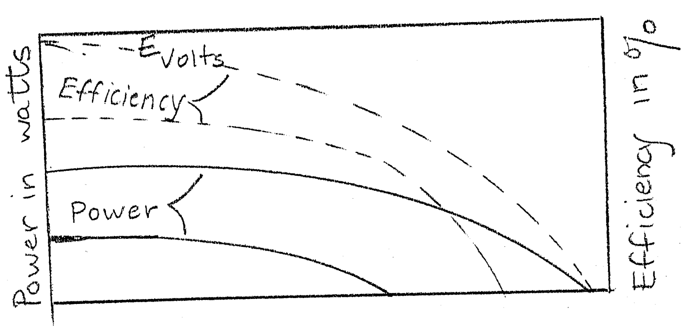

Figure 2.4

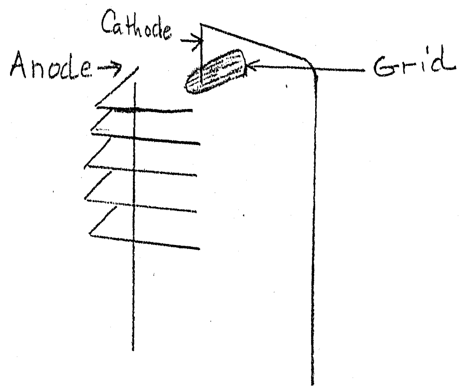

Figure 2.5

Figure 2.6

The results obtained with a tube with dual leads are illustrated by the data in Table 2.3.

Table 2.3

Table of the Frequency Limits Obtained with Dual-Lead Tubes

Tube	Wave-length centimeters	Frequency megacycles	Power watts	Efficiency percent
[1]	[2]	[3]	[4]	[5]
Taraskov tube with "bookcase" anode:				
(a) one-sided leads	40	750	6	~8
(b) two-sided leads	40	750	7-8	~10-12
Samuel tube with two-sided leads (368-A)	25	1200	3	~5

[1]	[2]	[3]	[4]	[5]
Samuel tube with two-sided leads (368-A)	20	1500	2	~3
Samuel tube with two-sided leads (368-A)	17.7	1700	1	-
Samuel tube with two-sided leads (368-A)	16.0	1870	0.01	Wave-length limit

Figure 2.9 illustrates the same data graphically.

Another, no less important trend in the development of the ultra-high-frequency tube with negative grid uses as the basis of design of the tube a flat arrangement of electrodes. This makes it possible to obtain a substantially larger mutual trans-conductance (up to 10 to 12 milliamperes volt) and to achieve a more convenient mode of securing the electrodes. The first tubes of this type were developed by Soviet designers [11] and made it possible to obtain waves as short as 16 centimeters in length. The experimental tubes which made it possible to obtain such short waves have a cathode in the form of a flat box which is covered with oxide and heat from within by an Alundumized tungsten spiral (Figure 2.10). The grid is made in the form of parallel tungsten wires stretched in the aperture of the metal disk G. The anode A is in the form of a cylinder which passes into a truncated cone inside which there is located a copper bushing which has good thermal contact with the base of the truncated cone, which in turn faces the grid. The distances between the electrodes are measured in tenths of a millimeter (0.2-0.4 millimeters).

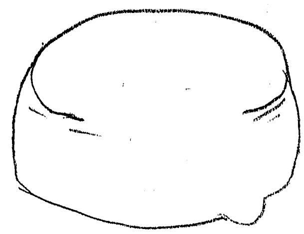

Figure 2.7

The design of these tubes makes it possible to combine them conveniently with coaxial oscillating systems so that the oscillator proves to consist of three circuits connected to the tube (Figure 2.11): the plate-grid circuit (1), the grid-cathode circuit (2), and the cathode-heater circuit (3). All of these are tuned by means of capacitance bridges, which, with sufficient blocking capacity (200-300 micromicrofarads), provide a separation of the constant voltages fed to the tube. The length of the generated wave depends mainly on the tuning of the plate-grid circuit, and the tuning of the other oscillating systems, in making very little change in the wave-length, affects chiefly the amplitude of the oscillations obtained. Changing the parameters of the system (principally U_a) also leads to a change in the power as well as the wave-length.

Declassified in Part - Sanitized Copy Approved for Release 2012/04/09 : CIA-RDP82-00039R000200090009-2

Figure 2.8

The table below describes the results obtained with the experimental tubes which have been described.

Table 2.4

THE RESULTS OBTAINED WITH EXPERIMENTAL TUBES

Tube	centimeters	Va volts	I_a milliamperes	V_g volts	I_g milliamperes	S milliamperes/volt	μ	P_a watts	R_i ohms
DTs-21	15.8	190	74	0	1	10.0	18	14	1800
	17.0	150	69	0	1	7.0	18	14	2700
	20.0	134	62	0	1	7.	18	14	2700
DTs-21	18.0	130	40	0	1	10.0	20	10	2000
	19.0	120	32	0	1	10.0	20	10	2000
	22.8	110	25	0	1	10.0	20	10	2000
DTs-21	18.3	146	51	0	1	11.0	18	9	1800
	20.0	138	46.8	0	1	11.0	20	9	1800
	22.1	134	46.2	0	1	10.5	20	9	1800
	24.4	120	48	0	1	10.0	18	9	1800
	25.8	110	39.3	0	1	10.0	18	9	1800

The tube design described was subsequently adapted by the same authors [12] to mass production in the form of the DTsM-1 metallic tube (Figure 2.12). The structure of the electrodes of this lamp is the same as that of the foregoing. It is also included in an analogous system of three coaxial lines. Testing of the DTsM-1 tube has shown that with plate voltages not exceeding 200 volts it may serve as a low-power oscillator at wave lengths from 20 to 25 centimeters. More powerful oscillations (from 1 to 5 watts) may be obtained with this tube at wave lengths from 30 to 60 centimeters. In addition, it may be used as high-frequency amplifier in the same frequency ranges.

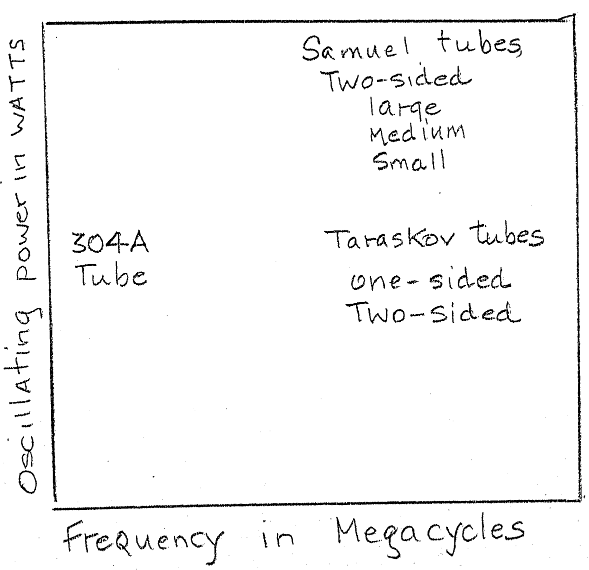

Figure 2.9

The flat arrangement of electrodes introduced by Soviet designers has disclosed an interesting technical aspect in the

Declassified in Part - Sanitized Copy Approved for Release 2012/04/09 : CIA-RDP82-00039R000200090009-2

design of the so-called "lighthouse" tubes, which are externally reminiscent of a lighthouse tower. The arrangement of the cathode, grid, and plate is essentially identical to the one described. The electrode leads are made through metal disks to which glass cylinders are soldered (Figure 2.13). This design of the leads makes it convenient to include "lighthouse" tubes in the coaxial circuits of which we have seen an example in Chapter I (Figure 1.58). Below are given the data for two "lighthouse" tubes -- receiving and oscillating (Table 2.5).

Table 2.5

"Lighthouse" Tube Data

	V_k	I_k	V_a	I_a max	P_a	P_{osc}	f_{max}
2C40 Tube	6.3 v.	0.75 a.	500 v.	25 ma.	6.5 watts	0.075 watts	1400 meg.
GL-3C22 Tube	6.3 v.	2.0 a.	1000 v.	150 ma.	125 watts	50 watts	600 meg.

The few examples which have been considered show that, thanks to the application of specially-designed tubes, the ordinary oscillator circuit with negative grid may provide an opportunity to obtain oscillation over the entire band of decimeter waves. Their basic design and application advantages are preserved, although the power of the oscillations falls rapidly with a shortening of the wave-length, as low as fractions of a watt in the lower range of the decimeter spectrum. This fact insures for oscillator circuits with a negative grid a broad application in cases where it is necessary to have a source of stable oscillations of small power, which is portable, well modulated, and simple to control.

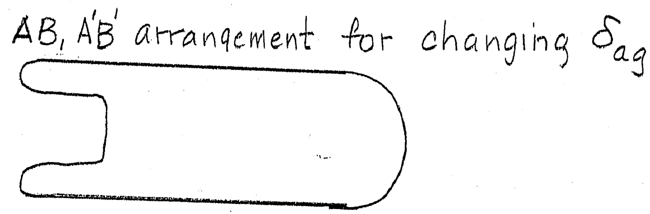

Figure 2.10

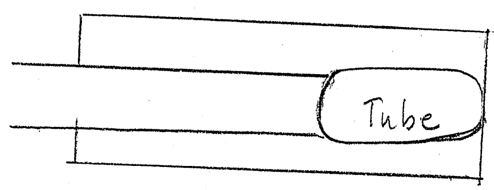

Figure 2.11

Section 2.3 Retarding-field Oscillator Circuits

We have already noted at the beginning of the preceding section that the operation of a tube in a circuit with reverse connection is characterized by the application of the principle of static control of the electron current. The braking-field was the first thermionic instrument in which another principle was used -- the principle of dynamic control of the electron stream. Dynamic control of the electron stream is basically the reaction of an ultra-high-frequency alternating electric field on an electron stream which already possesses a high velocity due to the action of a constant potential which considerably exceeds the saturation potential. A result of the action of the alternating electric field is the period changing of the velocities of the electrons in the stream, which leads, for finite transit times, to an interruption of the static nature of the current and the formation in it of dense spots which are periodically changing in time and space; in these densifications the instantaneous values of the current may exceed considerably the saturation current of the electron emitter which feeds the system. The utilization of such periodically occurring densifications in the electron stream in conjunction with a well-designed oscillating system is one of the basic processes in devices for generating micro-waves.

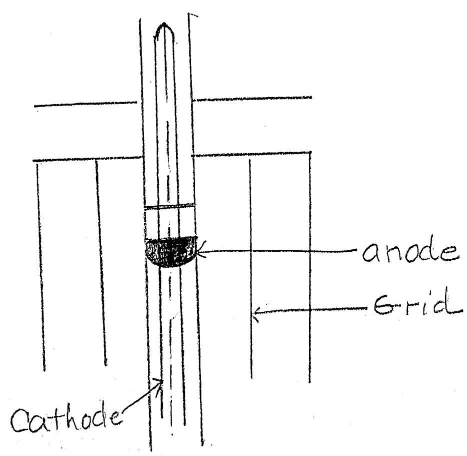

Figure 2.12

Declassified in Part - Sanitized Copy Approved for Release 2012/04/09 : CIA-RDP82-00039R000200090009-2

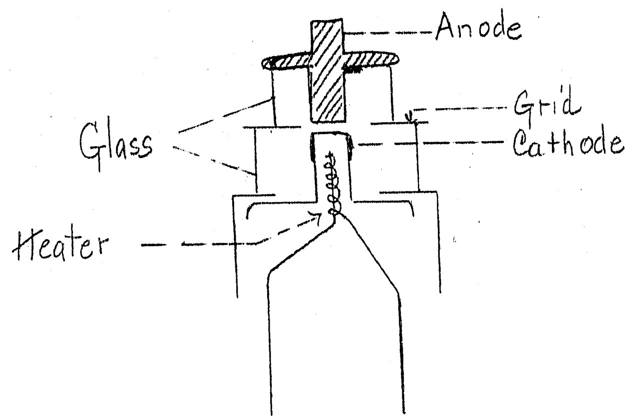

Figure 2.13

However, these facts have been understood for only a comparatively short time, and the retarding-field circuit has been used since 1919-1920. It is characterized by the fact that a high positive potential is fed to the triode grid (Figure 2.14) while the plate is at a zero or even negative potential. The occurrence of very high-frequency oscillations in this circuit has been explained by Barkhausen and Kurz [1] and by Zilitinkevich[2] by the "agitation" of the electrons around the positive grid. They obtained wave-lengths of up to 30 centimeters with ordinary tubes. The possibility of generating such short waves with a simple circuit has provoked a number of projects dedicated to the investigation of processes in the retarding-field circuit, as well as to its application. From simple deliberations based on the concept of "electron agitations" Barkhausen and Zilitinkevich found that the wave generated in the retarding-field circuit depends only on the geometrical dimensions of the tube and the potentials applied to it. For a flat electrode design where U_g is the grid potential in volts, U_a is the anode potential in volts, d_g is the distance between cathode and grid in centimeters, and d_a is the distance between the grid and plate in centimeters.

$$\lambda_{cm} = \frac{2000}{\sqrt{U_g}} \cdot \frac{d_a U_g - d_g U_a}{U_g - U_a} \qquad (2.4)$$

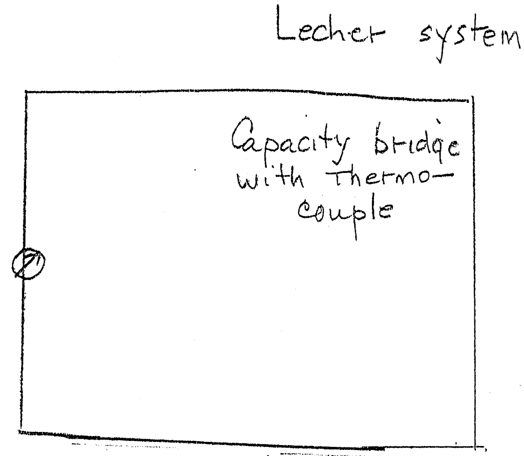

Figure 2.14

In the case where $U_a = 0$ formula (2.4) becomes

$$\lambda_{cm} = \frac{2000\, d_a}{\sqrt{U_g}} \qquad (2.5)$$

From this the "Barkhausen relationship" is obtained

$$\lambda \sqrt{U_g} = const, \qquad (2.6)$$

which is fulfilled more or less satisfactorily in all cases where the

Declassified in Part - Sanitized Copy Approved for Release 2012/04/09 : CIA-RDP82-00039R000200090009-2

oscillations are excited by means of a dynamically controlled electron stream.

In the first years of the existence of the retarding-field circuit (1920-1930) observations were made of the great complexity of the phenomena which take place in it and of the completely logical inconsistency of the theory of "electron agitations". This gave vent to the development of extremely diverse points of view, each of which attempted to explain with various degrees of precision -- and in part did explain -- the processes which take place in the circuit and the experimental facts which are observable. Many of these theories are now of only historical interest. Notice may be taken of two schools of thought: the kinematic theory, whose point of departure was the "kinematics of the electrons" in the retarding-field circuit and which attempted to create a sufficiently graphic concept of the mechanics of the oscillations, to accomplish which the representatives of this school often had recourse to mechanical models which illustrated their theory [13]; and another school of thought, which may be called the "power" school, proceeding from more general physical considerations and leading to certain quantitative results by somewhat more formal means, more or less independently of the concrete details of the operating mechanics of the circuit.

Most fruitful, however, were those theoretical deliberations which took into account both aspects of the phenomenon, applying considerations of a general power nature to an electron-kinematic mechanism which had been worked out in sufficient detail.

If we attempt to summarize the enormous quantity of experimental projects devoted to the retarding-field circuit [14], we may establish the following fundamental experimental facts:

(a) Electron oscillations are rather easily obtained in the retarding-field circuit with the majority of triodes of symmetrical design. Due to high grid potential and large grid currents, tubes with a high-power grid and a pure tungsten cathode operate with considerably more stability and make it possible to obtain shorter waves (a wave-length as low as 6 centimeters with tubes of the P-5 type).

(b) The power of these oscillations and their coefficient of efficiency are very small. Thus, for example, in the operation of specially constructed tubes ($\lambda \approx$ 30 centimeters) about 4 or 5 watts power is obtained with an efficiency of about 3/4 percent. Such low efficiency is caused by the enormous losses in the grid current circuit and also by the poor design of "ordinary" tubes with respect to the marriage of the electron stream to the oscillating system. Application of a system of grid-plate electrodes in the form of half-wave or quarter-wave segments of coaxial lines or hollow resonators (the "resotank" with retarding field) somewhat increased the effectiveness and stability of the oscillations in the retarding-field circuit, without relieving it, naturally, of the basic source of losses -- the grid current.

(c) Even with a fixed oscillating circuit, the intensity of the oscillations depends in a considerable degree, and to a

Declassified in Part - Sanitized Copy Approved for Release 2012/04/09 : CIA-RDP82-00039R000200090009-2

lesser degree the wave length, on the parameters of the circuit conditions of the tube, i.e. on the potential on the grid and the plate and the emission current.

(d) The basic elements which determine the frequency of oscillations generated in the retarding-field circuit are the oscillating systems which are directly connected to the tube's electrodes or which are formed by the electrodes themselves. As an example, mention may be made of the "grid spirals" which determine the oscillating frequency in the case of one of the most often used retarding-field circuit arrangements. Such self-exciting oscillating circuits are always present in ordinary tubes and manifest themselves as a rule with no regard to the external "controlled" oscillating circuits which are connected to the tube. As a result of this extremely complex and erratic "operating diagrams" (the function of the intensity of the oscillations and their wave length with respect to the parameters of the tube circuit and the tuning of the external circuit) are often obtained.

(e) If it is possible, by virtue of the multiplicity of possible oscillating conditions, to obtain different wave lengths with the same tube, then the function of λ with respect to U_g reproduces Barkhausen's condition rather closely -- with respect to currents -- but with values of the constant in formula (2.6) which are sometimes different. The Barkhausen constant most often observed with a given tube corresponds to an excitation of the first order. The successive, smaller values of the constant correspond to the excitation of "dwarf" waves, which are characterized by a small intensity of the oscillations and a lower efficiency, but which occur more easily under favorable conditions.

(f) With determinate values of U_g, U_a, and I_{em} (where I_{em} is the emission current) one or several maxima of intensity are obtained for each generated wave λ. The aggregate of these maxima creates an operating diagram which is characteristic of the retarding-field circuit and consists of a number of discrete excitation regions whose optima according to principle with respect to variation of all three of the parameters of the tube circuit which have been mentioned, U_g, U_a, and I_{em}.

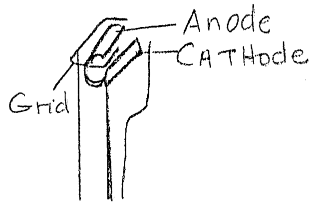

Figure 2.15

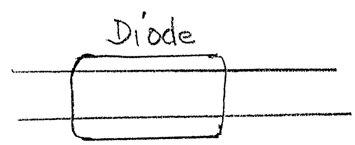

Figure 2.16

(g) A continuous variation of the wave length when any of these parameters is changed is observed only within the limits of one excitation region, and proves to be comparatively small with a fixed circuit. If then a change in the tuning of the oscillating system is made simultaneously with a change in one or several parameters of the lamp circuit, then changes in wave length may be accomplished over a wide frequency band located within the limits of the same excitation range. Thus a "continuous spectrum of electron oscillations" is obtained through the use of an aperiodic tube [15].

(h) In the case of the excitation of extremely short waves intra-tube circuits which possess inherent frequencies usually serve as the resonance systems, for example, the grid leads.

(i) Oscillations similar to the electron oscillations in the "normal retarding-field circuit", and conforming, to a first approximation, to the Barkhausen condition, also occur in systems with considerably distorted symmetry and in two-electrode systems, if an opportunity is created for the electrons to pass through a closed trajectory. As an example we may cite the one-sided tubes with semi-cylindrical plate and grid in the form of an open guard encompassing the plate, which were used back in 1928-1929 in Kohl's projects (Figure 2.15), and with which it was possible to obtain extremely short waves (as small as 4.5 centimeters in length), due evidently to the excitation of the grid guard. Oscillations have also been observed in "grid" and "filament" diodes [17, 18, 19], and have been explained by the fact that a part of the electrons accelerated by the field of the positive element of the system, which element possesses a certain degree of penetrability, passes through it due to inertia into the reverse field, is retarded, and returns backward. Figures 2.16 and 2.17 represent such systems with the possible trajectories of the electrons represented schematically.

In simple diodes with a continuous metallic anode the electrons may be caused to move along closed paths by means of a magnetic field applied to the system parallel to its axis. Thus the magnetron circuit was created, a circuit which has received widespread development in the field of micro-waves, but which under some conditions, for example under conditions of electron oscillations of the first order, does not differ in principle from the circuit of the retarding field.

Figure 2.17

(j) In the case of operation of a tube with retarding field, rather clearly evidenced phenomena of coupling are observed in the external tuned system (change in the frequency of the oscillations with tuning of the external circuit simultaneously with a change in their aplitude and trajectory, characteristic of tightly coupled oscillating systems). The latter have given a number of authors reasons for representing the retarding-field system as the aggregate of the intra-tube electron mechanism, which possesses a certain inherent frequency, and the outer system, which is coupled rather tightly to it.

However, as will be shown later it is extremely inexpedient to conceive of an electron-oscillation mechanism which is not dependant on any "circuit" systems, in consequence of which the observed phenomenon are due to some intra-tube oscillating system or to the reactive properties of the stream of electrons itself; the properties occur upon the interaction of the electrons with rapidly varying electric fields.

Such an explanation is also partially confirmed by the fact that the coupling phenomena described are considerably less vividly expressed in the magnetron than in the retarding-tube field, by virtue of the simple electrical design of the magnetron.

Section 2.4 The Magnetron Oscillator

Historically, the obtaining of ultra-high frequency oscillations through the use of the magnetron oscillator was reached as a result of investigation of the behavior of the retarding-field oscillator in a magnetic field. It was discovered that by placing the tube in a magnetic field oriented parallel to the axis of the electrodes or at a slight angle to it, it was possible to facilitate considerably the excitation of oscillations. With sufficiently large values of the intensity of the magnetic field, close to the "critical" values, it proved possible to obtain extremely high-frequency oscillations, even in a diode [20]. In so doing the oscillating system is enclosed between the anode and the cathode (Figure 2.18). The oscillations obtained in such a circuit are due in origin to the combined action of the electric and magnetic fields, which determine the motion of the electrons through closed trajectories inside the anode-cathode space. The trajectory of the electron in this inter-electrode space is closed when the magnetic field attains the critical value H_k

$$H_k = \frac{6.72}{r_a}\sqrt{U_a} \qquad (2.7)$$

where r_a is the radius of the anode in centimeters and V_a is the anode potential in volts.

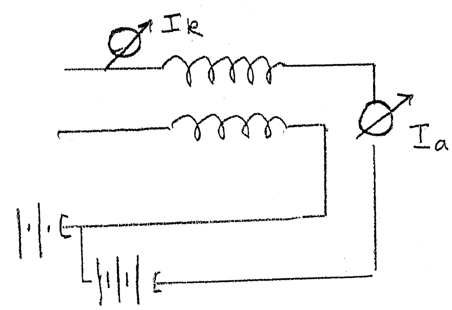

Figure 2.18

Due to axial symmetry of the entire system the process is determined mainly by the radial motion of the electrons, which occurs in analogous fashion to their motion in retarding-field circuit. The wave length of the oscillations obtained in the magnetron depends on the intensity of the applied magnetic field H_e, chaning in inverse proportion to the latter,

$$\lambda_{cm} = \frac{C_o}{H_{\text{э}}} \qquad (2.8)$$

Here C_o is the so-called "Okabe constant", which has a calculated value of 10,650. In practice the observed values of this constant range approximately from 7,000 to 16,000. Relationship (2.8) is equivalent to the Barkhausen formula

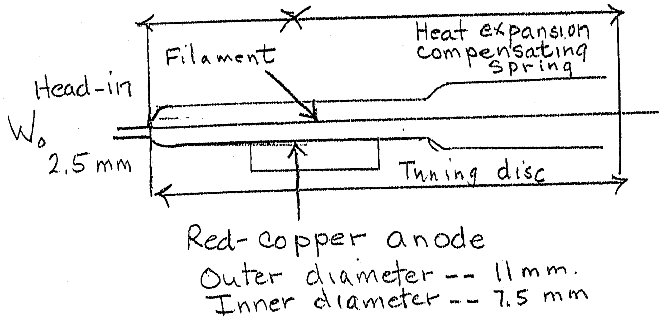

Figure 2.19

if by C' we understand the value

$$C' = \frac{C_0 r_a}{6.72}. \tag{2.9}$$

Oscillations of this type, designated as "electron oscillations" of the first order, are completely analogous to the oscillations in the retarding-field circuit.

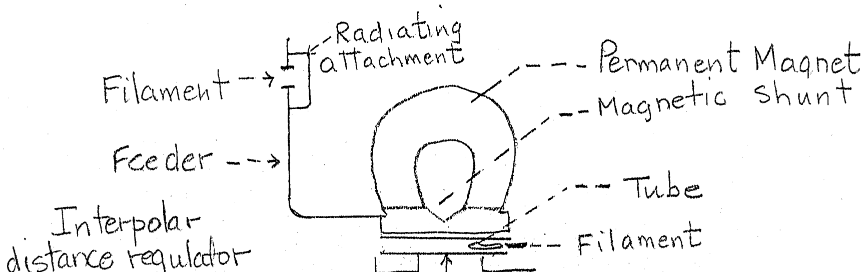

Figure 2.20

Declassified in Part - Sanitized Copy Approved for Release 2012/04/09 : CIA-RDP82-00039R000200090009-2

They are characterized by small intensity and a low efficiency factor, which does not exceed ten percent, in spite of the fact that losses due to grid current are not present in the magnetron. In this type of oscillation, however, very short undamped electromagnetic waves have been obtained. Here mention should be made of the above-noted work of Rice, and also of the work of Clinton and Williams [21] and Richter [22].

The magnetron tube and the Rice set-up are represented in Figures 2.19 and 2.20. This tube is a simple diode with a solid anode made up so that the anode and the filament serve as a section of a line with distributed constants, through which the oscillating power is fed off into a radiating dipole. The tube is located between the poles of a constant magnet and is cooled with water. The nature of its operation may be evaluated by means of the following data:

Plate diameter	7.5 millimeters
Cathode filament current	32.5 amperes
Emission current	115 milliamperes
Anode voltage	3050 volts
Intensity of the magnetic field	3300 oersteds
Wave-length	4.2-4.8 centimeters
Oscillating power	10 watts
Efficiency	3 percent

Clinton and Williams [21] went still farther, and obtained waves of 1.1 centimeters in length with tubes which had a dual-segment anode and an internal "frame" circuit. The data for one of their tubes are as follows:

Plate diameter	0.54
Length of the frame attached to the segments	4 millimeters
Plate voltage	870 volts
Magnetic field	11,000 oersteds

It is difficult to judge with sufficient precision the power of the oscillations obtained, since it is unquestionably below a milliwatt.

Richter, using an asymmetrically located filament in a "half-sectional" tube (2.21) achieved a reduction in operation radius and obtained waves to 4.9 millimeters in length.

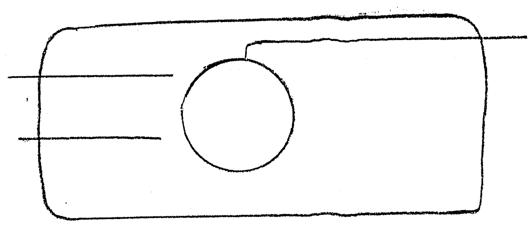

Figure 2.21

The difficulties arising from the generation of such short waves are clear from the fact that the electric fields used in these tubes reach gradients of the order of 10^5 volts/centimeter, by virtue of which the disturbing phenomenon of high-field emission from the cold surface of the metal begins to be of consequence. Richter tubes and their operating conditions are described by the data in Table 2.6 (page 61).

The conditions of electron oscillations of the first order are observed in magnetrons with solid anodes, as well as those with sectional anodes. However, for magnetrons with sectional anodes other oscillating conditions are characteristic: "electron oscillations of higher orders". It is customary to designate the ratio of the period of the oscillations to the time of return of the electron along its trajectory as the *n*th order of oscillation. By oscillations of higher orders we usually understand oscillations characterized by values of *n* from 2 to 10. Electron oscillations with values of *n* 10 become, in essence, so-called "dynatron" oscillations, which owe their occurrence to the statically falling-off characteristic in the inter-segmental circuit and are not associated in any respect with the transit time of the electrons. Most interesting and typical for sectional magnetrons in the region of the shortest waves in the condition under which electron oscillations of the higher orders are produced. Their excitation takes place at magnetic-field intensities which differ considerably from the critical values, and are due to the interaction of the rotating electron cloud inside the magnetron with the changing fields between the segments of the anode. While the oscillations of the first order are governed mainly by the radial components of the motion of the electrons, the leading role in the oscillations of higher orders belongs to the tangential components.

Table 2.6

RICHTER'S TUBE TABLE

No	r_a millimeters	Operating radius millimeters	Length of Lecher System, mm.	Filament diameter mm.	Centimeters	H Oersteds	H	U_a volts	I_a ma.	Oscillating power watts	Efficiency
1	2.5	2.5	10	0.2	8	1300	10400	2000	3.2	0.75	11.6%
2	1.5	1.5	6	0.15	4.8	2100	10100	1700	3	0.15	3%
3	1	1	5	0.12	2.8	3600	10000	2300	0.4	$2.5 \cdot 10^{-2}$	2.8%
4	1	1	4.5	0.12	2.44	4100	10100	2800	0.8	$4.2 \cdot 10^{-4}$	$1.9 \cdot 10^{-3}$
5	1	0.32	4.5	0.12	1.5	10000	15000	2000	1.4	$1.4 \cdot 10^{-5}$	$5 \cdot 10^{-6}$
6	0.4	0.22	2	0.1	0.75	13800	10300	1900	2.4	$3 \cdot 10^{-6}$	$6.5 \cdot 10^{-7}$
7	0.35	0.21	1.5	0.1	0.49	20000	9800	4000	0.6	$2.5 \cdot 10^{-7}$	$1 \cdot 10^{-7}$

In sectional magnetrons the oscillating system is usually connected to opposite segments (Figure 2.22a) in the case of the two-segment tube, or to two groups of segments whose elements are in alternate order (Figure 2.22b). Thus the densifications obtained by virtue of dynamic control of the tangential electron stream encounter an electric field which alternates 2p times for each rotation. By p we should understand the number of pairs slots (or segments). With relatively small angular velocities of the rotating electron space charge and a large number of segments, the possibility of generating oscillations of extremely high frequencies is realized in consequence of this. At the same time it is also necessary to note that the electron oscillations of the higher orders possess considerably higher efficiencies than the oscillations of the first order; their wave-length conforms rather closely to the relationship [23].

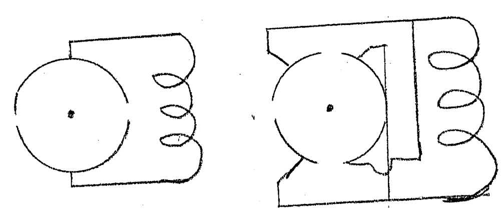

Figure 2.22

$$\lambda = \frac{C r_a^2 H}{p U_a} \qquad (2.10)$$

The constant C is approximately equal to 1000.

Table 2.7 which corresponds to certain Runge tubes, is given to show the characteristics of oscillations of higher orders and for comparison of them with oscillations of the first order [24].

Increasing the number of segments of the magnetron makes it possible to obtain very short waves under less severe conditions of operation. At the same time the oscillating system may be represented by the segments themselves, as shown in Figure 2.23, where the wave-length is fixed and determined by twice the length ABCD. Anode segmentation of this type was used by Linder in the two-segment "tank" anode of his magnetron, and by Gutton and Berline [25] and by Kuz'min [26] in multisegment magnetrons. A more complicated, but also more symmetrical oscillating system is formed if the segments consist of two groups, each of which is connected with its supporting ring, as may be seen from Figure 2.24 [25, 26, 27]. In this case the wave-length is determined by the oscillating system connected to rings A and B.

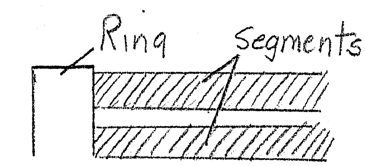

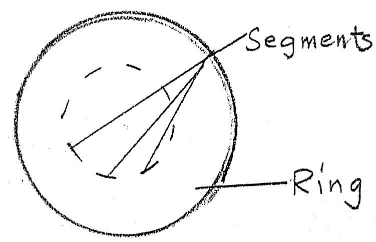

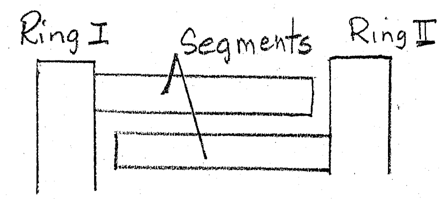

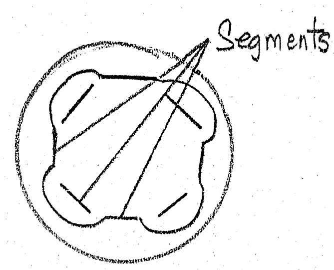

Figure 2.24/2.25

Table 2.7

RANGE TUBE DATA

Lamp No	r_a cm	l_a cm	λ cm	Number of slots --2p	Order of Oscillations -- n	V_a volts	H Oersteds	Oscillating Power watts	Efficiency percent
1	0.5	2	50	4	2	1000	400	60	40
2	0.25	1	25	4	2	1000	850	15	40
3	0.11	0.6	50	4	2	50	425	0.05	10
4	0.11	0.6	25	4	2	200	850	0.05	10
5	0.2	0.8	25	4	2	900	1100	11	40
6	0.22	1	10	2	1	1200	1070	0.5	5

The advantages of multi-segment magnetrons may be seen for example from a comparison of the geometrical and operating data of a two-segment and a twelve-segment (anode segmentation of the type of Figure 2.24) tube which are given in Table 2.8. Both tubes operate at a wave length of $\lambda = 10$ centimeters [25].

Table 2.8

DATA OF DUAL- AND MULTI-SEGMENT TUBES

	Two-Segment Tube	Twelve-segment tube
Plate diameter	4 millimeters	6.4 millimeters
Length of Plate	8 millimeters	10 millimeters
Anode Potential	1000 volts	600 volts
Magnetic-Field Intensity	1400 oersteds	500 oersteds
Oscillating Power	2.5 watts	7 watts
Efficiency	12 percent	15 percent

Of great interest are the multi-circuit or "multi-cell" magnetrons, whose operation does not differ in principle from the multi-segment types but which may be designed so that they permit the dissemination of high power and the provision of intensive water of air cooling. The results which have been obtained with magnetrons of this type are worthy of mention. The Soviet authors Alekseyev and Malyarov [28] were the first to design magnetrons whose oscillating system in the form of a cylindrical cell in a solid block of red copper, were connected to a narrow slot with an inner-anode space. (In Figures 2.25; d_a is the plate diameter; d_k is the "circuit" diameter.)

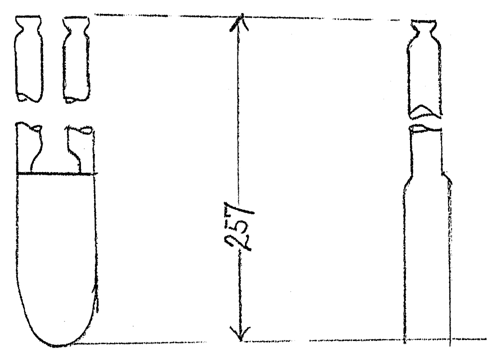

Figure 2.25a

Figure 2.25a represents the original design with one circuit; it is analogous to the ordinary two-sectional magnetron with circuit inside the tube. Figure 2.25b represents a two-circuit design, and Figure 2.25 a four-circuit design. The latter is analogous to a four-segment magnetron. Subsequently similar designs with a large number (6,8) circuit cells were used [26]. Alekseyev and Malyarov obtained up to 300 watts oscillating power at a wave length of $\lambda = 9$ centimeters with a sectional four-circuit magnetron with forced water cooling. An unsoldered tube of the same design developed a power of more than 100 watts at the same wave-length and under the same conditions of application. Finally, it proved possible in a magnetron of the same design to obtain a wave-length of 2.6 centimeters with a power of about 2 watts. The basic results of Alekseyev's and Malyarov's work are summarized in Table 2.9 (page 65).

Subsequent development of "multi-cell" magnetrons has led in past years to designs which have played an exceptionally important role in obtaining high-power centimeter waves. They have gained particularly broad application in radio-location equipment. The basic design elements of Alekseyev's and Malyarov's tubes have been preserved. The number of circuit-cells which surround the basic cylindrical chamber where the heating cathode is located reaches as high as eight, twelve, sixteen, and more. The dimensions of the cells are selected so that their inherent resonant frequency is equal to the generated frequency. In calculating the inherent frequency of the cells of magnetrons of this type they may be regarded, in a first approximation, as band circuits which conform to formulas (1.9) and (1.10) which were found by M. T. Grekhova.

Table 2.9

THE RESULTS OF ALEKSEYEV'S AND MALYAROV'S WORK

Tube Type	d_k/d_a	V_a, volts	I_a, milliamperes	H, oersteds	λ, centimeters	$P_{oscillating}$ watts	Efficiency percent	Remarks
One-Circuit	1.5	1700	140	2600	7.7	8	3	Oscillations of the 1st order
Two-Circuit	2.0	1800	45	2000	9.9	7	9	Oscillations of higher order
Four-Circuit Pump-cooled	1.5	2650	360	1350	9.0	170	18	
Same	1.5	4400	330	1950	9.0	300	20	
Four-Circuit Un-soldered	1.5	3220	160	1650	9.1	116	22.5	
Four-Circuit Un-soldered	1.4	1570	190	1600	5.5	20	7.0	Oscillations of the "half" order: $n = \frac{1}{2}$
	1.4	890	48	2560	2.6	2	4.5	

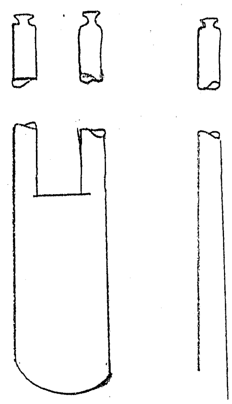

Figure 2.25b

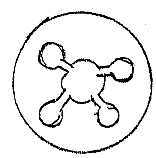

Figure 2.25c

The energy of oscillation is led off by means of a coupling loop located in one of the cells, as may be seen from Figure 2.26 which represents a schematic section of an 8-cell magnetron.

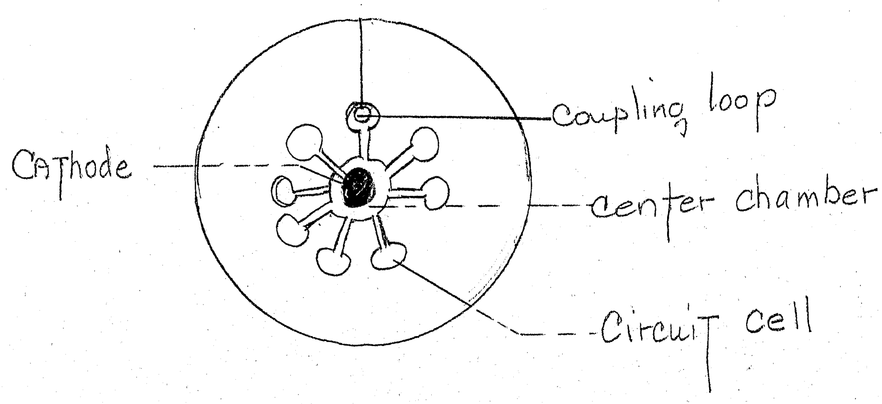

Figure 2.26

Declassified in Part - Sanitized Copy Approved for Release 2012/04/09 : CIA-RDP82-00039R000200090009-2

The maximum effect is obtained when these magnetrons are operated in impulse circuits where the tube operates only during the time of the impulse, which last one or several micro-seconds and "rests" in the intervals of time between the impulses, whose frequency normally does not exceed 600 to 1000 per second. During the impulse currents pass through the tube which are measurable in tens of amperes, and the oscillating power given off by the tube reaches, in present-day magnetrons, several megawatts at wave-lengths of the order of 10 centimeters. The principle of connecting the impulse magnetron is shown in the circuit in Figure 2.27. The anode is usually grounded, and the cathode is fed with negative impulses as rectangular in shape as possible. Data on magnetrons used in radio-location devices are given in Table 2.10 [29].

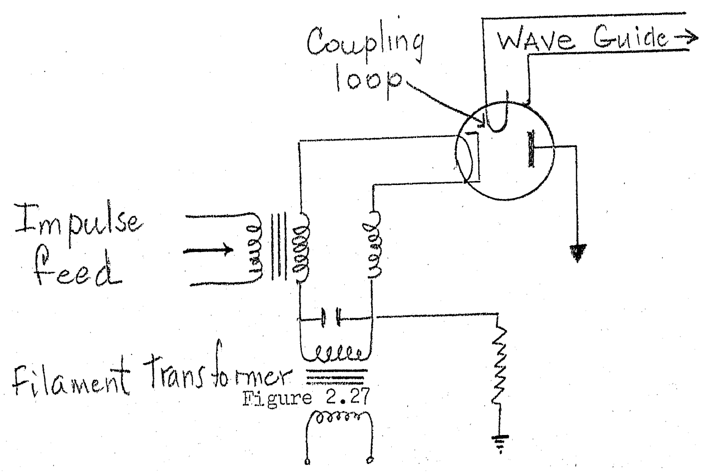

Figure 2.27

Table 2.10

PARAMETERS OF SEVERAL MULTI-CELL MAGNETRONS

Type [1]	Frequency Range Megahertz [2]	Maximum Oscillating Power Kilowatts [3]	V_a volts, I_a amperes in the impulse [4]	Ratio of Impulse Length to the Complete Cycle [5]	Maximum Duration of the Impulse [6]	Average Useful Power Watts [7]
I. L-Band (= 25 ÷ 50 centimeters)						
700A	680 (fixed)	100	12,000 10	1/400	2	120
5J21	1060 (fixed)	600	22,000 50	1/1000	2	750
4J21	1220 (fixed)	800	28,000 60	1/500	6	1500
5J26	1220 - 1350 (tunable)	800	27,500 60	1/500	6	1500
II. S-Band (= 8 ÷ 11 centimeters)						
720Ay	2720 (fixed)	1000	25,000 70	1/1000	2	1500
4J36	3400 (fixed)	850	24,000 43	1/1000	2.5	1000

Table 2.10 (Continued)

[1]	[2]	[3]	[4]	[5]	[6]	[7]
2J39	3333 (fixed)	12.5	5,400 5	1/500	2	27
III. X-Band (= 3 centimeters)						
725A	9400 (fixed)	60	12,000 12	1/10	2.1	120
2J56	9400 (fixed)	70	12,800 12	1/1000	2.5	150
2J51	8500 - 9600 (tunable)	60	14,000 10	1/800	2	200

Declassified in Part - Sanitized Copy Approved for Release 2012/04/09 : CIA-RDP82-00039R000200090009-2

When the input impulses are rectangular in shape the efficiency of these magnetrons is very high: from 20 to 60 percent. Thus, for example for the 10-centimeter 4J36 tube it reaches 47 percent. The frequency of the oscillations in tubes with fixed tuning systems may vary within the limits of 1 to 2 percent, depending on the tuning of the load circuit. The outer form of tubes with fixed circuits is represented in Figure 2.28, in which is shown a 10-centimeter magnetron with a million-watt impulse capacity. At the left are located the cathode leads, and the oscillating energy lead is at the right. An idea of the dimentions is given by means of a cubic inch shown in the same illustration. The design elements of similar tubes are represented in Figure 2.29. Figure 2.30 represents a 2-centimeter magnetron with a permanent magnet.

See Photograph
Text: page 68

Figure 2.28

Here notice should be given to the coaxial cathode lead-in and the wave-guide which takes off the oscillating energy. Figure 2.31 shows typical designs of magnets: at the left there is a 2900 gauss magnet for a 10-centimeter megawatt magnetron, and at the right there is a 3-centimeter tube with a 5500-gauss permanent magnet.

See Photograph: page 68

Figure 2.29

More substantial variations in frequency are obtained when moveable side-plates which limit axially the length of the chamber are added to the design of the magnetron. These are moved by means of the elastic walls, which are subjected to pressure from outside. The form of a magnetron with tuning mechanism is shown in Figure 2.32.

Declassified in Part - Sanitized Copy Approved for Release 2012/04/09 : CIA-RDP82-00039R000200090009-2

These few data on modern "multi-cell" magnetrons are evidence of the extremely broad and far-from-exhausted possibilities of utilization of them in the field of very short radio-waves.

See photograph: text: page 69

Figure 2.30

"Multi-cell" systems are a special case of polyphase systems, which, generally speaking, may consist of a closed series of oscillatory circuits whose phases are interrelated in a definite manner. Each of these circuits may also be excited as an individual system, for example, by means of a tube oscillator. In this case the excitation of each of the circuit cells which plays a part in the oscillations takes place in a corresponding phase associated with the angular velocity of the densifications in the rotating space charge, which in turn is interacting with the electrical fields of the circuits in the region of the slots. The guiding spirit of this school, N. A. Kuz'min [26] created "group radiators", magnetron systems whose anode consisted of a certain number of extremely short-wave oscillating circuits situated along a surface which described a cylinder. In the designs whose purpose was to obtain the shortest waves these circuits were resonance dipoles welded onto one supporting ring at the voltage nodes; along the axis of this ring the filament was located, in the form of a "pole circumference" (Figure 2.33). In similar fashion, systems with two "pole circumferences" were designed (Figure 2.34) It was possible to obtain waves of 2.4, 2.6, 3.2, and 3.4 centimeters with an intensity sufficient for laboratory application with devices of this type. The characteristics of the operating conditions of such systems are given in Table 2.11 (page 70).

See photograph

Text: page 69

Figure 2.31

The examples which have been cited are evidence of the fact that the magnetron, under conditions of electron oscillations, is an extremely convenient source of high-power oscillations in the decimeter and centimeter band. The possibility of making up light weight permanent magnets from the newest magnetic materials reduces

Declassified in Part - Sanitized Copy Approved for Release 2012/04/09 : CIA-RDP82-00039R000200090009-2

considerably the fundamental application shortcoming of the magnetron -- the presence of a heavy magnet or electromagnet.

Photograph
See
text: page 70

Figure 2.32

Data for Tubes with "Pole Circumferences"

	V_a volts	H oersteds	λ centimeters	H/H_k
MM-11 (Fig 2.33) r_1=0.34 centimeters; r_{11} = 0.40 centimeters; l=1.63 centimeters; number of dipoles N=12	1320	1680	2.4	2.33
	1480	1840	2.6	2.42
	1440	1840	2.6	2.45
MM-18 r_1 = 0.37 centimeters; r_{11}= 0.4 centimeters; l=0.7 centimeters; N=18	2800	1020	3.2	1.06
	2840	1020	3.4	1.05
	2760	1020	3.4	1.07

Declassified in Part - Sanitized Copy Approved for Release 2012/04/09 : CIA-RDP82-00039R000200090009-2

In concluding this section, a few words about the so-called "dynatron" oscillations of the magnetron (a term that is very unfortunate!). They likewise are observed only in magnetrons with sectional anodes, principally in those with two or four segments. The period of these oscillations is wholly determined by the inherent period of the oscillating system connected to the anode segments. The oscillations in the oscillating system are sustained due to the creation of a static negative resistance in the inter-segmental circuit. Essentially, the inertia of the electrons play no part in this. An important factor here is the nature of the trajectories of the electrons, which is responsible, under certain conditions of the electric and magnetic fields, for the incidence of a larger number of electrons on the least positive segment of the anode and the creation, in this manner, of a static negative resistance. The operation of the magnetron under the conditions of dynatron oscillations may be subjected to analysis by means of the usual methods of radio engineering. Dynatron oscillations are used principally for obtaining high-power oscillations in the long-wave portion of the decimeter band (30 centimeters), the efficiency reaching 50 percent and higher, and the absolute values of power capacity reaching several kilowatts at wave-lengths on the order of 60-80 centimeters with water cooling of tubes of suitable designs.

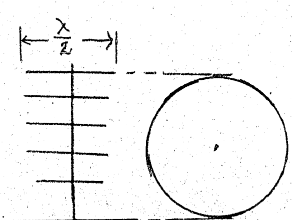

Figure 2.33

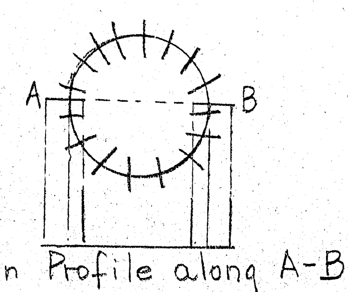

Figure 2.34

Section 2.5 Electron Beam Oscillators

In 1939 there appeared the report, mentioned in Chapter I, of the Varian brothers on a new oscillator and amplifier for ultra-high frequencies; the work was based on a completely new principle, as was made evident in the beginning. The arrangement of this instrument was as shown (Figure 2.35).

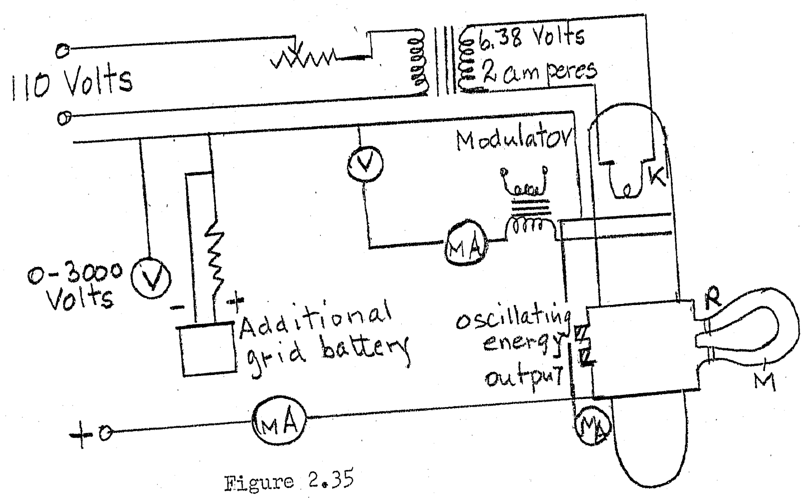

Figure 2.35

A stream of electrons emitted by the cathode K undergoes acceleration along the path to the surface A of the first grid of the toroidal endovibrator R and, possessing considerable velocity, passes through the zone of the electric field AB. As a result of variation of the latter with respect to time, the electron stream leave B with varying velocity -- "modulated velocity", as it has become conventional to call it. The space BC is shielded from the action of any fields, and the motion of the electrons in it occurs velocities but velocities different for different phases of the departure from B. As a result of the overtaking of some electrons by others in the stream densifications are formed which reach their maximum at some distance from B which is just where the electric field of the second toroidal circuit is located. With the help of the line M of reverse connection between the oscillations of both circuits, a phase relationship is set up due to which a densification of the electron stream is formed in the space CD at the moments of the maximum retarding alternating field in the second circuit. This causes, obviously, a transfer of energy by the "focus", as the densification in the electron stream is called, to the alternating field of the second circuit, and also caused sustained oscillations in it under certain conditions. The "worked out" electron stream which has passed the grid D is absorbed by the electrode-collector E. This device, which was named the klystron, made it possible to obtain a power on the order of hundreds of watts at wave-lengths on the order of several tens of centimeters with a coefficient of efficiency on the order of 40 percent. Naturally, these results differentiate the klystron favorably from other generators of ultra-high frequencies. The absence of a magnetic field, a single source of constant potential -- such are the advantages of the new-type oscillator.

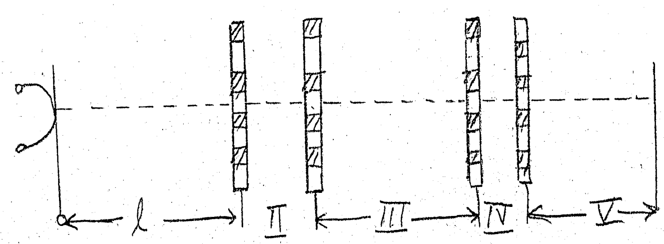

Figure 2.36

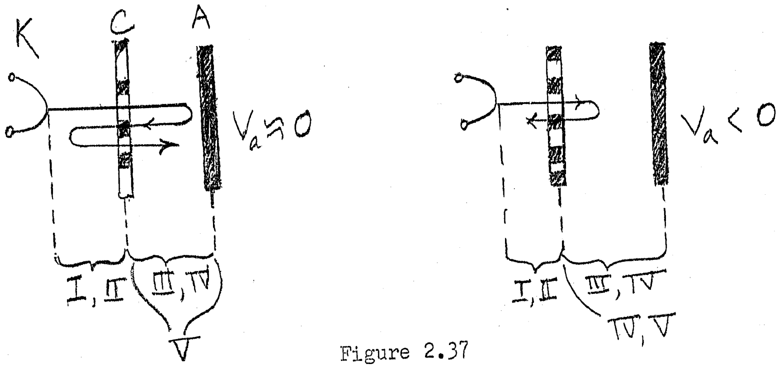

Figure 2.37

Nevertheless, the design and mode of operation of the klystron do not embody anything which is new in principle. In its design we have only a more effective utilization of the principle of <u>dynamic control</u> of an electron stream than in the retarding-field-circuit oscillator or in the magnetron. The potential of the first grid -- the accelerating potential -- considerably exceeds the saturation potential; consequently, a variation in current due to utilization of the static characteristic cannot take place. Control of the current must be such as to creat a variable current density not only in time, but also in space, between the electrodes. At the same time there occurs an interruption of the stationary nature of the current and the creation of densifications of the charge and current in the inter-electrode space, due to inertia of the electrons. Something similar also takes place, as we shall see further on, in the

Declassified in Part - Sanitized Copy Approved for Release 2012/04/09 : CIA-RDP82-00039R000200090009-2

retarding-field-circuit oscillator.

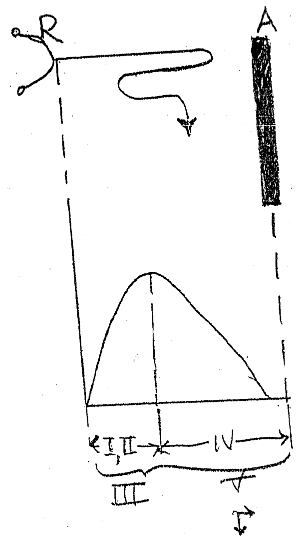

Figure 2.38

But for more complete utilization of the advantages of dynamic control it is necessary to take into consideration the "space" nature of the variation in density in the stream and to change correspondingly the design of the tube.

The klystron described above is of a design in which, with dynamic control, all of the fundamental moments of operation of the electron stream have been clearly divided in space. The "five-zone" circuit, which is identical to the klystron, may be represented as the most general circuit for processes which occur in instruments with dynamic control of the electron stream (Figure 2.36). Actually, the space KA, which may be called the "zone of acceleration", localizes the process of acceleration of

Declassified in Part - Sanitized Copy Approved for Release 2012/04/09 : CIA-RDP82-00039R000200090009-2

the electron stream which is necessary in all dynamically controlled instruments. Further along is zone AB, where the stream undergoes "dynamic control" in the form of the reaction of the ultra-high-frequency field between A and B, as a result of which "velocity modulation" is accomplished, that is, a certain variable component is superimposed on the constant velocity acquired in the zone of acceleration. Different parts of the stream, or in other words different bundles of electrons which make up the stream, will have different velocities in leaving the "zone of modulation" AB, and in the following zone BC, where the transit time is considerably greater than that of zone AB, individual groups of electrons will catch up with each other, thus creating densifications which follow one after the other in time but are localized in space. As a result of this type of "dynamic" conversion, "velocity modulation" involves "density modulation", which in theory may be as intense as is desired. Thus, zone BC may be called the "zone of conversion" of the stream. It is replaced by zone CD, in which the converted stream executes its basic function: it transfers energy to the oscillator circuit, if the device is an oscillator, or to the output circuit of the amplifier, if it is an amplifier. The zone CD may be called the "output zone" or the "zone of energy transfer". The subsequent fate of the electron stream is of interest to us only inasmuch as the stream must complete the circuit of the constant source, passing out into the electrode-collector E through the "purification zone" DE.

The applicability of the circuit dealt with here to any desiredcases of dynamic control of the electron stream may be shown by several simple examples. A clearly-defined differentiation of the zones in space and according to function, such as occurs in the klystron, is of course not always observed. In certain cases they may be combined, being localized in the same inter-electrode space. Thus, for example, in the triode with retarding field and the magnetron we may imagine a distribution of the zones in the spirit of Figures 2.37 and 2.38, in which the localization of the zones was designated in accordance with the following enumeration [30]:

I acceleration zone,

II modulation zone,

III conversion zone,

IV energy-transfer zone,

V purification zone

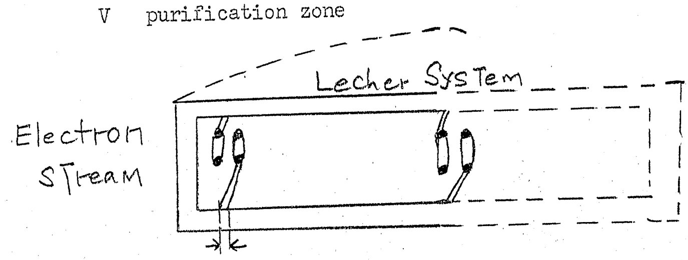

Figure 2.39

The common identify of the klystron with the electron-oscillation generators considered above is confirmed still further

Declassified in Part - Sanitized Copy Approved for Release 2012/04/09 : CIA-RDP82-00039R000200090009-2

by certain peculiarities which it discloses in its behavior:

(a) in the presence of an oscillating system tuned to a definite wave-length and of variation of the accelerating potential V_o, a number of discrete regions of oscillation are created;

(b) under conditions corresponding to optiumum output, Barkhausens's condition, $\lambda^2 V_o$ = const., is fulfilled;

(c) a continuous change in wave-length may take place only within the limits of one region of the oscillations.

Nevertheless, thanks to correct matching of the oscillating system with the electron stream the klystron, in spite of the presence of grids, possesses a considerable (20-40 percent) coefficient of efficiency by comparison with the retarding-field-circuit oscillator. Since it is related in principle to the retarding-field circuit, the two-circuit klystron (Figure 2.35) is at the same time characterized by certain peculiarities inherent in tubes with negative grids. Among these are: the possibility of using the klystron as an amplifier, the application of reverse coupling when used as an oscillator, separation of the output and input circuits.

The high quality of the oscillating systems which are used leads to the necessity of very precise tuning of both circuits to a single frequency for operation of the klystron as a generator. This fact limits its application as an amplifier, since the band-pass width is narrowed. We have already noted in Chapter I the difficulties and inconveniences which arise with endovibrators of the type used in klystrons. These inconveniences have led to the creation of various designs of the one-circuit klystron. Certain of these reproduce in principle the basic peculiarities of the two-circuit type: in them the "modulation zone" (M) and the "output zone" (G) are apart in space although they belong to one circuit. Thus, for example, are the designs of Lüdi [31] and Katsman [32], shown in Drawings 2.39 and 2.40. Other designs use essentially the retarding-field circuit, combining the zones of modulation and output and exciting a volume resonator by means of a stream "reflected" from the retarding electrode [33] (Figure 2.41). Such single-circuit klystrons have been called "reflex" klystrons.

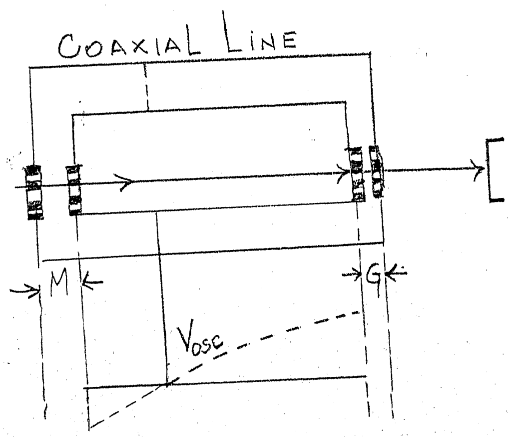

Figure 2.40

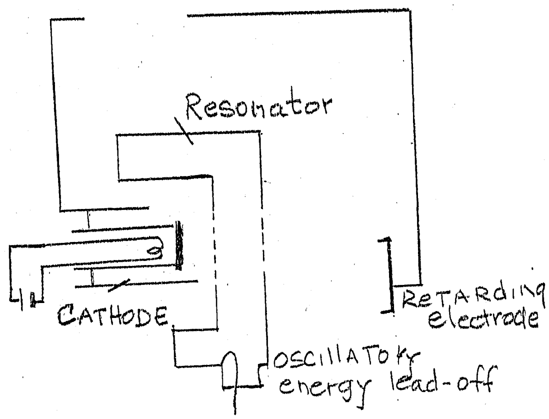

Figure 2.41

Together with electron-beam devices of the klystron type, which have been adapted for operation with volume resonators, still other electron-beam instruments which make partial or full use of the principle of dynamic control of the electron stream are known at the present time. We shall present several examples.

The Haeff amplifier [34], represented in Figure 2.42, offers a certain degree of perfection of tubes with the conventional static control, but is of interest by virtue of the design of the output circuit, in which the principle of inductive coupling of the electron stream with the oscillating circuit has been applied. The high-frequency potential being amplified is fed between the control grid G and the cathode K. A and B are the accelerating electrodes, and G is the collector, which is at a lower potential than A and B. A bi-cylindrical endovibrator with sectional inside tube E, placed on the tube, serves as the oscillating system of the output circuit. The electron stream, controlled by the grid G, interacts only with the circuit-field which penetrates through slot D over the extent of a small portion of its path, which causes almost complete absence of coupling between the input and output circuits. The device which has been described, which is controlled by a 10-watt magnetron oscillator at a frequency of 450 megacycles (λ = 67 centimeters), put 110 watts of oscillating power into the output circuit. The emission current was 150 milliamperes with 6000 volts on the electrodes A and B and 3000 volts on the collector C.

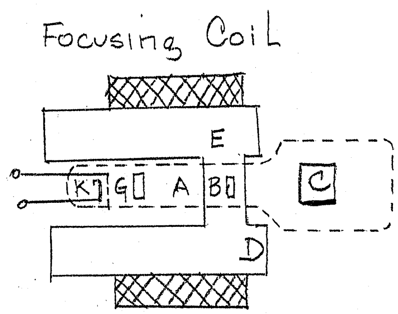

Figure 2.42

Tubes which operate on the principle of the Haeff amplifier, whose function is to operate in decimeter receivers (range λ = 25-100 centimeters), have been designed by Katsman [35] (Figure 2.43). By means of the metallic contact rings A, B, C, and D the tube is connected with the input and output circuits, which are made up in the form of rectangular boxes.

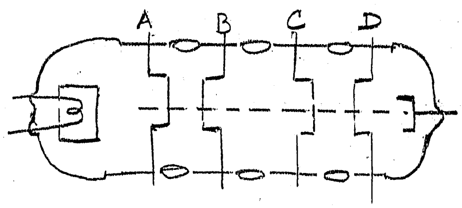

Figure 2.43

A certain improvement in the principle of velocity modulation of the electron stream is the "two-step modulation circuit". The modulating device, represented in Figure 2.44, differs from the modulating zone of the klystron by virtue of the fact that the electron stream undergoes the reaction of the alternating electric field twice: between the grid G and the cylindrical electrode B, and then, following its passage inside the latter, the electron stream passes through the second zone BG_2, where it is again exposed to the action of the alternating field. Greater effectiveness and degree of modulation are achieved by suitable selection of the voltages V_1 and V_3 (Figure 2.44) and of the time of passage inside the "Faraday cylinder" B. This time should be equal to half the period, and then the velocity of the electron will change in leaving G_2 from $\sqrt{2\frac{e}{m}(V_1+2V)}$ to $\sqrt{2\frac{e}{m}(V_1-2V)}$, where V is the amplitude of the variable difference in potentials between B and the grids.

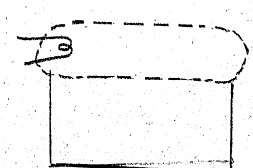

Figure 2.44

Declassified in Part - Sanitized Copy Approved for Release 2012/04/09 : CIA-RDP82-00039R000200090009-2

If the outer grids and the inner cylinder are connected to the conductors of the coaxial line, then, with a suitable choice of the time of passage of the electrons ($\sim\frac{\pi}{2}$) in the Faraday cylinder, the modulating device which has been described may act as a negative resistance, exciting oscillations in the line. The described circuit of the modulating device was applied by Hahn and Metcalf [36] in a whole series of amplifying, mixing, and oscillator tubes which operated with coaxial lines as oscillating systems.

Figure 2.45 shows a series of modulating devices tested at various frequencies by these authors. Figure 2.45a represents grids for a 5-centimeter wave, Figure 2.45b for a 30-centimeter wave, and Figure 2.45c for a 4.8 centimeter wave. The devices represented in Figures 2.45a and b operate with an angle of passage of π, and the device in Figure 2.45c with an angle of passage of 3π.

The Hahn and Metcalf amplifying tube is equipped with the two modulator devices M and K, which are connected with the input and output circuits (Figure 2.46). Thanks to the considerable distance between them, the electron beam is passed through a number of focussing electrodes; in the case of high powers magnetic focussing is also used, by means of a coil applied to the tube from outside.

Considerably more simple is the design of oscillator and mixer tubes in which use is made of the "retarding collector", to which has been given the best shape arrived at through experiment and calculational methods -- a spherical shape with a small (about

1 inch) radius. The Hahn and Metcalf oscillator tube, constructed in the usual metallic form with a standard base, is represented in Figure 2.47, where its external form (Figure 2.47b) and schematic (Figure 2.47a) are given. A tube of this type has oscillated over a very broad band of frequencies (frequency ration 5:1), with the voltages shown in the illustration and voltage variation in the Faraday cylinder, it being possible to obtain easily oscillations up to λ =14 centimeters with points in the beam of less than a milliampere.

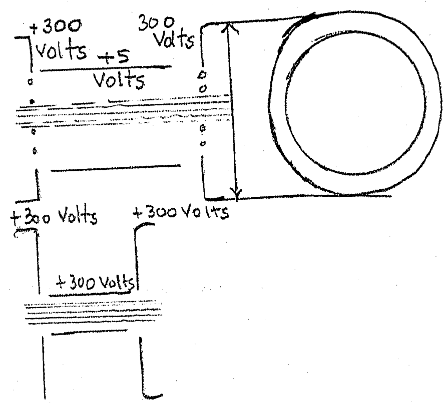

Figure 2.45

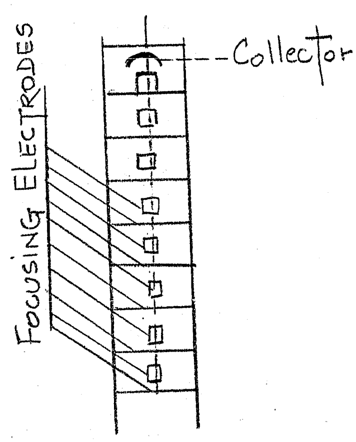

Figure 2.46

Of a similar design is the mixer tube represented in Figure 2.48. The signal is applied to grid No 1 (the detector grid), and modulates the beam with the corresponding frequency, while grid No 2 (the oscillator grid) modulates it with a heterodyne frequency. The "retarding collector" is slightly tilted toward the axis of the tube, so that the reflected beam is incident only on the oscillator gird, and not on the receiving grid. Tubes of this type have been tested at a wave-length of λ=37 centimeters with a subsequent amplification of the intermediate frequency at 18 megacycles, and have been completely satisfactory in operation.

From brief review which has been given, it may be concluded that contemporary progress in the field of sub-meter waves is indebted mainly to the development of oscillator devices with dynamic control of the electron stream. A few years ago -- in the first years after the appearance of electron-ray instruments (the klystron, Hahn and Metcalf tubes, etc.) -- it seemed that the "old" methods of generating micro-radio-waves (the circuit with reverse coupling, the retarding-field circuit, the magnetron) would revert to the background, leaving the field of activity open again. This, however, did not occur. The colossal progress of micro-radio-wave technology during World War II exposed both the strong and the weak aspects of all methods and as a result absolute preference could hardly be given to any of them. Concrete application of an oscillator of one type or another is in the last analysis determined by the function of the installation as a whole and the technical requirements imposed on it.

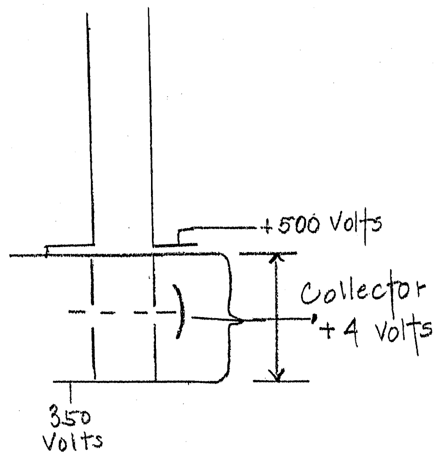

Figure 2.47

If a sufficiently compact and stable source of low-power (≦ 10 watts) oscillations in the 10-25 centimeter range is required, then tubes of special designs with negative grids and high-quality circuits may be used successfully.

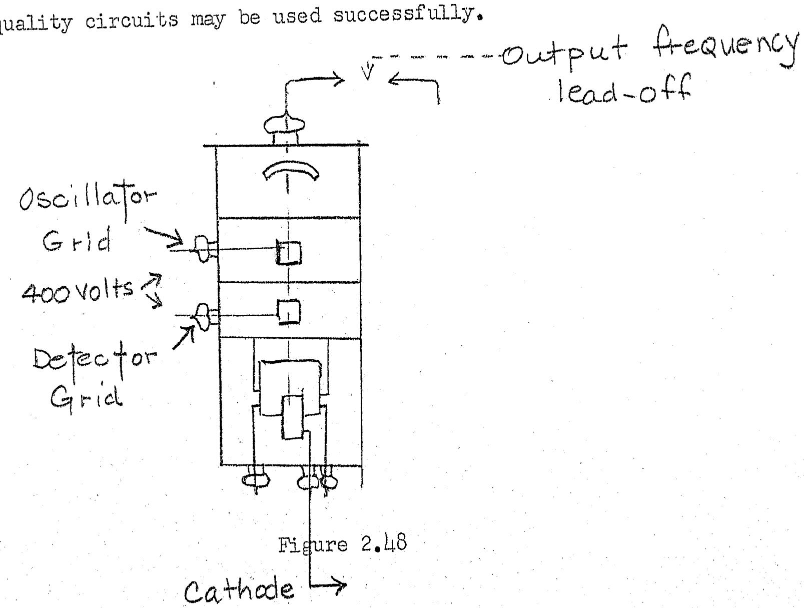

Figure 2.48

For laboratory purposes, the retarding field-circuit oscillator is extremely convenient in this same range. The magnetron makes it possible to obtain the greatest power at the shortest wave-lengths which have been obtained at the present time; its application is limited only due to the necessary presence of a magnetic-field source (an electromagnet, permanent magnet, or coil) which makes the installation somewhat bulky. Even electron-ray instruments which have approximately the same fields of application can hardly compete with the magnetron in the region of the short decimeter and centimeter waves.

With respect to obtaining the shortest waves ($\lambda \leq 1$ centimeter), the magnetron, and in particular "multi-cell" and polyphase systems, must be considered the most suitable device of all those which have been considered.

Literature Guide to Chapter II

1. H. Barkhausen and K. Kurz. Phys. ZS, 21, 1, 1920.
2. S. Zilitinkevich. TiTbp, No 18, 1923, 2; No 19, 1923, 166.
3. A. Slutskin and D. Shteynberg, Zhrfkho, VIII, 938, 1926; Ann. d. Phys. I, 658, 1929.
4. A. Zacek, ZS Hochfr. 32, 172, 1928.
5. K. Okabe, PIRE, 17, 652, 1929.
6. V. Kovalenko. IAN, s. fiz. 4, 449, 1940.
7. H. Hollmann. Sitsber. d. Pr. Ak. Wiss., Phys. Mat. Kl. VI, 1933.
8. A. Samuel. PIRE, 25, 1343, 1937.
9. B. Tsvetovskiy and N. Dzhibelli. IEST, No 5, 33, 1939.

10. I. Taraskov. "New Designs of Oscillator Tubes" (Trudy NIISO, M. 1943).
11. Devyatkov, Danil'tsev, and Khokhlov. IEST, No 2, 56, 1940.
12. Devyatkov, Gurevich, and Khokhlov. Zhtf, XI, 756, 1941.
13. Ye. Studenkov. UFN, XXIII, 417, 1940.
14. V. I. Kalinin. "Decimeter and Centimeter Waves", 1939, Chapter III.
15. V. I. Kalinin. Zhtf, III, 131, 1933.
16. K. Kohl. Ergebn d. ex. Naturwiss. 1930.
17. H. Hollmann. ZS techn. Phys. 10, 424, 1929.
18. E. Djakov. Hochfr. and Elektroak. 50, 41, 1937.
19. W. Gerber, ZS. Hochfr. 36, 98, 1930.
20. A. Lerbs and K. Lammchen. Hochfr and El. 52, 186, 1938.
21. Cleeton and Williams. Phys. Rev. 45, 234, 1934.
22. H. Richter. Hochfr and El. 51, 10, 1938.
23. K. Posthumus. Wir. Eng. 12, 127, 1935.
24. W. Runge. Telef. Ztg. 15, 3, 1934.
25. H. Gutton and S. Berline. Bull. Soc. Fr. Rad. El. 2, 30, 1938.
26. N. Kuz'min "Excitation of Electromagnetic Oscillations of Ultra-High Frequency in Polyphase Systems". Candidate's dissertation, LGU, 1941.
27. V. I. Kalinin and I. I. Vasserman. IAN, s. fiz., 1946.
28. N. Alekseyev and D. Malyarov ZhTf, X, 1297, 1940.
29. Electronics No 1, 1946.
30. V. I. Kalinin. IAN s. fiz., 93, 1946.
31. F. Ludi. Helv. Phys. Acta XIII, 498, 1940.

32. Yu. A. Katsman. IAN, s. fiz., X, 87, 1946.

33. J. Pierce. PIRE, 33, 112, 1945.

34. Yu. A. Katsman. "Tubes for Ultra-High Frequencies", Doctoral dissertation, LETI, 1945.

35. W. Hahn and G. Metcalf. PIRE, 27, 106, 1939.

CHAPTER III

INTRODUCTION TO THE ELECTRONICS OF ULTRA-HIGH FREQUENCIES

Section 3.1. Motion of the Electron in Electric and Magnetic Fields

The electron, which possesses a negative charge $e = 1.59 \times 10^{-19}$ coulombs and a mass $m = 9.03 \times 10^{-28}$ grams, situated and moving in electric and magnetic fields is exposed on the part of the latter to the action of forces which may be expressed by the following equations:

$$\left.\begin{aligned} \bar{F}_E &= e\bar{F} \\ \bar{F}_M &= e[\bar{v}\,\bar{H}] \end{aligned}\right\} \qquad (3.1)$$

Here $\bar{F}_E$ and $\bar{F}_M$ are the forces of the action of the electric and magnetic fields on the electron, $\bar{E}$ and $\bar{H}$ are the vectors of their intensity, and $\bar{v}$ is the velocity vector of the electron's motion. From these equations it may be seen that $\bar{F}_E \parallel \bar{E}$, but that $\bar{F}_M \perp \bar{v}$ AND $\bar{F}_M \perp \bar{H}$. The magnetic field acts only on an electron moving perpendicular to $\bar{H}$. In a combined field the total force acting on the electron is written as:

$$\bar{F} = \bar{F}_E + \bar{F}_M = e\left(\bar{E} + [\bar{v}\,\bar{H}]\right). \qquad (3.2)$$

The equation of motion of the electron is represented in general form in the following manner

$$\ddot{r} = \frac{e}{m}\left(\bar{E} + [\bar{v}\,\bar{H}]\right), \qquad (3.3)$$

where r is the displacement of the electron ($r^2 = x^2 + y^2 + z^2$). Projected on the axes of coordinates, equation (3.3) assumes the form:

$$\left.\begin{aligned} \ddot{x} &= \frac{e}{m}E_x + \frac{e}{m}(\dot{y}H_z - \dot{z}H_y) \\ \ddot{y} &= \frac{e}{m}E_y + \frac{e}{m}(\dot{z}H_x - \dot{x}H_z) \\ \ddot{z} &= \frac{e}{m}E_z + \frac{e}{m}(\dot{x}H_y - \dot{y}H_x) \end{aligned}\right\} \qquad (3.4)$$

In all the equations the dots denote differentiation with respect to time.

Let us analyze a number of fundamental cases.

<u>a) Motion of the Electron in an Electric Field</u>

In this case $\bar{H} = 0$ and equation (3.3) assumes the form

$$\ddot{r} = -\frac{e}{M} \operatorname{grad} V \qquad (3.5)$$

where V is the potential of the field. If V is not a function of time, equation (3.5) has an integral of kinetic energies

$$\frac{mv^2}{2} + eV(x, y, z) = const, \qquad (3.6)$$

which with certain initial values of v_0 and V_0

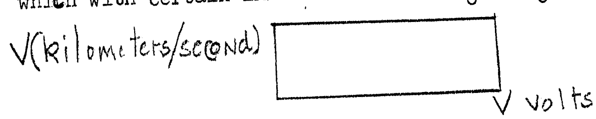

(Fig. 3.1)

lead to the equation $\frac{mv^2}{2} - \frac{mv_0^2}{2} = -e(V - V_0)$

and with $v_0 = V_0 = 0$ to the well-known expression for the speed acquired by an electron in an electric field in passage through a difference in potentials V

$$v = \sqrt{2\frac{e}{M}V} \qquad (3.7)$$

or in numerical expression

$$v_{cm/sec} = 0.594 \cdot 10^8 \sqrt{V_c}$$

Fig. 3.1 illustrates the relationship between the quantities v and V. Thus, an electron moving in an electric field in the direction of the force acting on it undergoes an acceleration and increases its kinetic energy due to the work of the field. An electron which is moving for some reason in an electric field against the force acting on it undergoes retardation and, decreasing in velocity, gives up its kinetic energy to the field. Thus there takes place -- in the simplest concept, of course -- an energy interaction of the electrons and the electric field.

b) Motion of the Electron in A Magnetic Field

From equation (3.1) it follows that the force of the action of the magnetic field on an electron is equal to

$$F_M = evH\sin\alpha \tag{3.8}$$

in magnitude, where α is the angle between $\bar{v}$ and $\bar{H}$, and the force of the field is directed perpendicular to the plane in which both these vectors lie. Let the direction of the magnetic field be along the axis OZ (Fig. 3.2).

Then: $H = H_z;\ H_y = H_x = 0,$

and the equations of motion are reduced to the following:

$$\ddot{x} = \frac{e}{m}\dot{y}H;\ \ddot{y} = -\frac{e}{m}\dot{x}H;\ \ddot{z} = 0 \tag{3.9}$$

If at the initial moment the electron was at the origin of the coordinates and possessed a velocity v_0, forming with $\bar{H}$ an angle , its subsequent motion will be determined by the equations:

$$\begin{aligned} x &= \frac{m}{eH} v_0 \sin\alpha \sin\left(\frac{eH}{m}t - \beta\right) \\ y &= \frac{m}{eH} v_0 \sin\alpha \cos\left(\frac{eH}{m}t - \beta\right) \\ z &= v_0 t \cos\alpha \end{aligned} \tag{3.10}$$

Here β is the angle formed by the projection of the velocity v_0 on the plane XOY with the X-axis (Fig. 3.2).

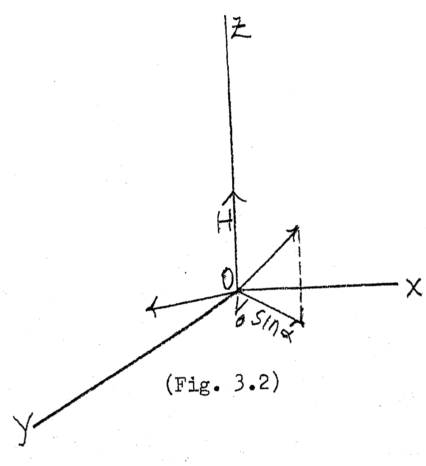

(Fig. 3.2)

Declassified in Part - Sanitized Copy Approved for Release 2012/04/09 : CIA-RDP82-00039R000200090009-2

The electron's trajectory, determined by the equations of (3.10), has the form of a helical line coiled on a round cylinder for which the axis OZ serves as the axis, and whose base in the plane XOY is the circle which is the projection of the trajectory on this plane. The equation of this circle is

$$x^2+y^2=\left(\frac{m}{eH}\right)^2 v_0^2 \sin^2\alpha \qquad (3.11)$$

Its radius is $r=\frac{m}{eH} v_0 \sin\alpha$

The projection of the electron on the plane XOY moves uniformly about the plane with a velocity $v_0 \sin\alpha$. The motion along the lines of force of the magnetic field, i.e. along the axis OZ, takes place with a uniform velocity $v_0 \cos\alpha$. The relationship between the vectors $\bar{v}$ and $\bar{H}$ and the direction of the revolution of the electron along the helical line is shown in Fig. 3.3. In this figure v_H and $v_\perp$ are the components of velocity of the electron in the direction of the magnetic field and in the direction perpendicular to this field. It is not difficult to see that the angular velocity of rotation of the electron about the axis of the cylinder is constant and equal to

$$\omega_H=\frac{He}{m} \qquad (3.12)$$

This frequently encountered value may be called the "inherent angular velocity of the magnetic field H", which may be expressed numerically (if H is given in oersteds) as

$$\omega_H=17.6\cdot 10^6 H_{oersteds}$$

and the frequency and period which correspond to it are:

$$f_{H_{hertz}}=2.8\cdot 10^6_{oersteds} \text{ and } T_{H_{sec}}=\frac{0.358\cdot 10^{-6}}{H_{oersteds}}$$

As a result of the action of the magnetic field on the moving electron, the latter accomplishes periodic motion with an angular velocity of ω_H. Considering it as in ideal classical oscillator, the length of the electromagnetic wave radiated by it may be expressed as:

$$\lambda_{centimeters}=\frac{2\pi c}{\omega_H}=\frac{2\pi c m}{e H}=\frac{10{,}650}{H_{oersteds}}$$

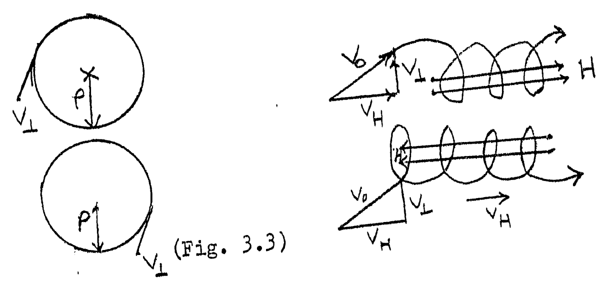

(Fig. 3.3)

In the special case where $\alpha = \frac{\pi}{2}$, i.e. the initial velocity of the electron lies in the plane XOY perpendicular to H, the electron describes a flat circular orbit with radius $r = \frac{mV_0}{eH}$ and the same angular frequency ω_H.

The magnetic field, as follows from what has been set forth, changes only the direction of the component of velocity of the electron which is perpendicualr to the lines of force of the field, and in so doing does not change its magnitude; the component of velocity of the electron which isparallel to the lines of force remains completely unchanged. Thus, the reaction of the magnetic field does not change the kinetic energy of the electron and may be utilized only curving the trajectory of the electron.

c) Motion of the Electron in Homogeneous Electric and Magnetic Fields

Let us consider the mutual effect of electric and magnetic fields on an electron. For purposes of simplicity let us analyze the case of mutually perpendicular electric and magnetic fields, practically the most interesting. Let $H=H_z$, $E=E_x$, and other components be lacking: $H_x=H_y=E_z=E_y=0$. We shall assume that at the initial moment the electron is passing through the origin of the coordinates with velocity $v_0 \perp H$. Then the motion of the electron should take place in the plane XOY, perpendicular to H. The equations of motion will take the form:

$$\begin{aligned} \ddot{x} &= \frac{e}{M}E + \frac{e}{M}H\dot{y} \\ \ddot{y} &= -\frac{e}{M}H\dot{x} \\ \ddot{z} &= 0 \end{aligned} \qquad (3.13)$$

By virtue of the conditions postulated the last equation gives z=0; from the first two, by means of the appropriate operations, the coordinates of the electron are obtained:

$$\left.\begin{aligned} x &= \frac{1}{\omega_H}\dot{x}_0 \sin\omega_H t + \left(\frac{e}{M}\cdot\frac{1}{\omega_H^2}\cdot E + \frac{1}{\omega_H}\cdot\dot{y}_0\right)(1-\cos\omega_H t) \\ y &= \left(\frac{1}{\omega_H^2}\cdot\frac{e}{m}E + \frac{1}{\omega_H}\dot{y}_0\right)\sin\omega_H t - \frac{1}{\omega_H}\cdot\dot{x}_0(1-\cos\omega_H t) - \frac{E}{H}t \end{aligned}\right\} \quad (3.14)$$

From the equations of (3.14) the equation of the trajectory may be obtained in the form:

$$(x-a)^2 + (y-b)^2 = \rho^2$$

where

$$\left.\begin{aligned} a &= \frac{1}{\omega_H}\left(\dot{y}_0 + \frac{E}{H}\right), \quad b = -\frac{1}{\omega_H}\left(\dot{x}_0 + \frac{e}{M}Et\right) \\ \rho^2 &= \frac{2}{M}\cdot\frac{1}{\omega_H^2}\cdot\left(\frac{mv_0^2}{2} + \frac{m\dot{y}_0}{H}\cdot E + \frac{M}{2H^2}\cdot E^2\right) \end{aligned}\right\} \quad (3.15)$$

The trajectory which has been obtained is described by a point on a rolling circle of radius ρ whose center has the coordinates a and b, i.e. is displaced rectilinearly and uniformly along a straight line parallel to the axis OY, i.e. along the equipotential straight line, with velocity $\frac{E}{H}$, being located at a distance a from the axis OY. The angular velocity of rotation [redacted] of the circle is constant and equal to the same value $\omega_H = \frac{He}{m}$.

If the initial velocity $v_0 = \dot{y}_0$ is parallel to the axis OY, i.e. perpendicular to the electric and magnetic fields, then the expressions of (3.15) become somewhat more simple:

$$a = \frac{1}{\omega_H}\left(\dot{y}_0 + \frac{E}{H}\right); \quad b = -\frac{E}{H}t; \quad \rho = a = \frac{1}{\omega_H}\left(\dot{y}_0 + \frac{E}{H}\right) \qquad (3.16)$$

In this case it is possible to obtain cycloidal curves of various shapes, depending on the relationship of the values of $\dot{y}_0$ and $\frac{E}{H}$, which is illustrated by Fig. 3.4.

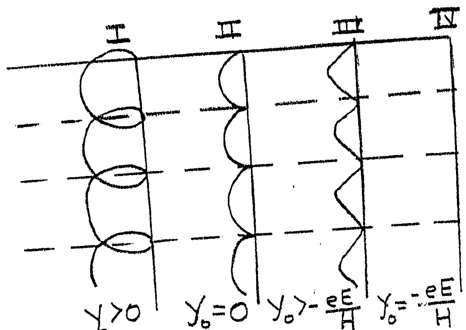

(Fig. 3.4)

Curve I corresponds to the case where $\dot{y}_0 > 0$ -- the electron had initially a velocity in the positive direction of the axis OY; in this case a curve with loops is obtained. The case of an electron initially at rest, when $\dot{y}_0 = 0$, yields an ordinary cycloid without slippage (Curve II). When there is an initial velocity in the direction of the negative semi-axis of OY, either a stretched-out cycloid is obtained when $|\dot{y}_0| < \left|\frac{E}{H}\right|$ (Curve III), or the trajectory degenerates into a straight line, $|\dot{y}_0| = \left|\frac{E}{H}\right|$ (Curve IV).

In the case of an ordinary cycloid, i.e. when $\dot{y}_0 = 0$, we have:

$$\left.\begin{aligned} x &= \frac{e}{m} \cdot \frac{1}{\omega_H^2} \cdot E\,(1 - \cos \omega_H t) \\ y &= -\frac{e}{m} \cdot \frac{1}{\omega_H^2} \cdot E\,(\omega_H t - \sin \omega_H t) \\ \rho &= \frac{E}{\omega_H H} = \frac{Em}{eH^2} \end{aligned}\right\} \qquad (3.17)$$

Thus, motion of an electron in mutually perpendicular electric and magnetic fields is made up of two components: uniform motion along a "guide", i.e. along the straight line along which the circle which describes the cycloid is rolling with velocity $\frac{E}{H}$, and uniform rotation along a "rolling circle" of radius ρ with angular velocity ω_H.

Section 3.2 Very Simple "Electron-Kinematic Mechanisms"

The problem of generating micro-radio-waves is linked closely, historically and in essence, with the solution of the problem of the

Declassified in Part - Sanitized Copy Approved for Release 2012/04/09 : CIA-RDP82-00039R000200090009-2

motion of an electron in electric and magnetic fields. Particularly interesting in this respect are cases of periodic motion. In the preceding section we have already seen that the action of a magnetic field leads to rotation of the electron with an angular velocity ω_H or introduces into its motion a periodic component characterized by the same angular frequency ω_H.

It is not difficult to see that any periodic motion of an electron in [redacted] an inter-electrode space which is fed with electric fields applied to the instrument may be evaluated to a first approximation as the cause of the occurrence in the attached conductors of alternating currents of the corresponding frequencies, i.e. as the basic operating process in very simple kinematic mechanisms of electron oscillations. Let us consider several such very simple mechanisms.

A. The Retarding-Field Circuit

According to the original concepts of many authors (A review of the basic work and theories may be seen in Kalinin, V.I. "Decimeter and Centimeter Waves". Svyaz'izdat, 1939, Chap. III and IV.) oscillations in the retarding-field circuit are due to periodic "agitation" of the electrons about the grid -- the electrode with the highest positive potential. A similar line of reasoning proceeds from consideration of the motion of a single electron which is not affected by the reaction of other electrons and connected oscillating systems, by virtue of which the potentials of all the electrodes are assumed to be constant.

(Fig. 3.5)

Let us imagine for purposes of simplicity a flat system of electrodes (Fig. 3.5) between which the electric field possess a linear distribution of potential. The plane K -- the cathode -- possesses a potential equal to zero and is a source of electrons with zero initial velocity. The accelerating electrode A (the grid) has a constant positive potential V_0, and the retarding electrode B (the anode) a potential V_b, which is capable of being negative as well. An electron leaving the cathode will move in the space KA with an acceleration

$$a_1 = \frac{e}{m} \cdot \frac{V_0}{d_1}$$

passing through the distance KA during the time τ_1, which is fixed in the following manner

$$\tau_1 = \sqrt{\frac{2d_1}{a_1}} = \sqrt{\frac{2m}{e}} \cdot \frac{d_1}{\sqrt{V_0}} = \frac{2}{0.594 \cdot 10^8} \cdot \frac{d_1}{\sqrt{V_0}} \text{ Sec.} \qquad (3.18)$$

In the space AB the electron undergoes retardation and reaches the point C, which possesses a zero potential, during the time τ_2, which is equal to

$$\tau_2 = \frac{2}{0.594 \cdot 10^8} \cdot \frac{d_2}{\sqrt{V_0}} \cdot \frac{V_0}{V_0 - V_b} \text{ sec.} \qquad (3.19)$$

Taking into consideration that the period of electromagnetic oscillations, T, is determined by the period of "complete agitation" of the electron, we obtain

$$T = 2(\tau_1 + \tau_2) \qquad (3.20)$$

which leads to the following expression for the wave-length:

$$\lambda_{cm} = cT = \frac{2000}{\sqrt{V_0}} \cdot \frac{(d_1 + d_2)V_0 - d_1 V_b}{V_0 - V_b} \qquad (3.21)$$

In the case of $V_b = 0$ this expression is simplified

$$\lambda_{cm} = \frac{2000}{\sqrt{V_0}} (d_1 + d_2) \qquad (3.22)$$

Consideration of the motion of a single electron in the retarding-field circuit leads to similar expressions for the length of the waves generated. Worthy of notice is the fact that the values of λ obtained from these expressions are in satisfactory agreement with the experimental data of many authors [1], in spite of the rough arrangement of this mechanism.

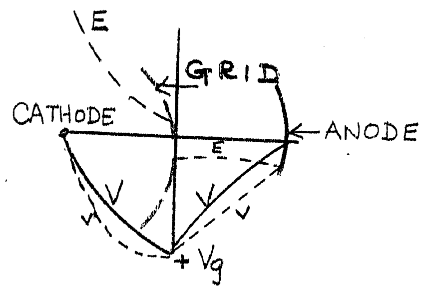

(Fig. 3.6)

In making the transition to cylindrical electrodes, with which it is more often necessary to deal in practice, the essence of the calculational process does not alter, and only the mathematical side is complicated, since it becomes necessary to consider the motion of an electron in fields with a logarithmic distribution of potential, which involves a corresponding complication of the nature of motion of the electron. Fig. 3.6 gives curves of the distribution of the potential V, the intensity of the field E, and the velocity of the electrons v for the case of cylindrical electrodes. A calculation of the "agitation" time of an electron in the retarding-field circuit has been performed by Zilitinkevich [2] and Scheibe [3]. According to Zilitinkevich the wave-length of the electron "agitations" is expressed as

$$\lambda = \frac{1000}{\sqrt{V_0}} \left(\frac{\delta_f}{\alpha_1} + \frac{\delta_p}{\alpha_2} \right) \qquad (3.23)$$

Here δ_f and δ_p are the distances from the surface of the grid

Declassified in Part - Sanitized Copy Approved for Release 2012/04/09 : CIA-RDP82-00039R000200090009-2

to the surfaces of zero potential around the cathode and around the anode, the quantities α_1 and α_2 depending on the geometry of the tube and being determined in the following manner:

$$\left.\begin{aligned} \alpha_1 &= \frac{2a_f}{\delta_f}\left[\frac{1}{3}\ln\frac{r_g}{a_f} + \frac{1}{1.5}\left(\ln\frac{r_g}{a_f}\right)^2 + \frac{1}{1.2.7}\left(\ln\frac{r_g}{a_f}\right)^3 + \dots\right] \\ \alpha_2 &= \frac{2a_p}{\delta_p}\left[\frac{1}{3}\ln\frac{r_g}{a_p} + \frac{1}{1.5}\left(\ln\frac{r_g}{a_p}\right)^2 + \frac{1}{1.2.7}\left(\ln\frac{r_g}{a_p}\right)^3 + \dots\right] \end{aligned}\right\} \quad (3.24)$$

where r_g is the radius of the grid, a_f is the radius of the surface of zero potential around the cathode, and a_p is the radius of the surface of zero potential between the grid and the anode (the return surface).

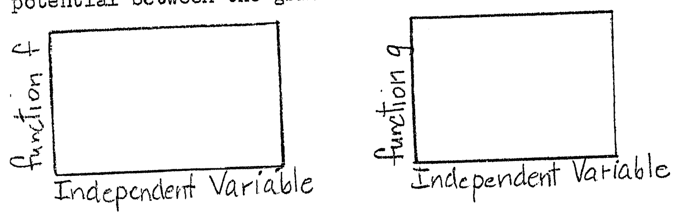

(Fig. 3.7)

Scheibe arrived at the formula

$$\lambda = \frac{1000\, r_g}{\sqrt{V_0}}\left[f(x) + g(y)\right], \qquad (3.25)$$

in which the functions f and g are determined by Table 3.1 and by the curves of Fig. 3.7. Their independent variables x and y depend on the geometry of the tube and are expressed as:

$$x = \sqrt{\ln\frac{r_g}{r_k}}\ ; \quad y = \sqrt{\frac{V_0}{V_0 - V_b}\cdot\ln\frac{r_b}{r_g}} \qquad (3.26)$$

r_k, r_g, r_b are the radii of the cathode, grid, and retarding electrode.

Table 3.1

TABLE OF THE FUNCTIONS f AND g

Independent Variables	Function f	Function g	Independent Variables	Function f	Function g
0	0	0	1.8	0.62419	40.36
0.1	0.00993	0.010	2.0	0.60268	98.01
0.5	0.21228	0.289	3.0	0.534	--
0.8	0.42568	0.988	4.0	0.516	--
1.0	0.53808	2.030	5.0	0.510	--
1.2	0.60872	4.080	7.0	0.504	--
1.5	0.65237	12.190	∞	0.500	--

Declassified in Part - Sanitized Copy Approved for Release 2012/04/09 : CIA-RDP82-00039R000200090009-2

All of the formulas which have been given for determining the wave-length have a common structure, which may be expressed by the Barkhausen relationship

$$\lambda\sqrt{V_0} = const. \qquad (3.27)$$

according to which the length of the generated wave, for a given geometrical structure of the electrodes which determine the constant, is related by a continuous function to the accelerating potential applied to the circuit.

B. Radial Electron Processes in the Magnetron

The periodicity of motion of an electron in the retarding-field circuit is caused by the combination of successive effects of the accelerating and retarding fields. In the magnetron a similar effect is obtained by the joint simultaneous action of the electric and magnetic fields on the electron. In the usual form the magnetron is an axially symmetrical system consisting of a cathode and a cylindrical anode which is continuous or broken up by longitudinal slots into some, usually even, number of segments. Magnetrons with a flat electrode construction have been used by only a few authors [4].

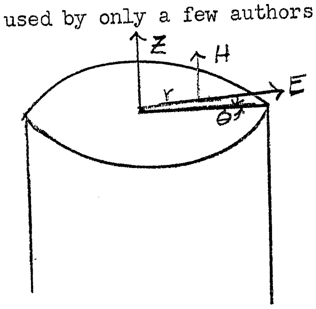

(Fig. 3.8)

The magnetic field is usually directed parallel to the cathode or at a slight angle to it. Assuming that $\bar{H}$ is parallel to the filament and associating a system of cylindrical coordinates r, θ, and z (Fig. 3.8) with the diode, it is possible according to Hull [5] to formulate the following equations for the motion of an electron leaving a point at a distance r_0 (radius of the cathode) with an initial velocity equal to zero:

$$\frac{1}{2}\frac{M}{e}\left[\frac{d}{dt}\left(\frac{dr}{dt}\right)^2 + 2r\left(\frac{d\theta}{dt}\right)^2\right] = E - Hr\frac{d\theta}{dt}$$

$$\frac{M}{e}\cdot\frac{d}{dt}\left(r^2\frac{d\theta}{dt}\right) = -r\frac{dr}{dt}H \qquad (3.28)$$

$$\frac{d^2z}{dt^2} = 0$$

By virtue of the complete axial symmetry of the system and the homogeneous radiation of electrons in all directions by the filament, the chief interest lies in the radial component of motion of the electron. Integration of the equations of (3.28) in the assumption that the electron leaves the filament with zero velocity leads to the following expression for the radial velocity of the electron

$$V_r^2 = \left(\frac{dr}{dt}\right)^2 = 2\frac{e}{M}V_r - H^2\left(\frac{e}{2M}\right)^2 r^2\left(1 - \frac{r_0^2}{r^2}\right)^2. \qquad (3.29)$$

Here V_r is the potential relative to the cathode at point r. The curvature of the trajectories of the electrons caused by the magnetic field becomes so large at a certain value of intensity of the latter, H_k, that the trajectory is confined to the inter-electrode space which is enclosed by the inner surface of the anode (Fig. 3.9). It is obvious that as a condition of this the radial velocity must be equal to zero when the electron reaches the anode:

$$\frac{dr}{dt} = 0, \quad V_r = V_a \quad \text{and} \quad r = r_a$$

The corresponding value of intensity of the magnetic field H_k bears the designation of critical value and may be obtained from expression (3.29). If we neglect the member r_0^2/r^2, which is entirely possible in the case where $r_0 < r$, then the expression for H_k will have the form

$$H_k = \sqrt{\frac{8M}{e}\cdot\frac{V_a}{r_a^2}} \qquad (3.30)$$

or in practical units

$$H_{k\,(oersteds)} = \frac{6.72}{r_{a\,(cm)}} \sqrt{V_{a\,(volts)}} \tag{3.31}$$

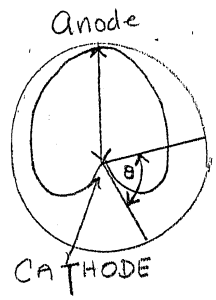

(Fig. 3.9)

The trajectory described during this by the electron (Fig. 3.9) is similar to a cardioid, lies in a plane perpendicular to the axis of the system, and is described by the equation

$$r = r_{max} \sin \tfrac{2}{3} \theta^{3/2} \tag{3.32}$$

The angular velocity of motion of the electron along this trajectory is

$$\frac{d\theta}{dt} = \frac{He}{2M}\left(1 - \frac{r_0^2}{r^2}\right) \tag{3.33}$$

and remains practically constant, changing only in the immediate vicinity of the cathode.

Thus, at any moment the velocity of the electron is made up of a radial and a tangential component. The role of these components is determined by the corresponding mode of operation of the magnetron. The following basic modes of electron oscillations of the magnetron are distinguished (i.e. oscillations in which the leading role is played by the inertia of the electrons): (a) electron Oscillations of the first order whose periodicity is related to the radial component of motion of the electrons, and (b) electron oscillations of higher orders, in whose process of occurrence and maintenance the tangential component of the electrons plays an important role. This, of course, is the elementary and schematic difference -- the details will be discussed later on.

In the case of electron oscillations of the first order the situation is defined by the periodicity of revolution of an electron about its cardioidal trajectory, represented in Fig. 3.9. The period of the oscillations may be taken to be twice the time of transit of the electron from the cathode to the anode, which for critical conditions is equal to $\tau = \int_{r_0}^{r_a} \frac{dr}{V_r}$,

Assuming for purposes of simplicity that $r_0=0$ or $r=\infty$ (which corresponds to the case of flat electrodes), Okabe found that the transit time τ yields in both cases the single expression

$$\tau = \frac{\pi M}{eH} \tag{3.35}$$

Hence, the period of revolution of an electron along the cardioidal trajectory is

$$T = 2\tau = \frac{2\pi M}{eH} = \frac{2\pi}{\omega_H} \tag{3.36}$$

The periodicity of motion of an electron is determined in this case by the same angular frequency ω_H.

Oscillations of the first order, observable in magnetrons, independently of the number of segments, occur under conditions close to the critical, and have a wave-length of $\lambda = \frac{2\pi cM}{eH}$ or

$$\lambda_{CM} = \frac{10650}{H_{oersteds}} = \frac{C_0}{H} \tag{3.37}$$

were C_0 is the so-called "Okabe constant".

In formula (3.37) the formula $H=H_k$ also includes, in this manner, a function of geometrical factors. Actually

$$\lambda = \frac{10650}{6.72\sqrt{V_a}} \tag{3.38}$$

which likewise leads, just as in the case of the retarding-field circuit, to the Barkhausen relationship $\lambda\sqrt{V_0}$= const. This is one of the most important evidences of the analogy between phenomena in the retarding-field circuit and electron oscillations of the first order in the magnetron.

The Okabe constant C_0, theoretically equal to 10,650, proves on the basis of experimental data to be equal to an average of 13,000, although rather considerable deviations from this value are observed on both sides (from 7,000 to 16,000). The nature of the wave-length function obtained under critical conditions of oscillation, then, with respect to the intensity of the magnetic field, which may be determined by formula (3.37), is confirmed rather well in practice.

Using the analogy between the magnetron and the retarding-field circuit, it may be shown rather simply that the so-called Okabe constant represents a value which, like the Barkhausen constant, is a function of the geometry of the tube. The curve of the variation of the radial component of velocity of the electron when it moves from the cathode to the anode under critical conditions, as represented for example in Fig. 3.10, exhibits a maximum at a certain distance r_m from the cathode, and then goes to zero at the anode. The quantity r_m may be found from the formula

$$r_M = \frac{r_a}{\sqrt{2 \ln \frac{r_a}{r_0}}} \qquad (3.39)$$

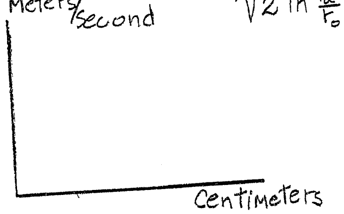

(Fig. 3.10)

Turning our attention away from the presence of a magnetic field, we may ascribe the variation in radial velocity of the electron which we have been considering to the action of some equivalent electric field whose potential V_{re} at every point r may be determined from the relationship [6]

$$v_r = \sqrt{2 \frac{e}{M} V_{re}} \qquad (3.40)$$

Hence, putting $r_0 < r$ on the basis of formula (3.29), we obtain

$$V_{re} = V_a \frac{\ln r/r_0}{\ln r_a/r_0} - H^2 \frac{e}{8M} r^2$$

which under critical conditons reduces to

$$V_{re} = V_a \left(\frac{\ln r/r_0}{\ln r_a/r_0} - \frac{r^2}{r_a^2} \right). \qquad (3.41)$$

At the point r_m, which may be determined from equation (3.39), this equivalent potential will have the maximum value

$$V_{rem} = V_a \left(1 - \frac{\ln\sqrt{2z}}{z} - \frac{1}{2z}\right) = CV_a \qquad (3.42)$$

Here we substitute z for $\ln\frac{r_a}{r_o}$ for the sake of brevity. The value $C = 1 - \frac{\ln\sqrt{2z}}{z} - \frac{1}{2z}$ is a purely geometrical parameter of the tube. The course of the curve of equivalent potential V_{re} is represented with a dotted line in Fig. 3.10, from which it may be seen that this curve may be approximated rather closely by two straight lines. Thus, we replace the magnetron with an equivalent flat system with retarding field, whose grid is located at the point r_m and has the potential V_{rem}. Then both the Okabe relationship (3.37) and the Barkhausen relationship (3.22) must be applied to the periodic "agitation" of the electrons in this equivalent system; on the basis of these relationships it is possible to express the wave-length by means of any one of the following relationships:

$$\left.\begin{aligned} \lambda &= \frac{C_o r_a}{6.72\sqrt{V_a}} \\ \lambda &= \frac{2000\,(r_a - r_m)}{\sqrt{CV_a}} \end{aligned}\right\} \qquad (3.43)$$

Comparing these expressions to each other, we find a connection between the Okabe constant C_o and the geometry of the tube

$$C_o = 13{,}440 \left[\frac{1 - \frac{1}{\sqrt{2z}}}{\sqrt{1 - \frac{\ln\sqrt{2z}}{z} - \frac{1}{2}}}\right] \qquad (3.44)$$

The limit value of the Okabe constant at $r_o \to 0$ proves in accordance with this formula to be equal to 13,440, i.e. is in considerably better agreement with experimental data than was the case with Okabe's calculations. Thus, for example, for the concrete case where $r_a = 0.5$ centimeters and $r_o = 0.005$ centimeters, the following data are obtained by the caluculation method: C=0.651; rm = 0.164; V_{em} = 0.651 V_a; $C_0 \approx$ 11,300.

The comparison given here of the magnetron under conditions of electron oscillations of the first order with the retarding-field circuit may also be extended, within the limits of the existence of oscillations of the first order, to conditions somewhat different from the critical. In these cases we may put $h=kH_k$, where k is not equal to unity but close to it. Then the expressions for the values r_m, V_{re}, and V_{rem} will assume a somewhat different form:

$$r_m = \frac{r_a}{k\sqrt{2z}} \tag{3.45}$$

$$V_{re} = V_a\left(\frac{\ln r/r_0}{z} - k^2\frac{r^2}{r_a^2}\right)$$

$$V_{reM} = V_a\left(1 - \frac{\ln\sqrt{2z}}{z} - \frac{1}{2z} - \frac{\ln k}{z}\right) = V_a C'$$

$$C' = C - \frac{\ln k}{z}$$

The region of application of these expressions, just as that of the whole of the equivalent retarding-field circuit which has been described, is naturally limited to conditions close to the critical, i.e. just to those which correspond to electron oscillations of the first order. Taking into consideration the role of the radial component of motion of the electrons in the kinematic process here described, oscillations of the first order may be characterized as "radial" oscillations.

C. Tangential Processes in the Magnetron

When the intensity H of the magnetic field, increasing, passes through the critical value, then all electrons emitted by the filament are forced to return from some cylindrical surface whose radius is inversely proportional to H. In consequence of the fact that the radial velocities of the electrons are equal to zero, there is formed in the region of this return surface a kind of rotating "virtual cathode" (the tangential velocity is not equal to zero). Looking upon the process obtained in the course of this as a simple picture of gradual contraction of the Hull cardioids, with preservation of the angular velocity and periodicity determined by the quantity ω_H, proves to be of no assistance. For the electrons which pass into the

Declassified in Part - Sanitized Copy Approved for Release 2012/04/09 : CIA-RDP82-00039R000200090009-2

outer regions of the virtual cathode a situation is created which is reminiscent of the case taken up in Section 3.1. We shall apply this case as a whole to the corresponding conditions in flat systems. With cylindrical coordinates, then, the electric field at a distance from the cathode is almost uniform, and therefore it may be assumed to a first approximation that the guiding line along which the circle which forms the cardioid is rolling and which always coincides with the equipotential line of the electric field, is transformed here into a circle of radius r on which the arcs of the cycloid rest. Depending on the relationships of the various values, it is possible to obtain cases which correspond to those taken up in Section 3.1, B. Fig. 3.11 represents the trajectory of the electron: it moves along a cycloid the height of whose arc is $b = \frac{2Em}{eH^2}$. The linear velocity of displacement of the center of the rolling circle along the guiding line is equal to $\bar{v}$, and the angular velocity $\bar{\omega} = \frac{\bar{v}}{r}$. The following cases, represented in Fig. 3.11, are possible:

(a) $b > \frac{\bar{v}}{\omega_H}$; (b) $b = \frac{\bar{v}}{\omega_H}$; (c) $b < \frac{\bar{v}}{\omega_H}$; (d) $b = 0$

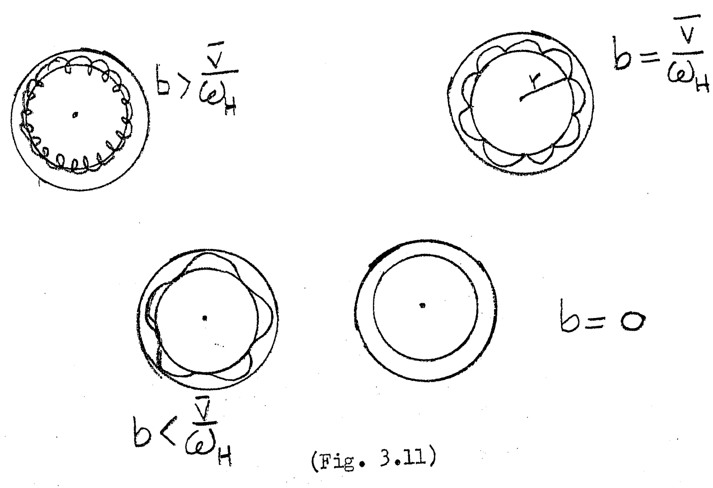

(Fig. 3.11)

For the case of a very small b or $\bar{\omega} < \omega_H$ we may take as a first approximation:

$$\bar{V} = \frac{E}{H} \quad \text{and} \quad \bar{\omega} = \frac{E}{Hr} \tag{3.46}$$

i.e. we may obtain relationships analogous to the case of homogeneous fields. However, in order that rotation along the guiding line be accomplished with constant velocity it follows from the relationships of (3.46) that the intensity of the electric field must increase linearly with distance.

$$E = H\bar{\omega}r \tag{3.47}$$

which, under conditions of the usual logarithmic distribution of potential and in the absence of a space charge between the cylindrical electrodes, cannot take place. If the path of the curve of intensity of the electric field required by equation (3.47) (curve b in Fig. 3.12) plotted together with the actual variation in intensity (curve a in Fig. 3.12), it turns out that only at the one point c does the quantity E satisfy the relationship of (3.47). Only at this distance from the axis is it possible, it would seem, for there to be stable motion along one of the trajectories shown in Fig. 3.11. Actually, however, this not the case. The crux of the matter is that we can do nothing in this case with the original hypotheses as to the complete absence of a space charge (consideration of the motion of a lone electron) and are forced to admit the existence of some space charge which manifests itself to a first approximation in a change in the path of potential and field intensity between the electrodes. Let us assume for simplicity that the density of the space charge is constant in the entire space between the electrodes. Then, proceeding from Gauss' theorem, it is not difficult to show that the intensity of the electric field at any point r will be expressed as

$$E = \frac{2V_a r}{r_a^2}, \tag{3.48}$$

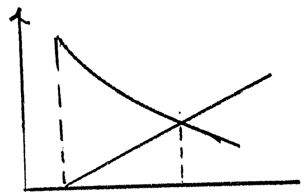

(Fig. 3.12)

i.e. that E varies proportionally to r, as is required in accordance with formula (3.47). In this case we may speak of a constant angular velocity ω at various distances r from the axis, i.e. of the rotation of the entire aggregate of electrons as a whole (See Chapter VIII). Thus another periodicity arises which is associated now only with the tangential component of motion of the electron. It is determined by the angular frequency of rotation along the guiding circle, which frequency may be expressed, taking into consideration the relationships of (3.46) and (3.48), as

$$\bar{\omega} = \frac{E}{Hr} = \frac{2V_a}{Hr_a^2} \qquad (3.49)$$

The wave-length which corresponds to this angular frequency, then, is

$$\bar{\lambda}_{cm} = \frac{942\,r_a^2 H}{V_a} \qquad (3.50)$$

A glance at formula (3.50) instantly reveals an essentially different dependency of λ on H than there was for oscillations of the first order from the Okabe relationship. Naturally, such a "tangential" electron mechanism is of interest only with respect to magnetrons with sectional anodes. The number of segments m, or what is used more frequency, the number of pairs of segments $p = \frac{m}{2}$, will play an essential role here.

Declassified in Part - Sanitized Copy Approved for Release 2012/04/09 : CIA-RDP82-00039R000200090009-2

As a matter of fact, the oscillating process, determined by only the one quantity , may take place only when b=0. If then $b \neq 0$ the phenomenon is characterized by two angular frequencies: $\bar{\omega}$, the frequency of revolution along the guiding line, and ω_H, the frequency of revolution of the rolling circle. If the guiding circle is made up of an integral number of arcs of the

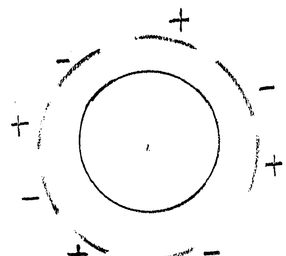

(Fig. 3.13)

cycloid, then there must be between $\bar{\omega}$ and ω_H some multiple relationship. It may be found from the following deliberations. Let the oscillating system connected to the anode segments have an inherent frequency of ω. Then we designate as the order of frequency n the ratio of the frequency ω_H, which determines the oscillations of the first order, to the given frequency ω

$$n = \frac{\omega_H}{\omega}. \qquad (3.51)$$

On the other hand, however, this matter is related in practice to the number of anode segments, since with the customary wiring of the oscillating system adjacent segments are always connected to opposite circuit leads. Therefore, in order to maintain the frequency ω by means of the "tangential" electron mechanism which we are discussing it is necessary that the angular frequency of rotation of the mechanism $\bar{\omega}$ be synchronized with the frequency of the circuit. The condition of such synchronization is the relationship

$$\frac{\omega}{p} = \bar{\omega} \qquad (3.52)$$

(Where p is the number of pairs of segments or pairs of slots). From the relationships of (3.51) and (3.52) it follows that upon excitation of oscillations of the n-th order in a 2p-segment magentron there must occur the following relationship between the basic frequencies which characterize the tangential electron mechanism

$$\frac{\omega_H}{np} = \bar{\omega} \qquad (3.53)$$

All of the deliberations given above may be properly applied to an electron which, being at a distance r from the axis of the system, has been included in the operation of the "tangential" mechanism and has begun to described a trajectory of the type represented in Fig. 3.13. This figure represents the case where n = 1, p = 4, and consequently $\omega_H = 4\bar{\omega}$. In this case maintenance of the oscillations stems from the fact that the cycloid enters into the region of the intersegmental alternating electric field at a place where at the given moment the field exercises a retarding effect, i.e. the electron in these slots gives its energy off to the field. Opposite the "accelerating" slots, on the other hand, it moves off into the tube, i.e. passes through a zone whose field is weaker. It is interesting to note that in multi-segmental systems oscillations may take place even when $n < 1$, if only the product np is equal to or greater than 1. Thus, for example, in quadri-segmental magnetrons oscillations of a "half order" are observed with $n = \frac{1}{2}$ [7], which leads for p=2 to the condition $\omega_H = \bar{\omega}$. This case may be illustrated by Fig. 3.14.

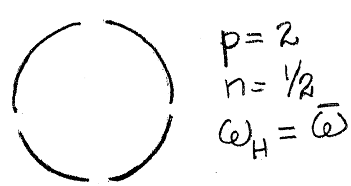

(Fig. 3.14)

Taking into consideration equation (3.50), a formula may be obtained from the condition of synchronization (3.52) for the wavelength of the circuit oscillations which are sustained by the "tangential" mechanism

$$\lambda = \frac{942\, r_a^2 H}{p V_a} \qquad (3.54)$$

This formula coincides with the formula of Posthumus (see Chap. II), which has been confirmed repeatedly by experimentation.

Thus, a very coarse and imperfect concept of a certain idealized electron-kinematic mechanism leads in this case, too, to results which have an indisputable bearing on reality and are satisfactorily confirmed in experiments.

More, however, cannot be obtained from investigation of the kinematics of the electron. A physically accurate, although approximate, and acceptable picture of the process may be arrived at only by taking into consideration the aggregate of electrons.

Section 3.3. Regulation of the Process in Terms of the Electron Aggregate

If electrons leave the cathode in a homogeneous stream and accomplish identical periodic motions in the inter-electrode spaces, it is then natural that the sum of all variable potentials applied to the electrodes must be equal to zero, and consequently, that oscillations cannot be observed, However, experiments testify to the contrary. Any system which consists of uniformly (on the basis of the foregoing analysis) moving electrons -- the circuit of the retarding field or the magnetron -- is a source of completely real and practically applicable ultra-high-frequency oscillations. This is evidence of the presence in the aggregate of electrons of some "collective" periodicity which lies in the periodic changes introduced into the aggregate of electrons under certain conditions of the mutual effect of the constant and variable potentials applied to the electrodes. The mechanism of this "collective periodicity" may be represented in simplest terms as a "sorting-out" mechanism. The essence of this idea is in the following: due to the presence of an alternating electric field created by the oscillating circuit connected to the electrodes the electrons which leave the cathode at moments corresponding to different phases of the alternating voltage behave differently, and form two basic groups -- "in-phase" and "out-of-phase" electrons. As "in-phase" electrons we may designate those the result in terms of power of whose individual periodic motion is a giving off of kinetic energy to the alternating electric field and correspondingly a decrease in the amplitude of their motion. "Out-of-phase" electrons behave exactly opposite: they land in the alternating fields under such phase conditions as to take energy from the latter and increase their own velocity and correspondingly the amplitude of their individual periodic motion. If the effects in terms of energy of these groups were to be absolutely identical, we would again be unable to observe oscillations in the external conductors. Operation of the "sorting-out" mechanism must also derive from the decreasing by various methods, in order to maintain oscillations, of the numbers of the group of "out-of-phase" electrons or their effect in terms of energy by comparison with the "in-phase" group. Let us illustrate these general considerations with a few examples.

a) The Retarding-Field Circuit

Let us consider the motion of electrons in a tube, beginning with

Fig. 3.15. Along the axis of abscissas we plot the time t, and along the axis of ordinates the path traversed by the electrons. Let the axis of abscissas correspond to the surface of the cathode K, the straight line gg' to the surface of the grid, and the straight line aa' to the surface of an anode with constant potential equal to zero. Let the oscillating system be connected to the grid and anode and the alternating potentials on these electrodes which are created by it be represented by sinusoids with period T. We shall analyze first the case where the time of motion of the electron from the cathode to the anode and back, τ, is equal to the period T of the alternating voltage on the electrodes. An electron which leaves the cathode at the moment I will pass through the cathode-grid space with a somewhat decreased acceleration, since the negative half-wave of the alternating voltage is on the grid at this time. The same thing awaits it in the grid-anode space, since when it passes the grid there begins to be a negative half-wave of voltage on the anode as well. In consequence of this the electron, at the moment I', reverses direction without reaching the anode and travels again toward the grid. An electron which has left the cathode a half period later behaves differently. It passes through the space kg under the action of a positive half-wave of alternating potential superimposed on the constant potential of the grid and consequently acquires a greater velocity then electron I. Electron II passes the grid at the moment when there appears a positive half-wave of voltage on the anode and a negative half-wave of voltage on the grid, and, due to the decreased potential gradient between the electrodes, lands on the anode and no longer participates in the electron oscillating mechanism. Electron III, which leaves the cathode half a period later than electron II, repeats the course of electron I, etc.

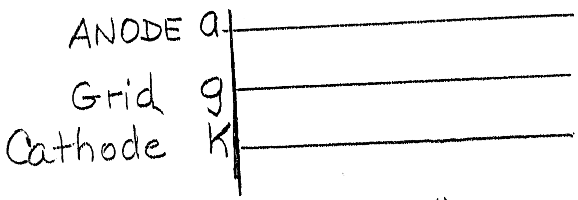

(Fig. 3.15)

The electrons I and II which we have considered are characteristic of the two groups into which the electron stream which has passed the grid is "sorted out". In accordance with the above-designated terminology electron I is "in phase", electron II is "out of phase", and the essence of the operation of the "sorting" mechanism (i.e. of the mutual action of the constant and alternating fields and the phase of the electron's departure from the cathode) consists of the fact that electron II "leaves the game" half a period after leaving the cathode, in consequence of which a periodically changing current is created in the anode-grid space. Its appearance is illustrated in Fig. 3.16. Motion of electrons toward the anode is occurring at any moment of time, but they move away from the anode only in the cross-hatched portions of the space-time graph represented in Fig. 3.16. Consequently, the grid-anode electron current is decreased at that time by a magnitude equal to the current created by the electrons returning from the anode.

This periodic changing of the electron stream, and at the same time of the anode current, maintains and controls the oscillations in the external circuit. The mechanism described has been called by Moller [8] "anode classification".

It may be shown that the period of change of the electron stream may also be unequal to the period of oscillating motion of an electron,

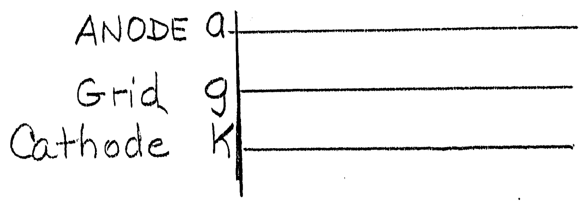

(Fig. 3.15)

The electrons I and II which we have considered are characteristic of the two groups into which the electron stream which has passed the grid is "sorted out". In accordance with the above-designated terminology electron I is "in phase", electron II is "out of phase", and the essence of the operation of the "sorting" mechanism (i.e. of the mutual action of the constant and alternating fields and the phase of the electron's departure from the cathode) consists of the fact that electron II "leaves the game" half a period after leaving the cathode, in consequence of which a periodically changing current is created in the anode-grid space. Its appearance is illustrated in Fig. 3.16. Motion of electrons toward the anode is occurring at any moment of time, but they move away from the anode only in the cross-hatched portions of the space-time graph represented in Fig. 3.16. Consequently, the grid-anode electron current is decreased at that time by a magnitude equal to the current created by the electrons returning from the anode.

This periodic changing of the electron stream, and at the same time of the anode current, maintains and controls the oscillations in the external circuit. The mechanism described has been called by Moller [8] "anode classification".

It may be shown that the period of change of the electron stream may also be unequal to the period of oscillating motion of an electron, provided that there is some multiple relationship between these values. In fact, let the circuit connected to the electrodes have a period of oscillation T three times less than the period of "electron agitation" (Fig. 3.17). Then electron I, having left the cathode at the moment of the maximum negative alternating potential on the grid, will pass it in 3/4T, and 3/4T later will reach the anode, which at that time is in the same phase as the grid at the moment the electron left the cathode. Thus there is superimposed on the motion of this electron a retardation caused by the negative half-wave voltage on the grid at the moment of the electron's departure from the cathode, and a similar retardation due to the negative half-wave voltage on the anode when the electron is approaching it. By virtue of this the electron will be forced to turn back from the anode. Electrons III, V, VIII, etc., will behave in a manner similar to electron I.

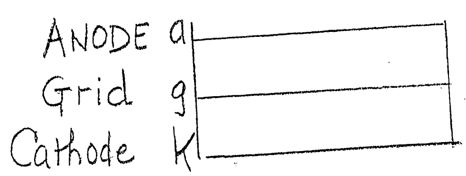

(Fig. 3.16)

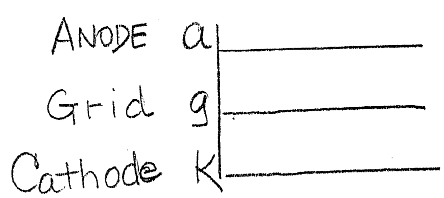

(Fig. 3.17)

Declassified in Part - Sanitized Copy Approved for Release 2012/04/09 : CIA-RDP82-00039R000200090009-2

The motion of electrons II, IV, VI, etc., which leave the cathode at moments of positive half-wave voltage on the grid, is accomplished in such a way that they also approach the anode at a time when there is a positive half-wave on it and are absorbed by it, leaving the picture; they are "sorted out".

By similar deliberations we may arrive at the conclusion that the electron stream will vary with a period equal to the period of the alternating potential on the electrons not only in the case represented by Fig. 3.17, but also in all cases where the period of the alternating voltage, T, is related to the period of electron oscillations, τ, by a simple repetitive relationship

$$T = \frac{1}{2}\tau;\ \frac{1}{3}\tau;\ \frac{1}{4}\tau;\ \ldots;\ \frac{1}{n}\tau$$

This explains the frequently observed maintenance of oscillations whose frequency is higher than the frequency of the "electron oscillations proper".

In all instances we follow the path of the first electron, for example, it may be observed that the amplitude of its oscillations about the grid gradually decreases, and in the limiting case, if it is not caught beforehand by the grid, it should stop on it. At the same time electron II, if it did not land on the anode at the end of its first passage, but were to reach the surface of zero potential, would return and increase the amplitude of its oscillations about the grid with each passage. This situation is possible, however, only in the case where there is a negative potential on the anode and the return surface is located somewhere between the electrodes. Then the classification of electrons may take place by a method somewhat different from the one described. Electrons I and II are the representatives of of the two groups -- "in phase" and "out of phase" -- which have the most considerable change in the amplitude of their oscillations. Generally, then, the change in amplitude of oscillations δ_x (Fig. 3.18) is a function of the moment of departure of an electron from the cathode, which is illustrated by Fig. 3.18. Let uu' be the return surface, aa' the anode, and gg' the grid. The sinusoids on aa' and gg' represent changes in potential on the anode and grid, and the sinusoid on uu' the course of δ_x as a function of time. Electrons of group I, for which δ_x is negative, return somewhat earlier than electrons of the second group, for which δ_x is positive. The representatives of both these groups begin their second oscillation with an altered phase difference. Due to this alternation an oscillation of the density of the electron stream with respect to time is obtained.

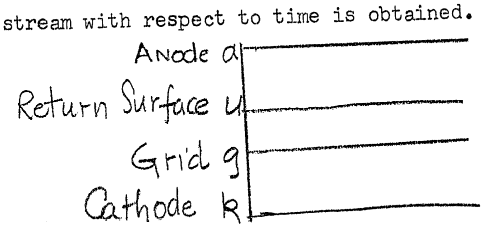

(Fig. 3.18)

Such a process of classification has been called "phase classification" by Moller [8]. For sufficiently large applitudes of the alternating potential, i.e. sufficiently large values of δ_x, "phase" classification may change over into "anode" classification, as evidenced by the electron current observed in many cases in the anode circuit Which Circuit accompanies the oscillations even with negative anode potentials.

It is clear that the sooner the "out-of-phase" electrons are removed from the field of action and the fewer of them there are by comparison with "in-phase" electrons, the higher will be the efficiency of

Declassified in Part - Sanitized Copy Approved for Release 2012/04/09 : CIA-RDP82-00039R000200090009-2

this process. The removal of "out-of-phase" electrons from the retarding-field circuit takes place by means of absorption of them by the anode or grid.

b) The Magnetron

Returning to the process of oscillations in the magnetron, we may also evoke the idea of "classification" to explain the occurence of organized oscillations. This is particularly easy to do with respect to oscillations of the first order, whose close analogy with oscillations in the retarding-field circuit has already been noted above. They occur, as is known, near critical conditions, which corresponds to a return surface lying in the direct vicinity of the anode. Since the transit time of an electron from the cathode to the anode (the grid of an equivalent tube with retarding field may be supposed to be located at the cathode itself) is equal to a half-period of oscillations, it is then obvious that an electron which has used for this transit a half-period, which corresponds to a positive half-wave of potential on the anode and a negative one on the cathode, will land on the anode, and with it also a group of others which are close to it with respect to departure phase. At the same time an electron, the half-period of whose flight is characterized by opposite half-waves of voltage (negative on the anode and positive on the cathode), will not reach the anode, since the radius of curvature of its trajectory will decrease. With respect to the alternating field between electrodes this electron is a representative of the "in-phase" group, since it gives off its energy to the field, diminishing its velocity and the radius of curvature of its trajectory. If an in-phase electron

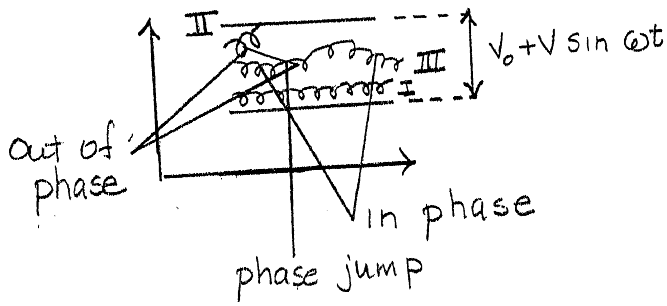

Figure 3.19

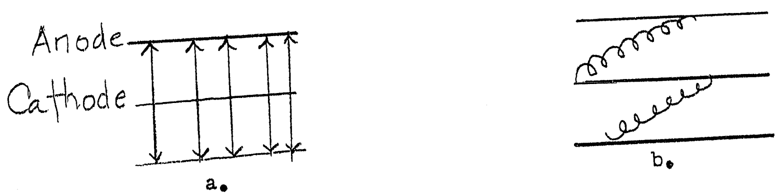

Figure 3.20

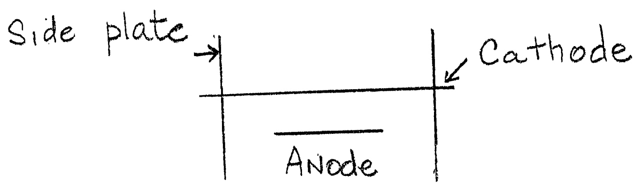

Figure 3.21

$\lambda = 42$ cm	I_R

Figure 3.22

describes a few loops of its trajectory with decreasing velocity and radius of curvature, it may, having expended all its initial energy, undergo "phase shift" and having begun, after almost completely halting, to move in phase with the alternation field, change into an "out-of-phase" electron. The possible behavior of different electrons is represented In Fig. 3.19, where a flat magnetron is represented for simplicity. It is assumed that the magnetic field is oriented perpendicular to the drawing. Without an alternating field the electron will move along a cycloidal curve of constant amplitude (curve I). In the presence of an alternating field there may occur the cases represented by curve II, which shows absorption of the field's energy but an electron landing after several revolutions on the anode, and by curve III, which illustrates the above described behavior of an "in-phase" electron when it makes the transition to the "out-of-phase" state. The desire to remove out-of-phase electrons from the inter-electrode space more rapidly causes the arrangement of the magnetron's axis at some angle α (usually several degrees) to the direction of the magnetic field's lines of force (Fig. 3.20), or the establishment on both sides of the anode of so-called side plates, superimposing on these a high positive potential for the creation of a longitudinal electric field (Fig. 3.21). Actually, experiment shows that proper selection of the angle between the direction of the magnetic field and the filament or of the voltage on the side plates plays a very essential role in the oscillating process. This may be seen from Fig. 3.22, which gives the curve of oscillating power of a magnetron with solid anode as a function of the angle α, and from Fig. 3.23, which represents change of the same value as a function of the potential on the side plates.

The concepts given here as to the mechanism of regulation of the motion of electrons in the simplest electron generators is, of course, purely qualitative in character. A few authors have tried, especially with respect to the retarding-field circuit, to introduce various numerical characteristics of this mechanism of "classification": for example, the phase of the electron's departure from the cathode, the phase of its passage through the grid, the displacement velocity of the return surface, etc. The pith of the matter, however, consists in all cases in demonstrating the predominance of the action of "in-phase" electrons over "out-of-phase" ones, i.e. in showing by virtue of this the possiblity of operations of a given device as an oscillator.

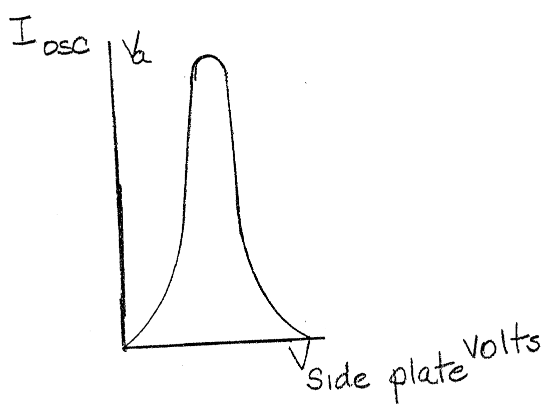

Figure 3.23

Literature Guide to Chapter III

1. V. I. Kalinin, Decimeter and Centimeter Waves, 1939.
2. S. I. Zilitinkevich. TiTbp, No 18, 2-22, 1923; No 19, 166-175, 1923
3. A. Scheibe. Ann. d. Phys. 73, 1924, 54-78.
4. Yu. A. Katsman. Elektrosvyaz', No 2, 39, 1939.
5. A. W. Hull. Phys. Rev. XVIII, 1921, 31.
6. V. I. Kalinin and I. I. Vasserman. IAN, ch. fiz. X. 103, 1946.
7. N. F. Alekseyev and D. Ye. Malyarov. ZhTF, X, 15, 1940, 1297-1300. PIRE, 32, 1944, 136-139
8. H. G. Moller. JddT, 34, 1929, 201-207. ENT, 7, 1930, 293-306. ENT 1930, 411-419.

The work with diodes is primarily of importance in establishing the principles involved, since it distinctly confirms the possibility of producing a negative resistance in a statistically regulated electron stream by means of the inertia of the electrons.

The theoretical considerations that have been briefly discussed above have been applied by various authors [1-6] to triode operation in U. H. F. Triodes with a negative grid are usually considered as the equivalent of the diode, for which the same conclusions are obtained, namely, the production of a complex internal resistance on account of the phase shift between current and voltage that results from the introduction of the inertia of the electrons. The phase shift ψ is not the result of a simple "mechanical lag" of the electron stream behind the voltage by the transit angle θ. Since there is a displacement current, the relationship between ψ and θ takes on a fairly complicated character:

$$\tan \psi = \frac{\sin\theta - \theta\cos\theta}{\theta\sin\theta + \cos\theta - 1} \qquad (4.22)$$

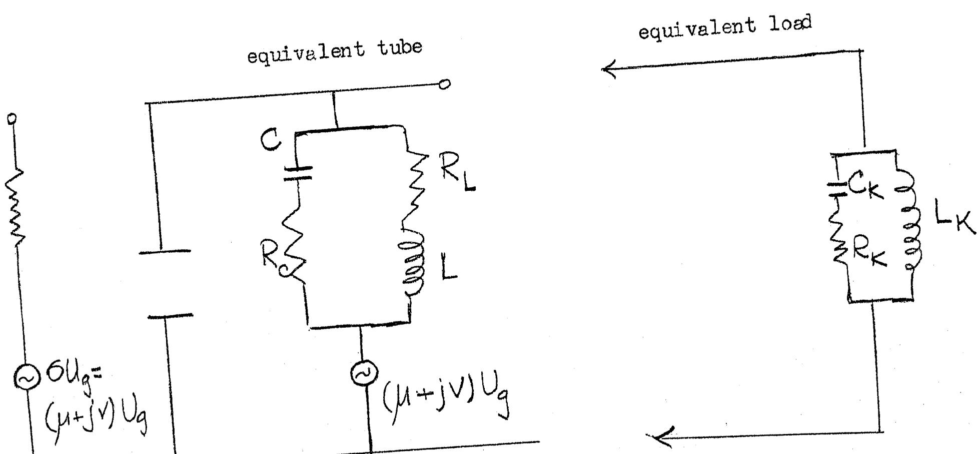

Figure 4.13

As ψ reaches the values π, 3π, $(2n+1)\pi$, an inversion of the internal resistance should be observed. Theoretically, the relationship between its active and reactive components may be considered analagous to that shown above for the diode. However, when a triode is operated in a feedback circuit, we must deal as a rule with very small transit angles, but in any case $\theta < \pi$. Thanks to this, it is possible to simplify very considerably the rather cumbersome expressions obtained by theoretical methods and thus to arrive at a number of approximate computational formulae. Representing the triode in the classic equivälent circuit, as an oscillator with electromotoive force μU_g and internal resistance R_i, where R_i and μ must be taken as complex quantities:

$$\bar{R}_i = r_i + i x_i \qquad (4.23)$$

$$\bar{\mu} = \mu + i\nu$$

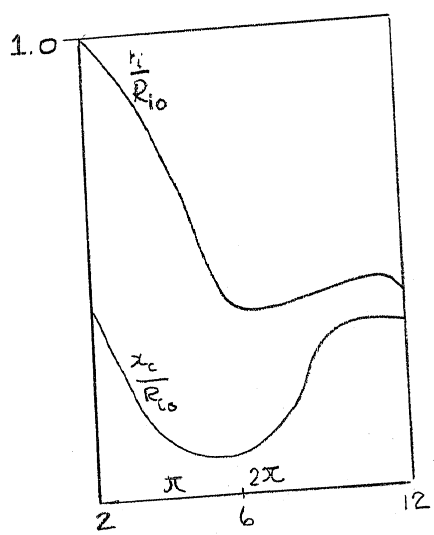

Figure 4.14

In connection with this, the equivalent tube circuit takes on the rather complicated form shown in Figure 4.13, with the quantities r_i, x_i, μ and ν being fairly complicated functions of the transit angle θ. The course of these functions is shown in the graphs of Figures 4.14, 4.15 and 4.16. Figure 4.14 represents the

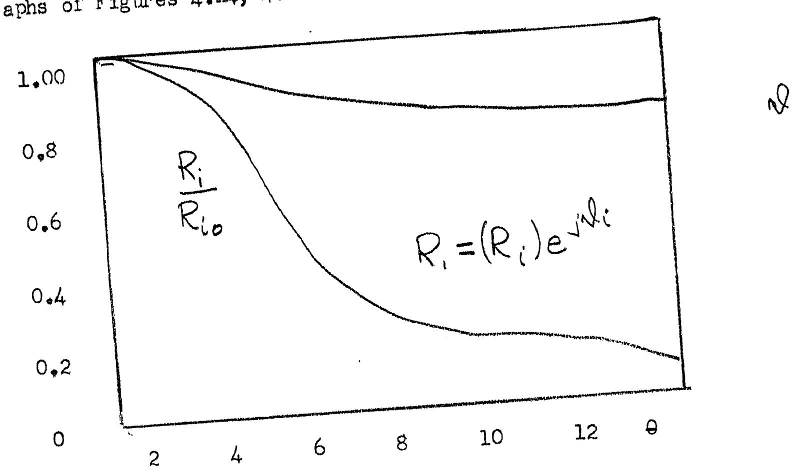

Figure 4.15

curves of the ratios r_i/R_{i0} and x_i/R_{i0}, where R_{i0} is the internal resistance of the tube at ω 0. Both these quantities, as may be seen, very rapidly become very small as θ increases. The tube resistance falls rapidly with increasing frequency, which is graphically illustrated by the curve $\left|\frac{R_i}{R_{10}}\right|$ in Figure 4.15. This circumstance manifests itself in the increasing loss caused by the tube in the oscillation circuit, and is one of the principal reasons for the rapid fall in the efficiency of oscillator tubes as we pass to VHF. The change in the complex amplification factor with increasing transit angle θ is shown by the graphs in Figure 4.16, which represent the curves μ/μ_o and ν/μ_o (μ_o being the static amplification factor for $\omega = 0$). As is clear from the drawing, the inertia of the electrons weakens the controlling action of the grid and reduces the amplification factor of the tube.

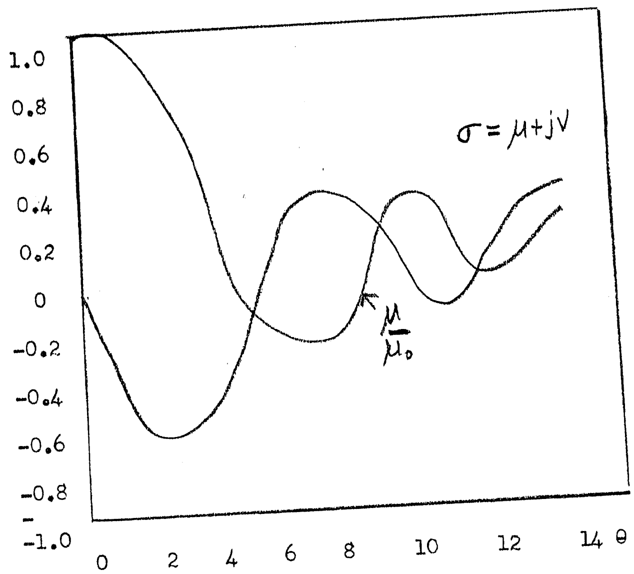

Figure 4.16

A third parameter of the tube also assumes the form of a complex expression: the transconductance of the plate current characteristic as a function of the grid voltage, in consequence of the phase shift, caused by the electron inertia between grid voltage and plate current. In accordance with the basic equation of the triode, the transconductance S may be represented in the form μ / R_i, which, when $\bar{\mu}$ and $\bar{R}$ are complex quantities takes the form

$$\bar{S} = \frac{\bar{\mu}}{\bar{R}_i} = \frac{\mu + i\nu}{r_i + ix_i} \tag{4.24}$$

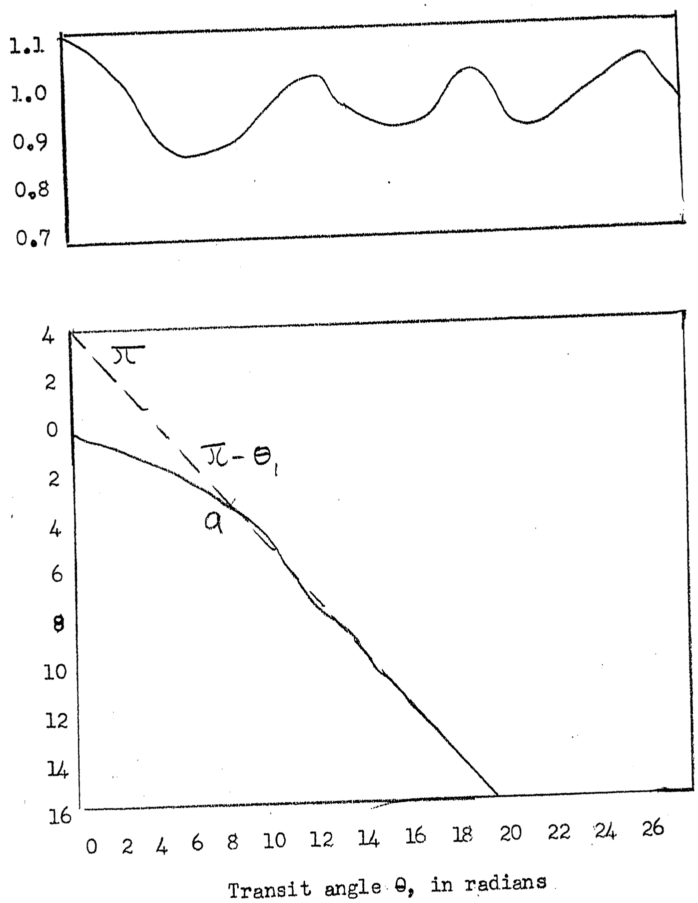

If $\bar{S}$ is represented in the form

(4.25)

then the modulus $|\bar{S}|$ and the phase angle θ of this complex quantity may be represented in dependence on the transit angle by the curves in Figure 4.17, on which

$$\frac{|\bar{S}|}{S_0} = f(\theta) \quad \text{and} \quad \vartheta = f(\theta)$$

are given, with $S_o = \mu_o / R_{io}$, the slope of the tube characteristic for $\omega = 0$.

4.3 THE PRESENT CONDITION OF THE THEORY OF CONDUCTIVITY OF ELECTRON TUBES

A very considerable number of investigations, most of them overloaded with their mathematical apparatus, have been devoted to the development of vacuum-tube theory, based on consideration of an equivalent circuit, and taking into account those phenomena that take place when the transit angles are appreciable. The work of Llewellyn and his school has long been manifesting tendencies to the construction of such a complex of equations as would cover, as diversely as possible, the relationships between the principal quantities that characterize the tube and the circuit elements connected with it. In recent years Llewellyn [10] and then Llewellyn and Peterson [11], have given a theory of equivalent tube circuits which is fairly well organized in spite of a certain unwieldiness. They point out that up to the present time there are two tendencies of treatment of vacuum-tube phenomena: either to study what goes on inside the tube, and thus coming to treat the tube as a certain conductance in combination with interelectrode capacitances, or, regarding the tube as a single element of a circuit, to apply the usual analysis of electric circuits to it, together with the other resistances, inductances, etc. In their latest work, Llewellyn and Peterson claim to have combined both these methods. The mathematical part of the problem is solved by them with reference to the processes that occur in the electron streams. They put their final questions in such a form as to assure relatively simple manipulation in applying them to equivalent circuits. Starting out from extremely simple geometrical picture of a diode with parallel plane electrodes a and b and an electron stream flowing perpendicularly to them, the authors operate with the data: total current, current conductivity and electron velocity on the plane a. Then, assuming electron velocity to be single-valued at all points of the interelectrode space, representing these quantities in the form of sums of direct and alternating components, and carrying out an analysis on a principle analagous to that described in the foregoing section, they obtain two groups of equations: one for direct current and a second for alternating current. These equations are written in the following form.

(a) The group of equations for direct current

$$\zeta = 3(1 - \tau_0/\tau)$$

$$x = (1 - \zeta/3)\,\frac{(v_a + v_b)\tau}{2} \qquad (4.26)$$

$$\left(\frac{\eta}{\varepsilon}\right) I_D = \frac{(v_a + v_b)\,2\zeta}{\tau}$$

Here $\eta = 1.76 \cdot 10^{15}$, $\varepsilon = \frac{1}{36\pi 10^{11}}$, $\frac{\eta}{\varepsilon} \cong 2 \cdot 10^{28}$, x is the distance in centimeters between planes a and b, is the transit time of the electrons for this distance, v_a and v_b are the electron-velocities on these planes, respectively, in centimeters/second, and I_d is the current density in amperes per square centimeter. The time τ_0 and the "space-charge factor" require some explanation: if there is only a single electron moving through the interelectrode space, it will require, to transverse the distance x, the time τ_0, which may be found from the relation

$$x = \frac{(v_a + v_b)\tau_0}{2} \qquad (4.27)$$

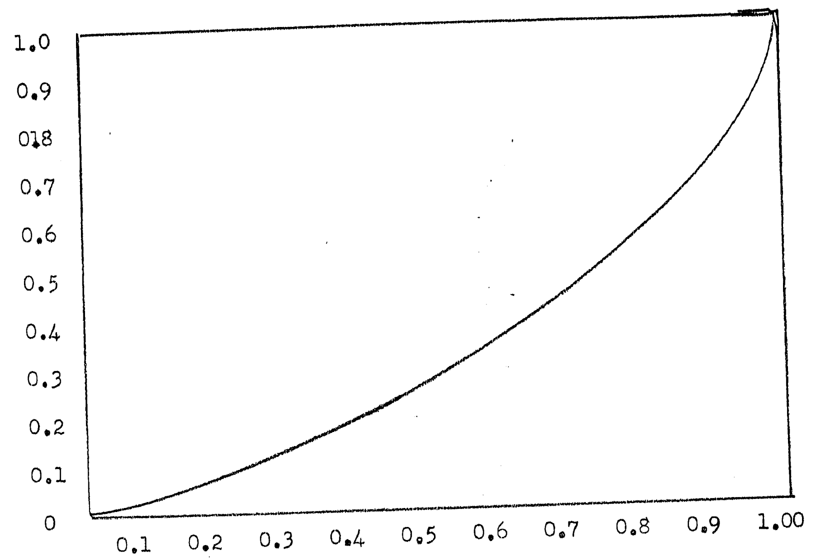

Figure 4.18

On comparing this expression with the second equation given in (4.26), it may be noted that τ_0 is a value that approaches τ as $\zeta \rightarrow 0$. The vanishing of the space-charge factor thus corresponds to the ideal case of the movement of a single electron between the electrodes. In practice we are always dealing, in a vacuum tube, with a great number of electrons and a factor ζ different from zero. The authors determine the value of ζ in such a way that it varies from $\zeta = 0$, under the conditions of the absence of any space charge, to $\zeta = 1$, when the electron stream reaches saturation (or speaking more precisely, constitutes all of the electrons impinging on electrode a), and is expressed by a certain maximum current value I_m. The relationship between I_D, I_m, and ζ may be written as

$$\frac{I_D}{I_m} = \left(\frac{9}{4}\right)\zeta\left(1 - \frac{\zeta}{3}\right)^2, \qquad (4.28)$$

The graph of the space-charge factor ζ in relation to the ratio of the currents I_D/I_m is presented in Figure 4.18. From the expressions (4.28) and (4.26) we can obtain

$$\frac{\eta}{\varepsilon} I_M = \left[\frac{2}{9} \cdot \frac{(V_a + V_b)^3}{X^2}\right] = \frac{2.33}{10^6} \cdot \frac{(\sqrt{U_{Da}} + \sqrt{U_{Db}})^3}{X^2} \qquad (4.29)$$

(where U_{Da} and U_{D_b} are the direct-current potentials of planes a and b), which leads ultimately to the Child equation. The space charge, as is clear from the foregoing, is thus taken into account by introducing the factor ζ, which is connected with the other quantities indicated by the equations and characterizes the increase in transit time due to the action of the space charge.

(b) The corresponding group of equations for the alternating current is as follows:

$$\begin{aligned} U_b - U_a &= A^*I + B^*q_a + C^*w_a \\ q_b &= D^*I + E^*q_a + F^*w_a \\ w_b &= G^*I + H^*q_a + I^*w_a \end{aligned} \qquad (4.30)$$

Here U is the alternating-current potential in volts, I is the alternating current in amperes, q the conduction current in amperes, and w the alternating-current velocity in centimeters/second. The indices a and b refer to the planes a and b. The coefficients A*.....I* are expressed according to Table 4.3. Tables 4.2 and 4.3 presented below contain a review of all formulae and give expressions for the coefficients both in the general form and for the limiting cases $\zeta = 0$ or $\zeta = 1$.

Table 4.2

FUNDAMENTAL EQUATIONS OF VACUUM TUBES USING THE NUMERICAL VALUES

$$\eta = 10^7 \frac{e}{m} = 1.77 \cdot 10^{15}; \ \varepsilon = \frac{1}{36\pi \cdot 10^{11}} \ ; \frac{\eta}{\varepsilon} \cong 2 \cdot 10^{28}.$$

Equations of Direct Current

Equation of energy.. $\eta U_D = \frac{1}{2}v^2$

Determination of space-charge factor.................... $\zeta = 3(1 - \tau_0/\tau)$

Distance.. $x = (1 - \xi/3)\frac{(v_a + v_b)}{2}\tau$

Current density....................................... $(\eta/\varepsilon) I_D = (v_a + v_b) 2\zeta/\tau^2$

Measure of space charge............................ $I_D/I_m \quad (9/4)\zeta(1 - \zeta/3)^2$

Limiting current density.................... $I_m = \frac{2.33}{10^6} \frac{(\sqrt{U_{Da}} + \sqrt{U_{Db}})^3}{x^2}$

Equations of Alternating Current

General equations:

$$U_b - U_a = A^*I + B^*q_a + C^*w_a,$$
$$q_b = D^*I + E^*q_a + F^*w_a,$$
$$w_b = G^*I + H^*q_a + I^*w_a.$$

The diode may serve as the first example to illustrate the application of these equations. Let there be no electrons between planes a and b. Then $\zeta = 0$, $q_a = 0$, and from equation (4.30) we have $U_b - U_a = A^*I$, from which the role of A^*, as a certain impedance, becomes plain. Taking the expression A^* for the case $\zeta = 0$ (Table 4.3), then $A^* = \frac{1}{\varepsilon}(v_a + v_B)\frac{\tau_0^2}{2} \cdot \frac{1}{\beta}$ and by comparing this with $x = \left[(v_a + v_b)/2\right]\tau_0$ we get

$$A^* = \frac{x}{\varepsilon i \omega}$$

and since, in the system of units adopted by Llewellyn and Peterson, $\frac{\varepsilon}{X} = C$ = capacity in farads per square centimeter of surface, then

$$A^{*} = \frac{1}{i\omega C}$$

i.e., it plays the role of the usual capacity reactance.

Table 4.3

VALUES OF THE COEFFICIENTS IN THE EQUATIONS OF ALTERNATING CURRENT

$$A^{*} = \frac{1}{\varepsilon}(V_a+V_b)\frac{\tau^2}{2}\cdot\frac{1}{\beta}\left[1-\frac{\zeta}{3}\left(1-\frac{12S}{\beta^3}\right)\right]$$

$$B^{*} = \frac{1}{\varepsilon}\frac{\tau^2}{\beta^2}\left[V_a(P-\beta Q)-V_bP+\zeta(V_a+V_b)P\right]$$

$$C^{*} = -\frac{1}{\eta}\cdot 2\zeta(V_a+V_b)\frac{P}{\beta_2}\,; \qquad G^{*} = -\frac{\eta}{\varepsilon}\frac{\tau^2}{\beta^3}\left[V_b(P-\beta Q)-V_aP+\zeta(V_a+V_b)P\right]$$

$$D^{*} = 2\zeta\left(\frac{V_a+V_b}{V_b}\right)\frac{P}{\beta^2} \qquad H^{*} = -\frac{\eta}{\varepsilon}\cdot\frac{\tau^2}{2}\left(\frac{V_a+V_b}{V_b}\right)(1-\zeta)\frac{e^{-\beta}}{\beta}$$

$$E^{*} = \frac{1}{V_b}\left[V_b-\zeta(V_a+V_b)\right]e^{-\beta} \qquad I^{*} = \frac{1}{V_b}\left[V_a-\zeta(V_a+V_b)\right]e^{-\beta}$$

$$F^{*} = \frac{\varepsilon}{\eta}\cdot\frac{2\zeta}{\tau^2}\left(\frac{V_a+V_b}{V_b}\right)\beta e^{-\beta}$$

Values of the coefficients for the limiting cases:

(a) Full space charge ($\zeta = 1$); (b) No space charge ($\zeta = 0$)

(a)

$$A^{*} = \frac{1}{\varepsilon}(V_a+V_b)\frac{\tau^2}{3\beta}\left(1+\frac{6S}{\beta^3}\right)$$

$$B^{*} = \frac{1}{\varepsilon}\frac{\tau^2}{\beta^3}V_a(2P-\beta Q)$$

$$C^{*} = -\frac{2}{\eta}(V_a+V_b)\frac{P}{\beta^2}$$

$$D^{*} = 2\left(\frac{V_a+V_b}{V_b}\right)\frac{P}{\beta^2}$$

$$E^{*} = -\frac{V_a}{V_b}e^{-\beta}$$

(b)

$$A^{*} = \frac{1}{\varepsilon}(V_a+V_b)\frac{\tau_0^2}{2}\cdot\frac{1}{\beta}$$

$$B^{*} = \frac{1}{\varepsilon}\cdot\frac{\tau_0^2}{\beta^2}\left[V_a(P-\beta Q)-V_bP\right]$$

$$C^{*} = 0$$

$$D^{*} = 0$$

$$E^{*} = e^{-\beta}$$

$$F^* = \frac{\varepsilon}{\eta} \cdot \frac{2}{\tau^2}\left(\frac{V_a + V_b}{V_b}\right)\beta e^{-\beta}$$

$$G^* = -\frac{\eta}{\varepsilon} \cdot \frac{\tau^2}{\beta^3}(2P - \beta Q)$$

$$H^* = 0$$

$$I^* = -e^{-\beta}$$

$$F^* = 0$$

$$G^* = -\frac{\eta}{\varepsilon} \frac{\tau_o^2}{\beta^3} \cdot \frac{1}{V_b}[V_b(P - \beta Q) - V_a P]$$

$$H^* = -\frac{\eta}{\varepsilon} \cdot \frac{\tau_o^2}{2}\left(\frac{V_a + V_b}{V_b}\right)\frac{e^{-\beta}}{\beta}$$

$$I^* = \frac{V_a}{V_b} \cdot e^{-\beta}$$

A Few Symbols Used in the Formulae of These Tables:

$$\beta = i\theta, \ \theta = \omega\tau, \ i = \sqrt{-1}$$

$$P = 1 - e^{-\beta} - \beta e^{-\beta} \approx \frac{\beta^2}{2} - \frac{\beta^3}{3} + \frac{\beta^4}{8} + \cdots$$

$$Q = 1 - e^{-\beta} \approx \beta - \frac{\beta^2}{2} + \frac{\beta^3}{6} - \frac{\beta^4}{24} + \cdots$$

$$S = 2 - 2e^{-\beta} - \beta - \beta e^{-\beta} \approx -\frac{\beta^3}{6} + \frac{\beta^4}{12} - \frac{\beta^5}{40} + \frac{\beta^6}{180} + \cdots$$

Let us now consider a second example, in which plane a is the cathode, and the conditions for the space charge correspond to saturation, i.e., for $\zeta = 1$. Then by virtue of the absence of the alternating current component on the cathode and the fact that electron velocity on plane a is 0, the first of the equations in (4.30) is written again as follows:

$$U_b - U_a = A^* I.$$

But the expression for A^* must now take account of the fact that $\zeta = 1$. By performing an operation analogous to that in the preceding example, we may obtain an expression for A^* as the impedence, in the following form

$$A^* = Z = \frac{2}{3} \frac{\left(\sqrt{U_{Da}} + \sqrt{U_{Db}}\right)^2}{I_D}\left[\frac{2}{\beta} + \frac{12S}{\beta^4}\right] \quad (4.31)$$

By writing $r_o = 2(\sqrt{U_{Da}} + \sqrt{U_{Db}})^2/3\ I_D$, and remembering that this quantity is inversely proportional to the transconductance of the diode characteristic, if $U_{Da} = 0$, we may express Z as

$$Z = r_o\left(\frac{2}{\beta} + \frac{12S}{\beta^4}\right). \qquad (4.32)$$

At exceedingly high frequencies, this impedance approaches the value $Z_\infty \approx r_o\left(\frac{2}{\beta}\right) = \frac{x}{\varepsilon i\omega}$, i.e., the value of the "static" capacity of the resistance. At very high frequencies the diode becomes equivalent to a simple condenser, the properties of which are not altered by the presence of electrons, as was remarked in the preceding section. A study of formula (4.32) leads to the conclusion that at transit angles corresponding to

$$\theta = 2\pi n + \pi/2 = \pi/2\ (1+4n)\ (n = 1, 2, 3\ldots\ldots), \qquad (4.33)$$

maxima are obtained for the negative active resistance of the diode

$$r = -12\frac{r_o}{\theta^3} \qquad (4.34)$$

Consideration of the case "partial space charge", when $0 < \zeta < 1$, leads to a somewhat more complicated expression for impedance A*:

$$A^* = \frac{2}{3}\zeta^2\frac{(\sqrt{U_{Da}} + \sqrt{U_{Db}})^2}{I_D}\frac{12}{\theta^4}\left[2(1-\cos\theta - \theta\sin\theta)\right] - i\,\frac{2}{3}\zeta^2\frac{(\sqrt{U_{Da}} + \sqrt{U_{Db}})^2}{I_D}\frac{12}{\theta^4}\left[\frac{\theta^3}{6} + \theta(1+\cos\theta) - 2\sin\theta\right] - i \times \frac{x}{\omega\varepsilon}\cdot\frac{1-\zeta}{1-\zeta/3}. \qquad (4.35)$$

The quantity r_o may be defined here as

$$r_o = \frac{2}{3}\zeta^2\frac{(\sqrt{U_{Da}} + \sqrt{U_{Db}})^2}{I_D} \qquad (4.36)$$

It follows from equation (4.35) that the impedance of a diode consists in the general case of three consecutively connected resistances: active and reactive, which vary in dependence on θ (Figure 4.14), and are represented by the first two terms of formula (4.35), together with that of the simple capacity defined by the third term of this formula. This capacity represents a static capacity which is somewhat varied by the existence of a space charge.

At very high frequencies, A* may be expressed as

$$A^*_{\omega \to \infty} \approx - \frac{12 r_0 \sin\theta}{\theta^2} - i \frac{x}{\omega \varepsilon} \qquad (4.37)$$

It is clear from this that as approaches infinity, the impedance of a diode for any space-charge condition whatsoever approaches the ordinary capacity reactance.

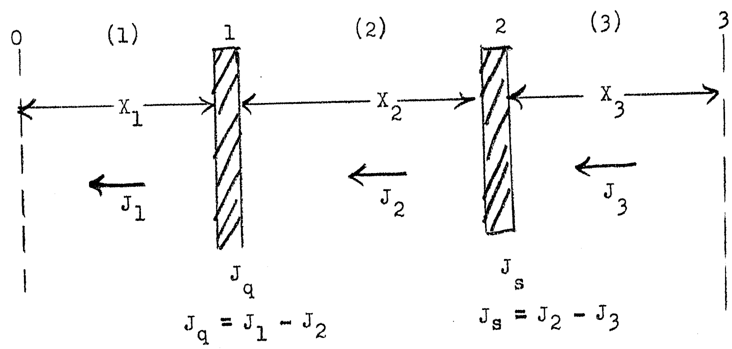

Figure 4.19

The general equations we have presented, of which we have just demonstrated the application to the already well-known properties of diodes, enable us to set up rational circuit equivalents for multi-electrode tubes as well. Such tubes have the form of a series of successive diodes with plane parallel electrodes, as depicted in Figure 4.19 for a tetrode. Here the conditions between the cathode and the control grid L are analagous to those in the diode we have been considering. Between the control grid 1 and the screen grid 2 the situation is already somewhat different on account of boundary conditions that differ from those in the first diode. Roughly the same is true between the screen grid and the anode 3. This series of diodes has its elements connected by the corresponding boundary conditions characterized by effective potentials. These effective potentials are naturally different from the actual potentials of the wires in the grids. The grid current is represented as the difference between the total current to the right of the corresponding grid and that to the left of it (Figure 4.18).

The diode equations are directly applicable to interval (1). The conditions in region (2) are not so simple. The fact is that the electrons on passing through grid 1 are already subject to the action of the alternating field in the first diode. Equations (4.30), however, enable us to calculate the initial current and velocity in space (2), since these coincide with their final values in space (1), if grid (1) is negative. If it is positive and carries a certain current, then the number of electrons entering region (2) is less than that of those leaving region (1). If a certain part αq of the alternating component of the conduction current q enters region (2), then the share $(1 - \alpha)q$ characterizes the grid current. Thus, each interval (1), (2), (3), etc is characterized by its own current I_1, I_2, I_3... The application of the equations of Table 4.2 gives the following expressions for these currents:

$$I_1 = U_1 y_{11}$$

$$I_2 = (U_2 - U_1) y_{22} - U_1 y_{12}$$

Declassified in Part - Sanitized Copy Approved for Release 2012/04/09 : CIA-RDP82-00039R000200090009-2

$$I_3 = (U_3 - U_2)y_{33} - (U_2 - U_1)y_{23} - U_1y_{13} \qquad (4.38)$$

$$I_4 = (U_4 - U_3)y_{44} - (U_3 - U_2)y_{34} - (U_2 - U_1)y_{24} - U_1y_{14}$$

etc, where the quantities y_{11}, y_{22},... represent conductances and yield the equations:

$$y_{11} = \frac{1}{A_1^*};\quad y_{22} = \frac{1}{A_2^*};\quad y_{33} = \frac{1}{A_3^*}, \text{ etc.}$$

$$y_{12} = \frac{1}{A_1^*A_2^*}(D_1^* \alpha_1 B_2^* \quad G_1^*C_2^*)$$

$$y_{23} = \frac{1}{A_2^* A_3^*}(D_2^* \alpha_2 B_3^* \quad G_2^*C_3^*) \qquad (4.39)$$

$$y_{13} = \frac{1}{A_1^*A_2^*A_3^*}\Big[A_2^* \Big\{\alpha_2 B_3^*(D_1^* \alpha_1 E_2^* + G_1^*F_2^*) + $$

$$+ C_3^*(D_1^* \alpha_1 H_2^* + G_1^*I_2^*)\Big\} - \Big\{\alpha_2 B_3^* D_2^*(D_1^* \alpha_1 B_2^* +$$

$$+ G_1^*C_2^*) + C_3^*G_2^*(D_1^* \alpha_1 B_2^* + G_1^*C_2^*\Big\}\Big]$$

The formulae (4.38) allow any region on Figure 4.19, for example the third one, on Figure 4.19, to be represented by the equivalent circuit of Figure 4.20. Here this region is represented by a circuit into which and out of which, the current I_3 flows. The conductance y_{33} is fed by two sources of current from each of the preceding regions. One source gives the current $I_b = (U_2 - U_1)y_{23}$, while the other gives $I_c = U_1y_{13}$, where the quantities y_{23} and y_{13} are "mutual conductances" corresponding to the regions or to the sharpness of their respective characteristics. The sum of all the currents arriving at point U_2 is equal to $I_3 = I_a - I_b - I_c$ in accordance with equations (4.14). The equivalent circuit for the entire electron stream of the tetrode in Figure 4.19 may be represented in Figure 4.21. The sources of direct current here play a role analagous to that of $\mu\ U_g$ -- the oscillation in the old equivalent circuit for the vacuum tube in Figure 4.13. The currents here are expressed through the equivalent grid potentials. Whatever connection may be known between the actual grid potentials and their equivalents calculated by formulae (4.39), the conductances may, so to speak, be "reduced to the terminals" of the tube, i.e. correspond to the relations between the actual currents flowing in the tube and the actual voltages applied.

As an example of the more detailed application of the general equations, the tetrode circuits of Figure 4.19 are analyzed, with a full space charge present in region (1) and its practical absence from the following intervals. Such conditions, as the reader has

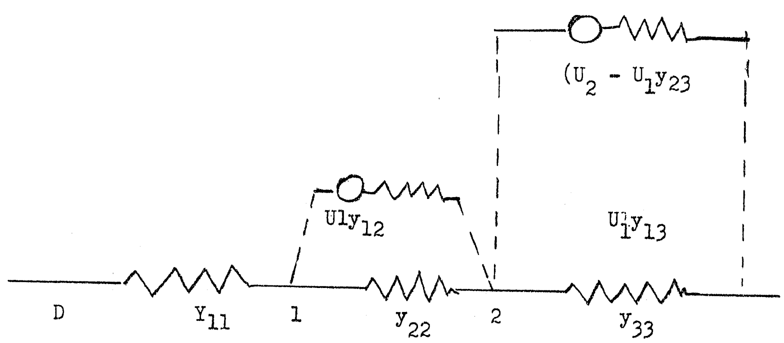

Figure 4.21

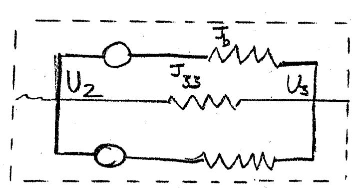

Third Region

Figure 4.20

Declassified in Part - Sanitized Copy Approved for Release 2012/04/09 : CIA-RDP82-00039R000200090009-2

already been reminded, entirely correspond to those of operation. The expressions for conductance are simplified in this way, and give the following equations:

$$y_{11} = \frac{1}{A_1^*} \; ; \quad y_{22} = \frac{1}{A_2^*} \; ; \quad y_{33} = \frac{1}{A_3^*}$$

$$y_{12} = \alpha_1 D_1^* B_2^* / A_1^* A_2^*$$

$$y_{23} = 0 \qquad (4.40)$$

$$y_{13} = \alpha_1 \alpha_2 D_1^* E_2^* B_3^* / A_1^* A_3^*$$

The conductances y_{12} and y_{13} are particularly interesting here; they define the transconductance of the characteristics of the respective currents in their dependence on the control-grid voltage. They may be expressed somewhat more in detail:

$$y_{12} = \frac{\alpha_1 \, 2P_1}{A_1^*} \cdot \frac{(2/\beta_1^2)}{(v_1 + v_2)} \left[v_1(P_2 - \beta_2 Q_2) - v_2 P_2 \right]$$

$$y_{13} = \alpha_1 \alpha_2 \frac{2P_1}{\beta_1^2 A_1^*} \cdot e^{-\beta_2} \frac{(2/\beta_3^2)}{(V_1 + V_2)} \left[V_2(P_3 - \beta_3 Q_3) - V_3 P_3 \right]$$

It is also of interest to bear in mind the limiting values, at very low and very high frequencies, of the quantities entering into these expression (Table 4.4)

Table 4.4

Quantities	$\left(\frac{2P_1}{\beta_1^2 A_1^*}\right)$	$\frac{2}{\beta_n^2}\left[\frac{V_{n-1}(P_n - \beta_n Q_n - V_n P_n}{V_n + V_{n-1}}\right]$
Low frequencies: $\beta \cong 0$	g_o	(-1)
High frequencies: $\beta \cong \infty$	$-g_o e^{-\beta_1}$	$-\frac{2}{\beta_n^2} \frac{(V_{n-1} - V_n e^{-\beta_n})}{V_{n-1} + V_n}$

The quantity $2P_1/\beta_1^2 A_1^*$, which in essence represents the sharpness is particularly interesting in this case. For $\beta > 0$ it is a complex quantity, and its behavior in relationship to the transit angle is described, as we have already shown, by the curves of Figure 4.17. A detailed analysis of the equations (4.41) leads us to the conclusion that the influence of transit time reduces down to causing variation in the phase angle of the transconductance, without exerting much of an influence on the value of the modulus (cf. Figure 4.17).

Where the transit angles are large in all regions of the stream, equations (4.41) reduce to the following set:

$$y_{12} = \alpha_1 g_0 e^{-i\theta_1} \frac{\sqrt{U_{D_1}} - \sqrt{U_{D_2}}\, e^{-i\theta_2}}{\frac{1}{2} i\theta_2 \left(\sqrt{U_{D_1}} + \sqrt{U_{D_2}}\right)}$$

$$y_{13} = \alpha_1 \alpha_2 g_0 e^{-i(\theta_1+\theta_2)} \frac{\sqrt{U_{D_2}} - \sqrt{U_{D_3}}\, e^{-i\theta_3}}{\frac{1}{2} i\theta_3 \left(\sqrt{U_{D_2}} + \sqrt{U_{D_3}}\right)} \qquad (4.42)$$

The course of the variation in the modulus value y_{13} is a little different from that of Figure 4.17 and is shown in Figure 4.22, from which it will be seen that the transconductance of the corresponding characteristic approaches zero as the transit angle increases.

To adapt this analysis to the conditions in actual tubes, we must take account of the fact that there also exist certain angles of flight and space-charge factors between the equivalent planes of the grids and the grids themselves, even though they are very small. For this reason we may introduce the concept of

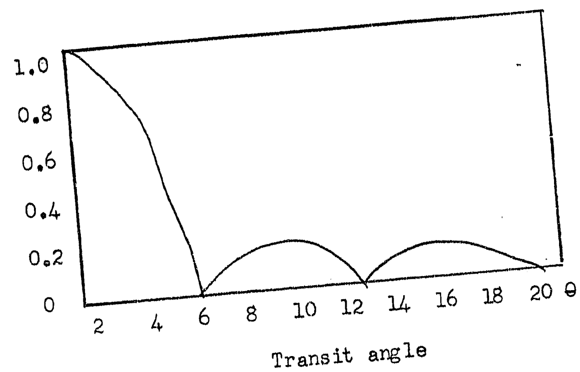

Figure 4.22

the conductances between the equivalent planes and the grids themselves, with values that may correspond to the expressions. The existence of these conductances somewhat complicated the general equivalent tube circuit, which here takes the form shown in Figure 4.23 (for the same tetrode, with a space charge only in the first region; if the voltage is negative on grid 1, the generator of current between 1 and G is eliminated).

The capacities C_{22}, C_{23} etc are here the electrostatic capacities between the conducting surfaces that coincide with the surfaces of the electrodes. The capacities C_g and C_s are the capacities between the electron stream and the grid wires, which in their relation to C_{22} and C_{33} condition the static amplification factor of the grids in question.

The general relationships of Tables 4.2 and 4.3 may be applied by an analagous method to systems with any number of electrodes. For tubes with statically controlled electron streams this method yields rather convenient computational formulae, which are also the most general, for the various parameters at different transit angles.

The authors of the work under discussion, Llewellyn and Peterson, also point out the possibility of applying the general equations to velocity-modulated devices as well, i.e. to systems having dynamic control of the electron stream. The physical operating conditions for the electron stream in such devices are, however, so peculiar that the method of equivalent circuits can hardly lay claim to being broad and general enough to take in the treatment of devices with dynamic control, taking into account the specific nature of their electronic mechanism. Katsman [12] has very correctly remarked that it is possible to employ confidently the theory being considered as long as the individual electrons or groups of electrons do not overtake each other, i.e. as long as phase focusing does not commence in the electron stream, for once it does, the above-postulated single-valued velocity for all points of the interelectrode space is at an end.

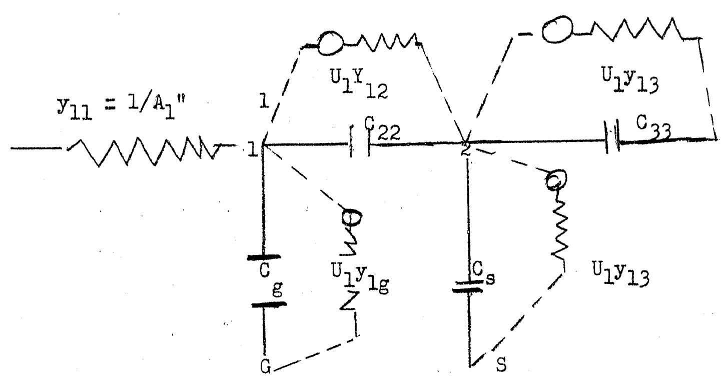

Figure 4.23

4.4 THE DIELECTRIC PERMEABILITY OF THE ELECTRON INTERVALS

It has been noted above that the capacity of the electron interval is less than the "cold" capacity of the electrodes on

Declassified in Part - Sanitized Copy Approved for Release 2012/04/09 : CIA-RDP82-00039R000200090009-2

account of the presence of electrons, resulting in the variation of dielectric permeability -- which becomes less than unity -- and consequent reduction of capacity. According to Benham /1/ and Müller /6/, the value of the dielectric permeability, which is defined as the ratio of the operating electrode capacity C to the "cold" electrode capacity C_1 -- depends on the transit time of the electrons through the interelectrode space. At $\omega = 0$, and a full space charge, the interelectrode capacity reaches 60 percent of its "cold" value. The course of the variation of the dielectric permeability of the gap as θ increases is shown in Figure 4.24, from which it will be seen that ε approaches unity as the transit angle increases. For insignificant values of θ the dielectric permeability of the electron gap depends also on the density of the space charge. The dielectric permeability of a space containing free charges, may be expressed /13/ as:

$$\varepsilon = 1 - \frac{4\pi N e^2}{m\omega^2} = 1 - \Delta\varepsilon \qquad (4.43)$$

where N is the number of electrons per [redacted] cubic centimeter and ω is the angular frequency of oscillation.

Thus, the value of $\Delta\varepsilon$, which shows the deviation from unity of the value of the dielectric permeability, is equal to

$$\Delta\varepsilon = \frac{4\pi N e^2}{m\omega^2}$$

The influence of the time spent by the electron in the interelectrode gap, however, is not reflected in these formulae. To take this factor into account as well, Benner /14/ has given the formula

$$\Delta \varepsilon = - \frac{4\pi N e^2}{m \omega^2} \left(1 - \frac{\sin \omega \tau}{\omega \tau}\right) \qquad (4.44)$$

In this case N is the number of those electrons in 1 cubic centimeter of the interelectrode space which remain there during the time τ. Benham /1/ gives a formula somewhat different from the foregoing:

$$\Delta \varepsilon = - \frac{4\pi N e^2}{m \omega^2} f(\theta) \qquad (4.45)$$

where the function $f(\theta)$ may be expressed in the following manner:

$$f(\theta) = \frac{1}{5} \theta^2 \left(1 - \frac{69}{12{,}600} \theta^2\right) \qquad (4.46)$$

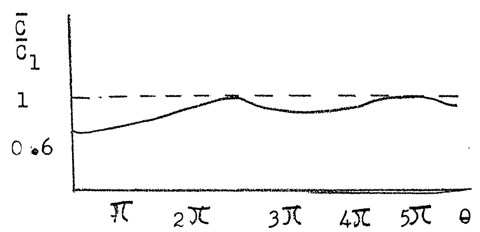

Figure 4.24

In consequence of the periodic variation in certain parameters of the electron stream (for instance, current density and electron velocity) that occurs in the interelectrode space, the dielectric permeability of that space may vary periodically in time, and with it the capacity of the interelectrode gap may also vary. Since interelectrode capacity usually forms a part of circuit capacity, this should involve modulation of the parameter and, under certain

Declassified in Part - Sanitized Copy Approved for Release 2012/04/09 : CIA-RDP82-00039R000200090009-2

conditions, parametric excitation of oscillations in the circuit connected to the electron gap. If the minimum and maximum values of N can be calculated for any specific case, and also of together with them, then the coefficient of modulation of the parameter can be found by definition, since

$$M = \frac{C_{max} - C_{min}}{C_{max} \quad G_{min}} = \frac{\varepsilon_{max} - \varepsilon_{min}}{\varepsilon_{max} + \varepsilon_{min}} \qquad (4.47)$$

and expressed by the values characterizing the properties of the electron gap, for example by the current density, the applied direct current voltage, the geometric dimensions, etc. When this has been done, the results of the theory of parametric excitation of oscillations, developed in the works of academecians N. D. Papaleks' and L. I. Mandelshtam and their students, can be applied to the system being considered.

Unfortunately, however, the question of the determination of the dielectric permeability of the electron gap cannot be considered to have been sufficiently clarified either from the theoretical or experimental side.

The experimental work performed by various authors is evidence that in most cases -- specifically in those cases where we are definitely dealing with a pure electron gap, uninfluenced by an possible ions of the residual gas -- the dielectric permeability is less than unity, and depends on: (a) the frequency of the alternating current voltage applied to the gap; (b) electron concentration; and (c) the time spent by the electrons in the gap. Investigations in the meter-wave field have shown that the variation in dielectric permeability with variation in frequency and the other parameters of the system is of resonant character. This phenomenon may be connected with the peculiar "anomalous dispersion" of the electron gap and the existence in it of its own natural frequencies. All of this shows that there is still a certain degree of uncertainty in the application of the ideas connected with the dielectric permeability of the electron gap to the interpretation of the mechanism of the operation of ultra-high frequency generators. Only when applied to gaps with very small transit angles may we hope to obtain results that are close enough by using the simple formula $\Delta\varepsilon = \frac{4\pi N e^2}{m\omega^2}$ if the mechanism by which the gap functions is well enough known and is simple enough to make it possible to calculate the variation in N, and together with it the capacity. The attempt of V. P. Gulyayev [15] to apply the theory of parametric excitation to the klystron generator has been fairly successful, and we shall consider it in the balance of this chapter.

Gulyayev takes the two-circuit klystron scheme of Figure 4.25 and assumes that the electrons fly from the cathode and modulator through equal time intervals, and that the forces of mutual repulsion between the electrons may be disregarded. He obtains the following expression for the number of electrons in 1 cubic centimeter of the output zone (the electric field of the second resonator):

$$N = \frac{N_0}{V_0\left(1 - \frac{1/2\,\varepsilon\omega s \cos\omega\tau_0}{V_0(1 + 3/2\,\varepsilon \sin\omega\tau_0)}\right)}, \qquad (4.48)$$

where

N_0 is the number of electrons emitted per second per square centimeter of cathode; $v_0 = \sqrt{2^{e/m} U_0}$ is the velocity acquired by the electron in the zone of acceleration; $\xi = U_1/U_0$ is the coefficient of "voltage modulation"; and s is the distance between the centers of the two resonators of the klystron.

Bearing in mind that the current density in the electron beam $i_0 = N_0 e$, the dielectric permeability may be expressed:

$$\varepsilon = 1 - \frac{4\pi N e^2}{m\omega^2} = 1 - \frac{2\pi i_0 V_0}{\omega^2 U_0\left(1 - \frac{\frac{1}{2}\xi\omega S \cos\omega\tau_0}{V_0\left(1+\frac{3}{2}\xi \sin\omega\tau_0\right)}\right)} \quad (4.49)$$

Whence, by formula (4.47), the coefficient of capacity modulation (assuming that $\xi \ll 1$) is obtained as the expression:

$$M \approx \frac{\pi i_0 \xi S}{\omega U_0} \quad (4.50)$$

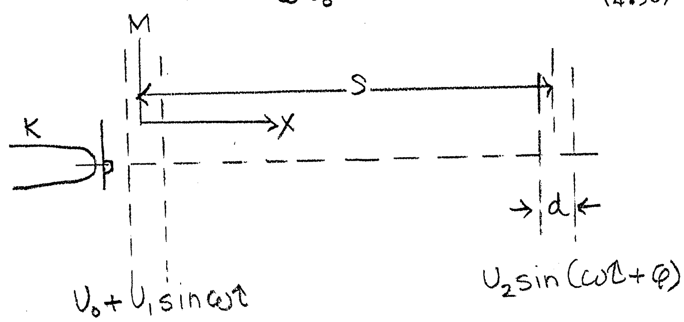

Figure 4.25

The modulation frequency of the parameter in this case is equal to the oscillation frequency, and the condition for excitation is obtained in the form

$$M^2 \geqslant 8\,\frac{R}{\omega L}$$

or

$$\frac{i_0^2 \xi^2 S^2}{U_0^2} \geqslant \omega \frac{R}{L} \cdot 10^{-23} \quad (4.51)$$

if i_o is expressed in amperes, and U_o in volts. Since $\mathcal{E} = U_1/U_o$, the initial value of the potential on the modulator U_{10} at which oscillation can be maintained may be expressed, from this equation, as follows:

$$U_{10} \geqslant 3.16 \cdot 10^{-12} \frac{U_o^2}{i_o s} \sqrt{\frac{\omega R}{L}} \qquad (4.52)$$

The condition for the excitation of oscillations and the other conclusions obtained for the klystron by Gulyayev, correspond satisfactorily to the experimental data and to the other theories.

The application of the theory of parametric excitation to the various types of ultra-high frequency generators is of great interest and will probably lead to, in a fairly simple way, fundamental results. One of the principal factors that is responsible for the physically grounded applicability of this theory is the reliable calculation of the dielectric permeability of the electron gap with varying space charge, which at the present time is hardly possible for the magnetron or even for the retarding-field circuit ("reflex klystron").

BIBLIOGRAPHY FOR CHAPTER IV

1. W. Benham, Phil. Mag., March 1928, p. 641; February 1931, 457.
2. F. Llewellyn, PIRE: 21, 1532, 1938; 22, 947, 1934; 23, 112, 1935.
3. C. Bakker and G. De Vries, Physica, I, 1045, 1934; II, 683, 1935.
4. G. Grünberg, Techn. Phys. USSR, III, 65, 1936.
5. Yu. Katsman, Elektrosvyaz' (Electrical Communication), No 7, 47, 1940.
6. J. Müller, Hochfrequenz & El., 41, 156, 1933; 43, 195, 1934; 46, 145, 1935.
7. S. Ramo, PIRE, 27, 584, 1939.
8. F. Llewellyn and A. Bowen, BSTJ (Bell System Technical Journal) 18, 280, 1939
9. F. B. Levellin (F. B. Llewellyn) Inertsiya electronov (The Inertia of Electrons), GTI, 1936.
10. J. Sahanek, Phys. ZS, 33, 693, 1932.
11. F. Llewellyn and L. Peterson, PIRE, 32, 144, 1944.
12. Yu. A. Katsman, Lampy dlya ul'travysokikh chastot (Ultra-High Frequency Tubes), Doctoral dissertation, 1945.
13. A. N. Shchukin, Rasprostraneniye radiovoln (The Propagation of Radio Waves). Svyaz'izdat, 1940.
14. S. Benner, Ann. d. Phys., 3, 993, 1929.
15. V. Gulyayev, ZhTF, XI, 101, 1941.